Design and Implementation of Piecewise-Affine Observers for Nonlinear Systems

AZITA MALEK

A Thesis

in

The Department

of

Electrical and Computer Engineering

Presented in Partial Fulfillment of the Requirements

for the Degree of Master of Applied Science (Electrical and Computer Engineering) at

Concordia University

Montréal, Québec, Canada

November 2013

CONCORDIA UNIVERSITY

School of Graduate Studies

This is to certify that the thesis proposal prepared

By: **AZITA MALEK**

Entitled: **Design and Implementation of Piecewise-Affine Observers for Non-linear Systems**

and submitted in partial fulfilment of the requirements for the degree of

Master of Applied Science (Electrical and Computer Engineering)

complies with the regulations of this University and meets the accepted standards with respect to originality and quality.

Signed by the final examining committee:

_____ Dr. M. Z. Kabir, Chair

_____ Dr. Y. M. Zhang , External Examiner

_____ Dr. A. Aghdam , Examiner

_____ Dr. Sx . Hashtrudi Zad , Examiner

_____ Dr. K. Khorasani, Supervisor

_____ Dr. L. Rodrigues, Supervisor

Approved by _____

Dr. W. E. Lynch, Chair

Department of Electrical and Computer Engineering

_____

Dr. C. W. Trueman

Interim Dean, Faculty of Engineering and Computer Science

ABSTRACT

Design and Implementation of Piecewise-Affine Observers for Nonlinear Systems

AZITA MALEK

This thesis is divided into two main parts. The contribution of the first part is to design a continuous-time Piecewise-Affine (PWA) observer for a class of nonlinear systems. It is shown that the state estimation error is ultimately bounded. The bound on the state estimation error depends on the PWA approximation error. Moreover, it is shown that the state estimation error is still convergent and ultimately bounded when the output of the system is only available at sampling instants. The proof of convergence is presented in two parts: conditions dependent on the sampling time and conditions independent of the sampling time. In addition, ultimate boundedness of the state estimation error is proven in the presence of norm bounded measurement noise. It is shown that the bound on the state estimation error is dependent on the sampling time, PWA approximation error and the bound on the norm of the noise. The proposed approach for observer design leads to a convex optimization which can be solved efficiently using available software packages.

The contribution of the second part is to implement the proposed PWA observer on a real setup of a wheeled mobile robot (WMR) available at the Hybrid Control Systems (HYCONS) Laboratory of Concordia University. Although some researchers have applied different types of observers to experimental applications, practical implementation of PWA observers has not been given much attention by researchers. In this thesis for the first time a PWA observer is applied to the WMR. The WMR is an example of a nonlinear system with

a sampled output in the presence of measurement noise. The results of the experimental implementation validate the proposed theoretical results in the first part.

"If we knew what it was we were doing, it would not be called research, would it? "

— Albert Einstein

ACKNOWLEDGEMENTS

First and foremost, I would like to thank my supervisors, Dr. Luis Rodrigues and Dr. Khashayar Khorasani. This thesis could not have been accomplished without their patient guidance, encouragement and support. I learnt from them; not only the scientific matters, but also lots of knowledge which are very helpful in all aspects of my life. I am very grateful to my supervisors for giving me this opportunity to come to Concordia University and join their research group.

I would like to convey my gratitude to all my committee members for devoting their valuable time in evaluating my work. Moreover, I must thank the professors, administrative and the technical staff of the department who have played an important role in my success.

I would like to thank all my HYCONS friends Behzad, Miad, Sina, Camilo, Hadi, Jamila, Amin, Tiago, Arthur, Javier, Qasim, Jesus, Manuel and Ram with whom I spent great moments during this period of my life. I would like to thank Miad in particular, which spent lots of time answering all my questions with patience. I also would like to thank Farzad for being such a good and supportive friend during the past few years.

Last, but by no means least, I would like to thank my parents for all of their unconditional love, help and support which cannot be put into words. Also, I would like to thank my lovely brother and sister for always being there for me.

To my parents.

TABLE OF CONTENTS

LIST OF FIGURES

xi

xv

LIST OF TABLES

Chapter 1

Introduction

This chapter includes the motivation and a review of the relevant literature on main topics of this thesis. The main contributions and the structure of the thesis are also stated in this chapter.

1.1   Motivation

It is not always possible to measure all the states of real systems. This might happen due to the high cost or limitations of the sensors. Generally, it is desired to have information about all states of the system in control applications. For example, applying a state feedback controller to the system requires information about all states of the system. Observable states can be estimated by state observers. Observers estimate the states of the system using the system's model, its inputs and its outputs. The estimated state, which is obtained by the observer, can be used in different observer-based applications [3, 4, 5]. Therefore, it is very important to have accurate and reliable estimation of the states. There are different ways to test an observer's performance and accuracy. A commonly used parameter to show the reliability and accuracy of the observers is the state estimation error, which is the deviation of the estimated state from the measured state [6, 7, 8].

Starting with the work of Luenberger, [6, 7, 8] the problem of observer design for

linear systems has been discussed in the literature. However, most of the dynamical systems exhibit nonlinear behavior. Consequently, it is very important to study the problem of observer design for nonlinear systems.

Designing observers for nonlinear systems is a difficult and challenging task. There is no method for observer design that works for all classes of nonlinear systems. Some methods of nonlinear observer design are based on the linearized models of the nonlinear systems [9, 10, 11] and only work within a small range around the equilibrium point for which the system is linearized. This is a motivation to study more general methods that work at a global scale.

Piecewise-Affine (PWA) systems are natural models for dead zone [12, 13], saturation [13, 14], relays [15, 16] and hysteresis [17, 18]. PWA systems are also good approximations for nonlinear systems [19, 20, 21]. All smooth nonlinear functions can be uniformly approximated by a PWA function over a simplicial partition [20, 22, 23]. Therefore, PWA observer design could be an alternative approach to design observers for a more general class of nonlinear systems. PWA systems have been an active area of research [17, 24, 25, 26, 27, 28, 29, 30, 31, 32, 33, 34]. Observer design for PWA systems has also been studied in the literature [35, 36, 37, 38]. In this thesis, an observer is designed for the PWA approximation of a class of nonlinear systems yielding a convergent state estimation error.

Designing observers for a PWA approximation of nonlinear systems leads to a method that is a convex optimization approach in terms of Linear Matrix Inequalities (LMIs). Convex optimization programs minimize convex functions over convex sets. There are many efficient and reliable ways to solve such problems with analysis tools and computer-aided programs [39]. This has made convex optimization as one of the most popular problems in many areas such as control [40].

In real applications, the observer is implemented inside a computer. The output of the system, which is given to the observer, is measured at sampling instants. The system with

the output that is only available at sampling instants is considered a sampled-data system. In this thesis, the observer is designed such that the state estimation error still converges when the output of the system is only available at sampling instants. Furthermore, in real environments noise exists almost everywhere and affects the operation of the systems. It is very important to consider the existence of noise in theoretical work. In this thesis, it is proven that the state estimation error is ultimately bounded in the presence of norm bounded measurement noise. In other words, the proposed observer is robust to norm bounded measurement noise.

The experimental motivation of this theoretical work is the application to a Wheeled Mobile Robot (WMR) available at the Hybrid Control Systems (HYCONS) Laboratory of Concordia University. The WMR is modeled by nonlinear equations that can be approximated by a PWA model. The states of this system are the position, the heading angle and the heading angle rate. The position is measured by capturing images by a camera and the heading angle can be calculated based on the information from the camera, but the heading angle rate is not measured. The measurements are affected by image noise which one of its common types is Gaussian [41]. Furthermore, according to the sampling time of the sensors, the output is only available at sampling instants. A PWA observer is proposed in this thesis that is able to estimate all the states of the system with convergent state estimation error.

This thesis addresses the design of continuous-time PWA observers for a class of nonlinear systems with a sampled output. At first, the problem is discussed by assuming that noise does not exist in the system. Then, the problem is studied by considering the presence of norm bounded measurement noise. To validate the observer design approach, the observer is applied to the real setup of the WMR.

1.2   Literature Survey

This section will be broken into five subsections. The first part presents a literature review on linear observer design methodologies. The second part will review the literature of nonlinear observer design approaches. The third and the fourth parts will present literature reviews on PWA observers and sampled-data observers, respectively. The last part of the literature survey studies the existing work on experimental implementation of observers.

1.2.1   Linear Observers

Commonly, the problem of estimating the states of a system is referred to as the problem of observer design for the system [11]. For linear observers the state reconstruction has a close relation with observability and can be used in connection with the design of linear regulators [42]. Starting with the work of Luenberger [6, 7, 8], the problem of observer design for linear systems has been discussed in the literature [43, 44, 45, 46, 47, 48] and references therein. The proposed observer by Luenberger [8], has the same structure as the linear system except it contains a linear function of the difference between the estimated output and the measured output, which is injected to the observer. This method is frequently called output injection. The observer gain can be designed by arbitrarily placing the eigenvalues such that the state estimation error is stable. The observer can be full-order or reduced-order. In full-order observers all the states of the system are estimated while in reduced-order observers only some of the states are estimated.

There exist also sliding mode observers for linear systems which are designed by transforming the linear system into block-observable form [49, 50, 51, 52, 53]. One of the differences between the sliding mode observer and Luenberger observer is injection of a nonlinear discontinuous term into the sliding mode observer. The discontinuous term enables the observer to reject disturbances and a class of mismatch between the system and the observer [54]. Hence, sliding mode observers are more robust than other existing types

of observers [52, 54]. The discontinuous term drives the observer trajectories such that the state estimation error goes to a surface in the error space. The sliding surface is usually set so that the deviation of the observer's output from the system's output is forced to go to zero [54]. Also, a wide variety of parameter estimation problems can be solved by the sliding mode observer design approach [52].

Although the mentioned methods are applicable to all linear systems with observable states, many real systems exhibit nonlinear behavior. For example, vehicle models such as autonomous land vehicles [20], rotorcraft unmanned aerial vehicles [21] and a helicopter pitch model [19]. Thus, it is very important to study observer design approaches for nonlinear systems.

1.2.2 Nonlinear Observers

Designing observers for nonlinear systems is considered a difficult problem, since there is no unique method that works for all classes of nonlinear systems. For a linear observable system, any input distinguishes any two distinct states, while for nonlinear systems this is no longer true [55]. Several research studies have been conducted on nonlinear observer design [10, 42, 52, 55, 56, 57, 58, 59, 60, 61, 62, 63, 64, 65, 66, 67, 68, 69, 70, 71, 72, 73, 74, 75, 76, 77, 78, 79, 80, 81, 82, 83, 84, 85, 86, 87, 88, 89, 90, 91, 92, 93, 94, 95, 96, 97, 98, 99, 100, 101, 102, 103, 104, 105, 106, 107, 108, 109] and this is still an open area of research.

There are different methods for nonlinear observer design such as: Lyapunov-based, geometric, sliding, Lie-algebraic, backstepping and high-gain observers. Some examples of Lyapunov-based observers are the ones suggested in [42, 56, 57, 58, 59, 60, 61, 62, 63]. In [42], a procedure is proposed to check the stability of the state estimation error for a given observer gain but it does not suggest a method for designing the observer gain. Choosing the observer gain in [42] is a trial and error procedure that is not feasible for higher-order systems. In [56] some sufficient conditions for the existence of an observer are proposed

which are difficult to satisfy. One of the conditions is existence of a certain Lyapunov-like function. The author of [57] has generalized the method of [56], but the system still needs to satisfy some restrictive necessary conditions. In [58] an algorithm is presented to design an observer gain for a class of nonlinear systems. The procedure in [58] is a recursive algorithm that solves the Ricatti equation. The only information from the nonlinear part that is used by the method in [58] is the Lipschitz number. Reference [59] contains an observer design algorithm that uses the Lyapunov auxiliary theorem. The restriction in [59] is that the system should be either locally asymptotically stable at the origin or unstable with the eigenvalues that are all in the right half-plane. The author of [60] has provided the reader with a numerical approach for solving the methodology presented in [59]. The solution in [60] can be obtained by deriving a linear matrix equation. In [61] a nonlinear observer design methodology is proposed for a special class of systems. The authors of [62] have presented a nonlinear observer for a class of nonlinear discrete-time systems. Reference [63] contains a Lyapunov-based observer design method with application to diesel engines.

Geometric methods of observer design are based on transforming the nonlinear systems into linear systems [10, 64, 65, 66, 67, 68, 69, 70]. In [10], a methodology based on extended linearization is proposed for observer design. Extended linearization is the family of linearization of the nonlinear system parameterized by the constant operating points. Although extended linearization is better than linearization about a single point, it is not global. Extended linearization problems are solvable locally which means that some of the results are just valid in the presence of controlled dynamics [11]. An observer design methodology is presented in [67] that is based on transforming the system into nonlinear observer canonical form and performing an extended linearization for multi-input multi-output systems. With reference to extended Kalman filter, the method in [67] is called extended Luenberger observer.

Some other existing methods of nonlinear observer design are based on the Lie-algebraic approach [71, 72, 73, 74, 75, 76, 77]. The goal in such methods is to transform

the nonlinear system into a linear system by using Lie-algebraic tools and designing linear observers for it. Another common approach in Lie-algebraic methods is to transform the system into a system for which all the nonlinearities are measurable [71]. In the case that the nonlinearity just depends on the output, an observer can be designed easily by output injection and pole placement. The main drawback of this approach is to assume that the nonlinear term is perfectly known. Modeling errors can cause problems in stability of the state estimation error. Another difficulty in Lie-algebraic observer design methods is the existence of transformations for transforming the system into the linear or nonlinear observable form. Normally, it is extremely difficult to satisfy the conditions for this approach. Even if all the conditions are satisfied, it is very difficult to obtain the transformation and transform the system into the observable form. In [71], a transformation is proposed to transform single-input single-output nonlinear systems into the observable form. It is very difficult to satisfy the necessary conditions for the existence of the transformation. Moreover, it is very difficult to calculate the transformation if the transformation exists. Using the methodology in [71] for higher-order systems, requires many partial differential equations to be solved. The authors of [72] have extended the results of [71] to make it easier to solve, but there are still some restrictions. In [73] the same problem as [71] is discussed for multi-input multi-output systems. Reference [74] contains a transformation for single-input single-output nonlinear systems into the observer form in order to design adaptive observers. In [75], an extension to [74] is provided for multi-input multi-output systems.

High-gain observers are another class of observers that are robust to modeling errors [110]. Reference [78] provides the reader with a study on high-gain observers and their applications in controller design. The peaking phenomenon is an intrinsic feature of any high-gain observer that rejects the effect of the disturbances such as modeling error [78]. The Peaking phenomenon can destabilize the closed loop system by transforming an impulsive-like behavior from the observer to the plant [78]. When it is desired to design a controller for the system whose states are being estimated by a high-gain observer,

the controller has to be globally bounded in order to protect the system from the peaking phenomenon [78]. A High-gain observer is basically an approximate differentiator. This can cause practical limitations in cases such as existence of measurement noise [78]. High-gain observers are studied in different applications including, but not limited to, stabilization [79], adaptive control [80], sliding mode control [81, 82], switching control [83] and feedback control [84]

Another method for nonlinear observer design is based on the sliding mode theorem [111]. In comparison with other types of observers, sliding mode observers are more robust [52, 54]. The reason is injection of a nonlinear discontinuous term which rejects the disturbances and a class of mismatch between the system and the observer [54]. The trajectories of the observer are forced by the nonlinear discontinuous term to go to a surface in the error space. The equation of the surface is usually a function of the difference between the observer's output and the system's output, which is forced to converge to zero [54]. There are several research studies on sliding mode observers with different applications such as control, fault detection and isolation [52, 85, 86, 87, 88, 89, 90, 91, 92, 93].

Backstepping observer design is another method for estimating the states of nonlinear systems. This method is mainly applicable to the systems in triangular form. In [103] exponentially convergent backstepping observers are designed for a class of parabolic Partial Differential Equations (PDEs). The authors of [104] have proposed a methodology for designing backstepping observers for a class of nonlinear single-output systems. In order to design the observer proposed in [104] the system must be in a specific triangular observer form. The proposed method in [104] guarantees exponentially convergence of the state estimation error, if the initial estimation error is not too large. In [105] in order to control a nonlinear single-output system with adaptive output-feedback controller the derivatives of the output are needed which some of them are estimated using high-gain observer and the rest are estimated using backstepping observer. In [106] a backstepping observer is used as a residual generator for fault detection and isolation of a class of nonlinear systems. The

authors of [107] have designed a backstepping observer for a nonminimum-phase system in order to stabilize the system with output feedback. In [108] a backstepping observer design approach for a class of state affine systems is proposed. The authors of [109] have proposed an observer backstepping control for wind turbines.

Moreover, some researchers have studied the problem of Linear Parameter Varying (LPV) observer design in the literature. In [112] the problem of LPV observer design for an industrial semi-active suspension is studied. The authors of [113] have used LPV observer in order to perform fault detection. Also, in [114, 115] and the references therein, the problem of observer design for LPV systems is addressed.

Sometimes uncertainties exist in nonlinear systems. The reason could be the existence of unknown inputs or lack of knowledge about the system's nonlinearities. In [89, 94, 95, 116] some techniques are proposed to design observers for systems with uncertainties. In other words, in these methods not all the information about the system is needed for designing an observer. References [96, 97, 102, 117, 118] contain comparative studies on many different nonlinear observer design techniques including Kalman filter, Thau's method, adaptive observers, high-gain observers, multi-stage nonlinear observers, sliding mode observers and equivalent control-based sliding mode observers. There is no exact conclusion on the performance or ease of design of these observers.

Although there exist several research studies in the area of nonlinear observer design techniques, since no unique method exists for all classes of nonlinear systems, this is still an open area of research.

1.2.3 Piecewise-Affine Observers

PWA systems provide a powerful modeling framework for complex dynamical systems which are modeled by nonlinear functions. Furthermore, a broad range of nonlinear systems which are frequently used in engineering applications can be accurately approximated by PWA systems [119].

PWA systems [17, 24, 25, 26] and in particular observer design for PWA systems [35, 36, 37, 38] have been studied in the literature. There are different approaches for PWA observer design in the literature [120, 121, 122, 123]. The references that are discussed in this section are mostly the ones that design PWA observers through an LMI-based approach. The authors of [35] were the first to design an observer for PWA systems. Then, the work of [35] was extended in [3, 124]. In [36, 125] a methodology for designing a bimodal continuous-time PWA observer with asymptotically stable state estimation error is proposed. The proposed observer in [36, 125] is used for fault diagnosis. Reference [37] contains the problem of observer design for discrete-time PWA systems without considering the affine term. Another approach for state estimation that is presented in [37] uses particle filtering in a noisy environment. In [38] the problem of observer design is discussed for both continuous-time and discrete-time PWA systems, however, the affine term is neglected.

Many researchers have also studied the problem of observer design for switched linear systems [126, 127, 128, 129]. Switched systems are a class of systems containing both continuous dynamics and discrete events [40]. In [126], an observer design methodology is proposed which guarantees stability of the state estimation error for switched linear systems. The problem is discussed in both continuous-time and discrete-time, but the fact that the state of the system and the estimated state can be in different regions is not considered. Reference [127], consists of the problems of stability of the state estimation error, minimization of the error and a projection method for state estimation of discrete-time switched linear systems. The situation when the state and the estimated state lie in different regions is not considered in [127]. In [128], an observer design methodology with stable state estimation error is presented for discrete-time switched linear systems with bounded noise. The proposed method in [128] is not an LMI-based approach. The method in [128] is also applicable to mode estimation.

The problem of observer design for Piecewise-Linear (PWL) systems is also studied

in the literature [130, 131, 132]. PWL functions are made up of linear pieces. The difference between PWL and PWA systems is that in PWL systems there is no affine term while PWA systems contain affine terms. In [130], an observer is proposed for a PWL bimodal system in both discrete-time and continuous-time. The authors of [131] have discussed the problem of observer design for a continuous-time PWL system. In [132], the problem of observer design is studied for a PWL system that contains disturbance, process noise and measurement noise.

To the best of the author's knowledge there is no work in the literature that designs a continuous-time PWA observer for the PWA approximation of a nonlinear system with a convergent state estimation error when applied to the nonlinear system. Since many real systems which exhibit nonlinear behavior can be approximated by PWA systems, designing a PWA observer can be a good approach to deal with the problem of observer design for nonlinear systems. This thesis will present a method for PWA observer design for nonlinear systems with the output available only at sampling instants.

1.2.4 Sampled-Data Observers

As discussed in previous sections, for continuous-time systems with continuous-time outputs several methods for observer design have been proposed. In real applications observers are implemented inside computers. The output of the system that is given to the observer is measured at sampling instants. The system with an output only available at sampling instants is called a sampled-data system. The problem of observer design for linear and nonlinear sampled-data systems has been studied in recent years [133, 134, 135, 136, 137, 138]. Reference [134] contains the problem of observer design for a discrete-time approximation and emulation of a nonlinear sampled-data system. In [135], the problem of observer design for nonlinear sampled-data Lipschitz systems with exact and Euler approximated models is discussed. In [136], an observer-based fault-tolerant controller is designed for a class of nonlinear sampled-data systems. The authors of [137] have proposed an observer design

methodology for nonlinear sampled-data systems via approximate discrete-time models. Reference [138] addresses the problem of observer design for continuous-time systems with sampled output measurements. The author in [139, 140] has discussed stability of sampled-data PWA systems under state feedback. However, by assuming that all the states are measurable, no observer is designed in [139, 140].

Although in real observer implementations the output of the system is sampled and although PWA systems have proven to be good approximations for nonlinear systems, to the best of the author's knowledge there is no contribution in the literature on PWA observer design for nonlinear systems with a sampled output.

The problem in this thesis is not to design a sampled-data observer, but it is rather to apply a continuous-time PWA observer to a nonlinear system with a sampled output. The state estimation error is shown to be convergent when the continuous-time PWA observer is applied to the nonlinear system with a sampled output. The methodology of [139, 140] is used to discuss the stability of the state estimation error for a class of nonlinear sampled-data systems after designing a continuous-time PWA observer.

1.2.5   Experimental Implementation of Observers

Although PWA observer design has been studied in the literature as discussed in Section 1.2.3, unfortunately, its practical implementation has not been given much attention by researchers. However, some researchers have applied other types of observers to different experimental applications [131, 141, 142, 143, 144, 145, 146, 147, 148, 149, 150, 151, 152, 153, 154, 155]. In [141] a Luenberger observer is applied to a tethered wing wind power system in order to perform an observer-based control. In [142] a linear hybrid observer is used for battery state of charge estimation. The method of observer design in [142] is based on designing separate observers for each subsystem, which does not guarantee the stability of the state estimation error in case of arbitrary switching between the observers. The authors of [143] have presented a new methodology referred to as the smooth variable

structure filter, which is used for estimating the stator winding values of a brushless DC motor. In [144] a high-gain observer is applied to an experimental setup of an inverted pendulum on a cart. Reference [145] contains the problem of applying a nonlinear observer to a single-ended primary inductor converter. In [146] a cascade nonlinear observer that is designed for a class of cascade nonlinear systems is used for state estimation of an experimental induction motor benchmark. The authors of [147] have used an observer for estimating the velocities of two cooperative industrial robots. In [148] a nonlinear observer is used for state estimation and parameter estimation of an induction motor and the efficiency of the observer is shown on an experimental setup of an induction motor. The authors of [149] have applied interconnected high-gain observers to induction motors to perform the state estimation. Also, in [150] high-gain observers are designed to estimate the mechanical and magnetic variables of an induction motor and use the estimated states to control the system. The authors of [151] have proposed an extended state observer for experimental observer-based control of a flexible-joint robotic system. References [131, 152] contain the problem of implementation of a PWL observer on a harmonically excited flexible steel beam with a one-sided support, which is an example of flexible mechanical systems with one-sided restoring characteristics. Also, in [152] an observer is applied to an experimental setup of a dynamic rotor system that is a benchmark for motion systems with friction and flexibility. It should be noted that PWL functions are not as accurate as PWA functions in approximating nonlinear functions. In [153], an observer is designed based on the mean value theorem [156, 157] and it is used for estimating the slip angle of a Volvo XC90 sport utility vehicle. In [154] an observer is designed to estimate the position, velocity and disturbance torque in a surface permanent-magnet machine. In [155] an adaptive backstepping observer is designed for estimating the rotor-flux of an induction motor drive. To the best of the author's knowledge, there is no work in the literature that applies a PWA observer to an experimental setup. In this thesis a PWA observer is applied to an experimental setup of a WMR that is available at the HYCONS Laboratory of Concordia University.

1.3   Objectives and Contributions

This thesis addresses the design of continuous-time PWA observers for a class of nonlinear systems with a sampled output. Based on observer theory for PWA systems, sufficient conditions are proposed such that a continuous-time PWA observer can be used to estimate the states of a nonlinear system with a sampled output yielding a convergent state estimation error. The method for observer design is a convex optimization approach in terms of LMIs. It is shown that the state estimation error converges to a region and the size of the region depends on the sampling time and the PWA approximation error.

In the following the main contributions of this thesis are summarized:

• A continuous-time PWA observer is designed for a class of smooth nonlinear systems yielding a convergent state estimation error. It is proven that the state estimation error is ultimately bounded when the output of the nonlinear system is only available at sampling instants. It is shown that the proposed observer is robust to norm bounded measurement noise by proving the ultimate boundedness of the state estimation error in the presence of norm bounded measurement noise. The proposed design methodology can be cast as a set of LMIs which is based on a convex optimization approach that can be solved efficiently using available software packages. Using the proposed method leads to numerical values for the observer gains.

• A continuous-time PWA observer is implemented on an experimental setup of a WMR for the first time. The experimental setup of the WMR is available at the HYCONS Laboratory of Concordia University and is an example of a nonlinear system with a sampled output in the presence of measurement noise. The WMR is modeled by nonlinear equations that can be approximated by a PWA model. The state estimation results of this experiment validate the proposed theoretical results in this thesis. The state estimation errors regarding all states of the system (position, heading angle and heading angle rate) are shown to be ultimately bounded and convergent.

1.4 Structure of the Thesis

This thesis is structured as follows. Chapter 2 consists of preliminaries and prerequisites. After a brief review of PWA systems, the problem of PWA observer design is addressed. Then, a review on definitions of boundedness and ultimate boundedness is provided. Furthermore, some nonlinear observer design techniques are reviewed in Chapter 2. The problem of PWA observer design for nonlinear systems is presented in Chapter 3. After a brief introduction, the problem of designing continuous-time PWA observers for a class of nonlinear continuous-time systems is explained. It is followed by presenting the results on stability of the state estimation error for the nonlinear continuous-time system. Then, stability of the state estimation error for nonlinear sampled-data systems is studied in two parts: conditions dependent on the sampling time and conditions independent of the sampling time. The last problem discussed in Chapter 3 is to design continuous-time PWA observers for a class of nonlinear systems with a sampled output in the presence of measurement noise. Finally, some simulation examples are provided in Chapter 3 to show the validity of the results. Chapter 4 addresses the WMR modeling, wireless communication, and a discussion of the electronics and sensors related to the experimental setup. Chapter 4 is closed by presenting the results regarding the implementation of the proposed observer on the WMR setup. Finally, conclusions are drawn and suggestions for future studies are made in Chapter 5.

Chapter 2

Preliminaries and Prerequisites

2.1 Introduction

This chapter contains four sections. In Section 2.2 the mathematical representation of PWA systems is reviewed. Section 2.3 presents the structure of PWA observers. Section 2.3 also contains prerequisites needed for stability analysis of the state estimation error. Section 2.4 provides the reader with some definitions on boundedness and ultimate boundedness. Some approaches for nonlinear observer design are studied in Section 2.5.

2.2 Review of Piecewise-Affine Systems

Hybrid systems are a class of systems containing both continuous dynamics and discrete events [40]. PWA systems are a class of hybrid systems with affine subsystems. PWA systems are also a natural model for hybrid dynamical systems containing switching such as dead zone [12, 13], saturation [13, 14], relays [15, 16] and hysteresis [17, 18]. Furthermore, PWA systems may result from PWA approximations of nonlinear dynamics [125]. All smooth nonlinear functions can be uniformly approximated by a PWA function over a simplicial partition [20, 22, 23]. Although a PWA approximation of a nonlinear system

works at a global scale, it does not have the same complexity of the nonlinear system locally [125]. In other words, using a PWA model of a complex nonlinear system provides a global approximation of the system with locally simpler affine dynamics [125]. Some examples of nonlinear systems approximated by PWA dynamics are tunnel diode circuits [20], autonomous land vehicles [20], rotorcraft unmanned aerial vehicles [21] and a helicopter pitch model [19].

PWA systems are obtained by partitioning a subset of the state space X into a set of regions R_i such that each subsystem is affine [20, 40]. The state space representation of a PWA system is described as

$$\dot{x}(t) = A_i x(t) + B_i u(t) + b_i$$
$$y(t) = C_i x(t)$$

(2.1)

for $x \in R_i$, where $u(t) \in R^m$, $x(t) \in R^n$ and $y(t) \in R^p$ represent the input, state and output of the system, respectively. The matrices A_i, B_i and C_i are matrices with appropriate dimensions and contain real entries. The vector of constant values b_i is called the affine term and contains real entries. For the regions containing the origin in its closure the affine term is zero, i.e. $b_i = 0$.

In slab systems for which the switching just depends on one linear combination of the states, the regions are defined as

$$R_i = \{x | d_i < H^T x < d_{i+1}\}$$

(2.2)

with $i = 1, .., q$, where q is the number of regions, or equivalently

$$R_i = \{x | \|E_i x + f_i\| < 1\}$$

(2.3)

When the switching depends on only one state, H is a vector of zeros except for the element corresponding to the state that is responsible for the switching of the system and we have

$$E_i = \frac{2H^T}{d_{i+1} - d_i}$$

(2.4)

17
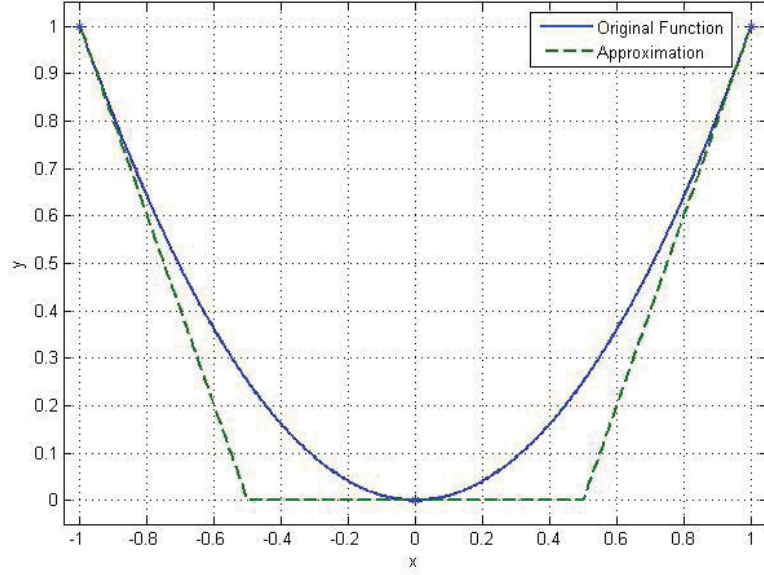
Figure 2.1: PWA approximation of $y = x^2$ for $x \in [-1, 1]$.

and

$$f_i = \frac{-(d_{i+1} + d_i)}{d_{i+1} - d_i} \tag{2.5}$$

Note that

$$\bigcup_{i=1}^{q} \bar{R}_i = X \tag{2.6}$$

and

$$\bar{R}_i \cap \bar{R}_j = \phi \tag{2.7}$$

Different algorithms exist in the literature to obtain PWA approximations of nonlinear systems [20, 21, 158, 159, 160, 161, 162, 163]. In Figure 2.1 a PWA approximation of nonlinear function $y = x^2$ for $x \in [-1, 1]$ is shown. This nonlinear function is approximated by a PWA function in three regions [21].

PWA systems have been studied in the literature in different subjects such as PWA approximations [20, 21, 158, 159, 160, 161, 162, 163, 164, 165, 166, 167], analysis of PWA control systems [17, 24, 25, 26, 27, 28, 29, 30, 31, 32, 33, 34] and controller/observer design for PWA systems [14, 25, 26, 35, 36, 37, 38, 168, 169, 170].

2.3 Review of Piecewise-Affine Observer Design

Designing observers for PWA systems leads to a convex optimization problem through an LMI-based approach. Convex optimization programs can be solved efficiently using software packages such as SeDuMi [171] and YALMIP [172]. This has made such programs as one of the most popular problems in many applications [39, 40]. Before presenting the PWA observers, the definitions of convex functions and convex optimization problems are provided.

Definition 2.3.1. *[39] A function $f_i : R^n \rightarrow R$ is convex if for all $x, y \in R^n$ and all $\alpha, \upsilon \in R$ with $\alpha + \upsilon = 1$, $\alpha > 0$ and $\upsilon > 0$, the functions satisfy*

$$f_i(\alpha x + \upsilon y) \leqslant \alpha f_i(x) + \upsilon f_i(y) \tag{2.8}$$

Definition 2.3.2. *[39] The following problem is called a convex optimization problem.*

minimize $f_0(x)$

subject to $f_i(x) \leqslant g_i$, $i = 1, ..., m$

where $f_0, ..., f_m : R^n \rightarrow R$ are convex and the constants $g_1, ..., g_m$ are the limits, or bounds, for the constraints.

For the system defined in (2.1), a PWA observer has the structure as follows [35]

$$\dot{\hat{x}}(t) = A_j \hat{x}(t) + B_j u(t) + b_j + L_j(C_i x(t) - C_j \hat{x}(t))$$
$$\hat{y}(t) = C_j \hat{x}(t) \tag{2.9}$$

for $\hat{x} \in R_j$, where $\hat{x}$ denotes the estimated state and the observer gain for R_j is given by L_j. The structure of the PWA observer is almost the same as the one for a linear observer except that the PWA observer includes the affine term and several regions. Moreover, the observer gain for each region has a different value. A scheme of the PWA observer is depicted in Figure 2.2.

The state estimation error is defined as

$$e(t) = x(t) - \hat{x}(t) \tag{2.10}$$
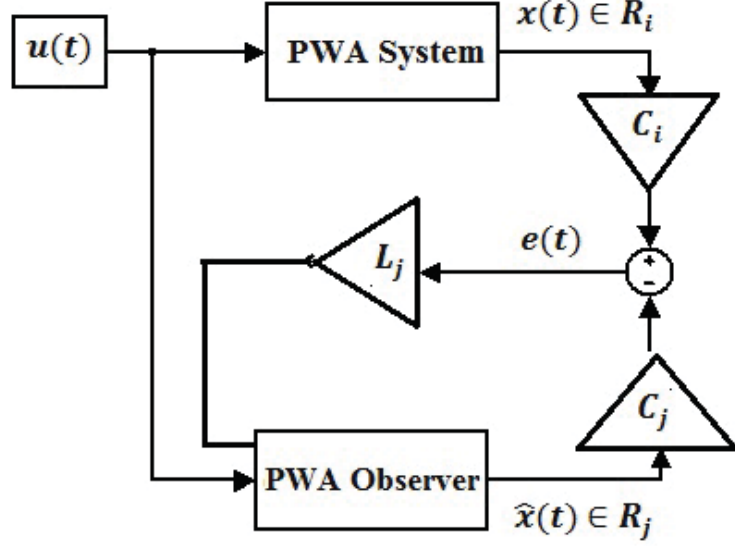
Figure 2.2: PWA observer schematic.

which is the deviation of the state $x(t)$ from the measured state $\hat{x}(t)$. The state estimation error is commonly used for discussing performance of observers. When the state estimation error converges to zero, it means that all the states are estimated correctly.

It should be considered that the state of the system and the estimated state generated by the observer can either be in the same or in different regions. Depending on q which is the number of regions, q^2 different cases can happen. To discuss stability of the state estimation error all the cases should be considered.

According to (2.10) the dynamics of the state estimation error for the system and the observer defined in (2.1) and (2.9), respectively, is

$$\dot{e}(t) = (A_j - L_j C_j)e(t) + (A_i - A_j + L_j(C_j - C_i))x(t) + (B_i - B_j)u(t) + (b_i - b_j) \quad (2.11)$$

for $x \in R_i, \hat{x} \in R_j$.

The objective is to design an observer with stable state estimation error. In order to design observer gains, stability of the state estimation error must be taken into account. Due to the structure of (2.11), it is not possible to provide stability of the state estimation error by pole placement in the same way as linear observers. To discuss stability of the

20

state estimation error, a candidate Lyapunov function should be defined. The complete discussion on this problem will be presented in Chapter 3.

One of the tools needed to prove stability of the state estimation error is the S-procedure, which is explained in Lemma 2.3.1.

Lemma 2.3.1. *S-procedure [173]: Let f_0 and f_1 be quadratic functions of the variable $\zeta \in R^n$. If there exist $\lambda \geqslant 0$ such that for all ζ*

$$f_0(\zeta) \geqslant \lambda f_1(\zeta) \tag{2.12}$$

Then $f_0(\zeta) \geqslant 0$ for all ζ such that $f_1(\zeta) \geqslant 0$.

Proof. See reference [173]. □

One of the advantages of using the S-procedure is that instead of studying stability of the state estimation error with dynamics for $x \in R_i$, $\hat{x} \in R_j$ in the whole state space, it can be just studied for $x \in R_i$, $\hat{x} \in R_j$. In this thesis, the S-procedure is applied in regions whose projection in the $x, \hat{x}$ plane are circles. The circles are an approximation of the rectangles that are the intersection of two slab regions, as shown in Figure 2.3. One of the slab regions is the region in which the state of the system is operating and the other one is related to the estimated state. The intersection is approximated by the circle with minimum area that contains the rectangle (see Figure 2.3). The circle is defined by

$$\varepsilon_{ij} = \{x, \hat{x} \mid \| H^T x - \gamma_i \|^2 + \| H^T \hat{x} - \beta_j \|^2 \leqslant r_{ij}^2\} \tag{2.13}$$

where γ_i, β_j and r_{ij} are coordinates of the center and radius of the circle related to the case $x \in R_i$, $\hat{x} \in R_j$ and are defined by

$$\gamma_i = \frac{d_{i+1} + d_i}{2} \tag{2.14}$$

$$\beta_j = \frac{d_{j+1} + d_j}{2} \tag{2.15}$$

$$r_{ij} = \sqrt{\left(\frac{d_{i+1} - d_i}{2}\right)^2 + \left(\frac{d_{j+1} - d_j}{2}\right)^2} \tag{2.16}$$
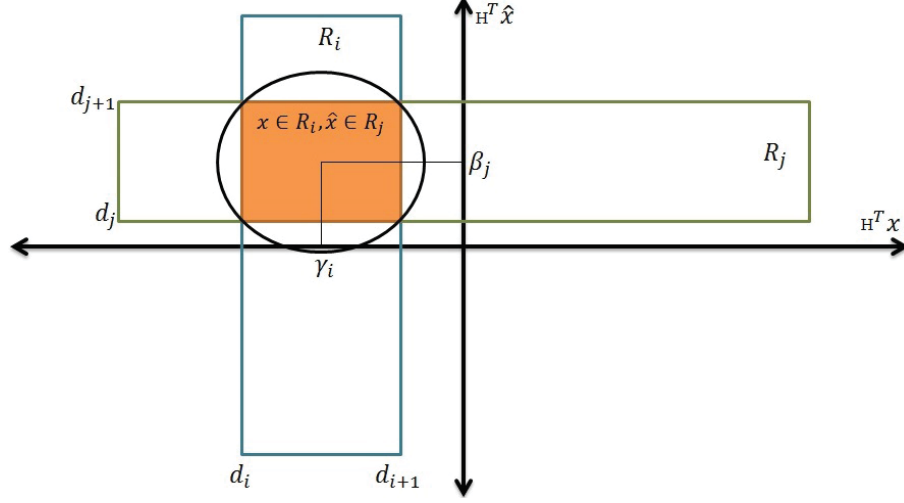
Figure 2.3: Covering circle with minimum area ($x \in R_i$, $\hat{x} \in R_j$).

2.4 Boundedness and Ultimate Boundedness

Lyapunov analysis can be used to show boundedness of the solution of the state equation (for example boundedness of the state estimation error defined in (2.11)) when there is no equilibrium point at the origin [110]. Before starting the discussion on boundedness and ultimate boundedness, some definitions will be presented.

Definition 2.4.1. *[110] Let $f(x)$ be defined on an interval I. Suppose that two positive constants L and α can be found such that*

$$|f(x_1) - f(x_2)| \leqslant L|x_1 - x_2|^\alpha \, \forall x_1, x_2 \in I \qquad (2.17)$$

Then f is said to satisfy a Lipschitz condition of order α.

Definition 2.4.2. *[110] A function $f(x)$ is globally Lipschitz if it satisfies the Lipschitz condition on R^n for $\alpha = 1$.*

Definition 2.4.3. *[110] A function $f(x)$ is Lipschitz on a set W if it satisfies the Lipschitz condition on W for $\alpha = 1$.*

Definition 2.4.4. *[110] A function $f(x)$ is locally Lipschitz on a domain $D \subset R^n$ if each point of D has a neighborhood D_0 in which f satisfies the Lipschitz condition for all points in D_0 with some Lipschitz constant L_0 and $\alpha = 1$.*

Note that, in Definition 2.4.3 the condition must be satisfied for all points in W, but in Definition 2.4.4 the condition must be satisfied for a small neighborhood of each point.

In what follows some definitions are provided on boundedness and ultimate boundedness [110]. Consider the system

$$\dot{x} = f(t, x) \tag{2.18}$$

where $f : [0, \infty) \times D \to R^n$ is piecewise continuous in t and locally Lipschitz in x where $D \subset R^n$ contains the origin.

Definition 2.4.5. *[110] The solutions of (2.18) are uniformly bounded if there exists a positive constant c, independent of $t_0 \geqslant 0$ such that for every $a \in (0, c)$, there is $\beta = \beta(a) > 0$ independent of t_0, such that*

$$\| x(t_0) \| \leqslant a \Rightarrow \| x(t) \| \leqslant \beta, \forall t \geqslant t_0 \tag{2.19}$$

Definition 2.4.6. *[110] If (2.19) holds for arbitrarily large a, the solutions of (2.18) are globally uniformly bounded.*

Definition 2.4.7. *[110] The solutions of (2.18) are uniformly ultimately bounded with ultimate bound b if there exist constants $b > 0$ and $c > 0$, independent of $t_0 > 0$, such that for all $a \in (0, c)$ there is $t_1 > 0$ independent of t_0 such that*

$$\| x(t_0) \| \leqslant a \Rightarrow \| x(t) \| \leqslant b \quad \forall t \geqslant t_0 + t_1 \tag{2.20}$$

Definition 2.4.8. *[110] If (2.20) holds for arbitrarily large a, the solutions of (2.18) are globally uniformly ultimately bounded.*

In what follows some mathematical properties regarding the matrix norm are presented.

Definition 2.4.9. *Let $R^{m \times n}$ denotes the vector space containing all $m \times n$ matrices with entries in R. If $\| A \|$ denotes the vector norm of matrix A in $R^{m \times n}$,*

$$\| A \| \geqslant 0 \quad and \quad \| A \| = 0 \quad iff \quad A = 0 \quad for \ all \quad A \in R^{m \times n} \tag{2.21}$$

23

$$\| \alpha A \| = |\alpha| \, \| A \| \quad \textit{for all} \quad \alpha \in R \quad \textit{and} \quad A \in R^{m \times n} \tag{2.22}$$

$$\| AB \| \leqslant \| A \| \| B \| \quad \textit{for all} \quad A, B \in R^{m \times n} \tag{2.23}$$

For $m = n$

$$\| A \|_2 = \sigma_{max}(A) \tag{2.24}$$

where $\sigma_{max}(A)$ defines the maximum eigenvalue of the square matrix A.

Moreover, it can be proven that [110]

$$\sigma_{min}(A) \leqslant \| A \|_2 \leqslant \sigma_{max}(A) \tag{2.25}$$

where $\sigma_{min}(A)$ is the minimum eigenvalue of the square matrix A. In this thesis, $\| A \|$ refers to the $\| A \|_2$.

2.5 Nonlinear Observers

A detailed literature survey on nonlinear observer design techniques is provided in Section 1.2.2. In this section, the nonlinear observer design methods that are applicable to the special class of systems considered in this thesis and in particular the WMR example that we are interested in, are studied. The following class of nonlinear systems is considered

$$\dot{x}(t) = f(x) + Bu(t)$$
$$y(t) = Cx(t) \tag{2.26}$$

where $f(x)$ is smooth and nonlinear in one of the states, $x(t) \in R^n$ is the state vector, $u(t) \in R^k$ is the input, $y(t) \in R^l$ is the measured output, B and C are real matrices with appropriate dimensions.

The methods that are studied in this section are later used in Chapter 3 to design observers for the WMR system in order to compare the results with the PWA observer.

• Nonlinear Observers with Output Injection

In this section, a nonlinear observer design approach is studied that is applicable to the systems for which the nonlinearity just depends on the input and the output. Furthermore, a method of transformation is presented for transforming the nonlinear systems into the observable form (2.27) in order to design observers. Consider the following class of nonlinear systems

$$\dot{x} = Ax + \gamma(y, u)$$
$$y = Cx$$

(2.27)

where x, y and u define the state, output and input, respectively. The nonlinear function γ depends on the input and the output of the system.

If (A, C) is observable, the following observer can be used to estimate the states of the nonlinear system defined in (2.27) [71].

$$\dot{\hat{x}} = A\hat{x} + \gamma(y, u) + L(y - C\hat{x})$$

(2.28)

where $\hat{x}$ is the estimated state and L is the observer gain.

The state estimation error defined in (2.10) for the system and the observer defined in (2.27) and (2.28) is given by

$$\dot{e} = (A - LC)e$$

(2.29)

Designing observer gain L such that $A - LC$ is Hurwitz, which means its eigenvalues have negative real parts, guarantees asymptotic stability of the state estimation error. As the poles of $A - LC$ are placed farther from the origin, the state estimation error converges faster. It should be noted that if the eigenvalues of $A - LC$ are placed very far from the origin, we get larger values for observer gains. On the other hand, since this value is multiplied by the state estimation error, it can cause problems such as amplification of any noise that might be obtained from measuring the output, for poles that are very far from the origin. For this reason it is not desired to place eigenvalues of $A - LC$ very far from the origin.

Although the proposed method for nonlinear observer design is very easy, it is just applicable to the special class of nonlinear systems defined in (2.27). However, there are systems for which the nonlinearity depends on the states that are not being measured. Therefore, the studied method is just an answer to a limited number of nonlinear observer design problems. Moreover, the main drawback of this method is that it is assumed that the nonlinear function $\gamma(y, u)$ is perfectly known. This assumption affects the state estimation error in case of modeling errors.

In [71] some conditions are proposed to transform the system

$$\dot{x} = f(x) + g(x)u$$
$$y = h(x)$$
(2.30)

into the observable form (2.27). Before presenting the conditions, two definitions are provided.

Definition 2.5.1. *[71] The Lie bracket of $[f, g]$ is defined as*

$$[f, g] = \frac{\partial g}{\partial x} f - \frac{\partial f}{\partial x} g$$
(2.31)

where $\frac{\partial g}{\partial x}$ and $\frac{\partial f}{\partial x}$ are Jacobian matrices. Also $[f, g]$ can be written as $ad_f g$ where

$$ad_f^k g = [f, ad_f^{k-1} g]$$
(2.32)

with

$$ad_f^0 g = g$$
(2.33)

Definition 2.5.2. *For a scalar function h and a vector field f the Lie derivative is defined as*

$$L_f h = \frac{\partial h}{\partial x_1} f_1 + \ldots + \frac{\partial h}{\partial x_n} f_n$$
(2.34)

Lemma 2.5.1. *[71] Sufficient conditions for existence of a transformation from system (2.30) into the observable form (2.27) are as follows*

$$Rank(\frac{\partial \phi}{\partial x}) = n$$
(2.35)

where

$$\phi = \begin{bmatrix} h \\ L_f h \\ . \\ . \\ . \\ . \\ L_f^{n-1} h \end{bmatrix} \tag{2.36}$$

and there must exist a vector τ such that

$$\frac{\partial \phi}{\partial x} \tau = b \tag{2.37}$$

with

$$b = \begin{bmatrix} 0 & 0 & . & . & . & 1 \end{bmatrix}^T \tag{2.38}$$

and τ must satisfy

$$\begin{cases} [ad_f^i \tau, ad_f^j \tau] = 0, 0 \leqslant i, j \leqslant n-1 \\ [g, ad_f^j \tau] = 0, 0 \leqslant j \leqslant n-2 \end{cases}$$

For the system defined in (2.26) which is linear in the input, $[g, ad_f^j \tau]$ is equivalent to $[B, ad_f^j \tau]$ and is calculated as follows

$$[B, ad_f^j \tau] = \frac{\partial (ad_f^j \tau)}{\partial x} B \tag{2.39}$$

Normally, it is very difficult to satisfy the conditions for existence of such transformations. In addition, if the transformation exists it is not easy to calculate the transformation and transform the system into the observable form.

- **Sliding Mode Observers**

The structure of the sliding mode observer is very similar to the standard full-order Luenberger observer with replacement of the linear innovation term (linear function of the difference between the estimated output and the measured output) by a discontinuous function. Two commonly used discontinuous functions in sliding mode observer design

are the *sign* function and the *saturation* function. Due to occurrence of chattering in the systems the saturation function is preferable to the sign function. Consider the following system [89]

$$
\begin{aligned}
\dot{x}_1^i &= x_2^i + b_1^i(y, u) \\
&\vdots \\
\dot{x}_{q_i-1}^i &= x_{q_i}^i + b_{q_i-1}^i(x_2^i, \ldots, x_{q_i-1}^i, y, u) \\
\dot{x}_{q_i}^i &= a_i(x_d, x_0) + b_{q_i}^i(x_d, x_0, u)
\end{aligned}
\tag{2.40}
$$

where i denotes the ith subsystem of a nonlinear system, q_i is the size of the ith subsystem and x_d is a vector containing $(x_1, \ldots x_{q_i})$ states of the ith subsystem of the nonlinear system.

Lemma 2.5.2. *[89] For the system defined in (2.40) the following sliding mode observer can be designed*

$$
\begin{aligned}
\dot{\hat{x}}_1^i &= \hat{x}_2^i + b_1^i(y, u) + \lambda_1^i sign(\overline{e_1^i}) \\
\dot{\hat{x}}_2^i &= \hat{x}_3^i + b_2^i(\hat{x}_2^i, y, u) + \lambda_2^i sign(\overline{e_2^i}) \\
&\vdots \\
\dot{\hat{x}}_{q_i-1}^i &= \hat{x}_{q_i}^i + b_{q_i-1}^i(\hat{x}_2^i, \ldots, \hat{x}_{q_i-1}^i, y, u) + \lambda_{q_i-1}^i sign(\overline{e_{q_i-1}^i}) \\
\dot{\hat{x}}_{q_i}^i &= a_i(\hat{x}_d, \hat{x}_0) + b_{q_i}^i(\hat{x}_d, \hat{x}_0, u) + \lambda_{q_i}^i sign(\overline{e_{q_i}^i})
\end{aligned}
\tag{2.41}
$$

where

$$
\overline{e_j^i} = (\lambda_{j-1}^i sign(\overline{e_{j-1}^i}))
\tag{2.42}
$$

for $j = 2, \ldots, q$ and

$$
\overline{e_1^i} = e_1^i = y_i - \hat{x}_1^i
\tag{2.43}
$$

where, $\lambda_{q_i}^i$ are large enough scalars.

Proof. See [89]. □

For the system defined in (2.26) which is linear in the input, (2.40) can be rewritten

as follows

$$
\begin{bmatrix} \dot{x}^i_1 \\ \dot{x}^i_2 \\ \vdots \\ \dot{x}^i_{q_i-1} \\ \dot{x}^i_{q_i} \end{bmatrix} = \begin{bmatrix} 0 & 1 & \ldots & \ldots & 0 \\ 0 & 0 & 1 & \ldots & 0 \\ \vdots & & & & \vdots \\ 0 & \ldots & \ldots & 0 & 1 \\ 0 & \ldots & \ldots & \ldots & 0 \end{bmatrix} \begin{bmatrix} x^i_1 \\ x^i_2 \\ \vdots \\ x^i_{q_i-1} \\ x^i_{q_i} \end{bmatrix} + \begin{bmatrix} b^i_1(y) \\ b^i_2(x^i_2,y) \\ \vdots \\ b^i_{q_i-1}(x^i_2,...,x^i_{q_i-1},y) \\ a^i_{q_i}(\hat{x}_d) + b^i_{q_i}(x_d,y) \end{bmatrix} + Bu \qquad (2.44)
$$

for which an observer can be designed with the following structure

$$
\begin{bmatrix} \dot{\hat{x}}^i_1 \\ \dot{\hat{x}}^i_2 \\ \vdots \\ \dot{\hat{x}}^i_{q_i-1} \\ \dot{\hat{x}}^i_{q_i} \end{bmatrix} = \begin{bmatrix} 0 & 1 & \ldots & \ldots & 0 \\ 0 & 0 & 1 & \ldots & 0 \\ \vdots & & & & \vdots \\ 0 & \ldots & \ldots & 0 & 1 \\ 0 & \ldots & \ldots & \ldots & 0 \end{bmatrix} \begin{bmatrix} \hat{x}^i_1 \\ \hat{x}^i_2 \\ \vdots \\ \hat{x}^i_{q_i-1} \\ \hat{x}^i_{q_i} \end{bmatrix} + \begin{bmatrix} b^i_1(y) \\ b^i_2(\hat{x}^i_2,y) \\ \vdots \\ b^i_{q_i-1}(\hat{x}^i_2,...,\hat{x}^i_{q_i-1},y) \\ a^i_{q_i}(\hat{x}_d) + b^i_{q_i}(\hat{x}_d,y) \end{bmatrix} +
$$

$$
\begin{bmatrix} \lambda^i_1 sign(\overline{e^i_1}) \\ \lambda^i_2 sign(\overline{e^i_2}) \\ \vdots \\ \lambda^i_{q_i-1} sign(\overline{e^i_{q_i-1}}) \\ \lambda^i_{q_i} sign(\overline{e^i_{q_i}}) \end{bmatrix} + Bu
$$

$$(2.45)$$

The WMR example can be rewritten such that its subsystems are in the form of (2.44).

- **Backstepping Observers**

To design a backstepping observer according to [108], the nonlinear system needs to be broken into state affine single output subsystems in the following form

$$
\dot{x}_1 = a_1(u,y)x_2 + b_1(u,x_1)
$$

$$\vdots$$

$$
\dot{x}_{n-1} = a_{n-1}(u,y)x_n + b_{n-1}(u,x_1,...x_{n-1}) \qquad (2.46)
$$

$$
\dot{x}_n = f_n(x) + b_n(u,x)
$$

$$
y = x_1
$$

An observer must be designed for each subsystem independently.

Lemma 2.5.3. *[108] The following backstepping observer can be designed to estimate the*
states of the system defined in (2.46)

$$\dot{\hat{x}}_1 = a_1(u,y)\hat{x}_2 + b_1(u,\hat{x}_1) + \phi_1(\hat{x})(y - \hat{x}_1)$$

$$\cdots$$

$$\dot{\hat{x}}_{n-1} = a_{n-1}(u,y)\hat{x}_n + b_{n-1}(u,\hat{x}_1,\ldots\hat{x}_{n-1}) + \phi_{n-1}(\hat{x})(y - \hat{x}_1) \qquad (2.47)$$

$$\dot{\hat{x}}_n = f_n(\hat{x}) + b_n(u,\hat{x}) + \phi_n(\hat{x})(y - \hat{x}_1)$$

where

$$\phi_i = \frac{g_{n+1,n-i+1}}{K_{n-i}K_{i-1}} + \frac{K_{n-1}}{K_{i-1}K_{n-i}}\left(\frac{\partial f_n}{\partial \hat{x}_{n-i+1}}\right) \qquad (2.48)$$

for $i = 1,\ldots,n$

    and

$$K_r = \prod_{i=0}^{r} a_i \qquad (2.49)$$

with $a_0 = 1$.

The formulas to obtain $g_{i,j}$ for different values of i and j can be found in the Appendix.

Proof. See [108]. $\qquad\qquad\qquad\qquad\qquad\qquad\qquad\qquad\qquad\qquad\qquad\qquad\square$

For the system defined in (2.26) which is linear in the input, (2.46) can be rewritten
as follows

$$
\begin{bmatrix} \dot{x}_1 \\ \dot{x}_2 \\ \vdots \\ \dot{x}_{n-1} \\ \dot{x}_n \end{bmatrix} =
\begin{bmatrix}
0 & a_1(y) & \cdots & \cdots & 0 \\
0 & 0 & a_2(y) & \cdots & 0 \\
\vdots & & & & \vdots \\
0 & \cdots & \cdots & 0 & a_{n-1}(y) \\
0 & \cdots & \cdots & \cdots & 0
\end{bmatrix}
\begin{bmatrix} x_1 \\ x_2 \\ \vdots \\ x_{n-1} \\ x_n \end{bmatrix} +
\begin{bmatrix} b_1(y) \\ b_2(x_2,y) \\ \vdots \\ b_{n-1}(x_2,\ldots,x_{n-1},y) \\ f_n(x) + b_n(x,y) \end{bmatrix} + Bu
$$

$$(2.50)$$

for which an observer can be designed with the following structure

$$
\begin{bmatrix} \dot{\hat{x}}_1 \\ \dot{\hat{x}}_2 \\ \vdots \\ \dot{\hat{x}}_{n-1} \\ \dot{\hat{x}}_n \end{bmatrix} = \begin{bmatrix} 0 & a_1(y) & \ldots & \ldots & 0 \\ 0 & 0 & a_2(y) & \ldots & 0 \\ \vdots & & & & \vdots \\ 0 & \ldots & \ldots & 0 & a_{n-1}(y) \\ 0 & \ldots & \ldots & \ldots & 0 \end{bmatrix} \begin{bmatrix} \hat{x}_1 \\ \hat{x}_2 \\ \vdots \\ \hat{x}_{n-1} \\ \hat{x}_n \end{bmatrix} + \begin{bmatrix} b_1(y) \\ b_2(\hat{x}_2,y) \\ \vdots \\ b_{n-1}(\hat{x}_2,...,\hat{x}_{n-1},y) \\ f_n(\hat{x}) + b_n(\hat{x},y) \end{bmatrix} +
$$

$$
\begin{bmatrix} \phi_1(\hat{x})(y-\hat{x}_1) \\ \phi_2(\hat{x})(y-\hat{x}_1) \\ \vdots \\ \phi_{n-1}(\hat{x})(y-\hat{x}_1) \\ \phi_n(\hat{x})(y-\hat{x}_1) \end{bmatrix} + Bu
$$

(2.51)

The WMR model can be broken into single-output subsystems in the form of (2.50) in order to design a backstepping observer based on Lemma 2.5.3.

- **High-Gain Observers**

Consider the following system

$$
\dot{x} = Ax + \beta \phi(x,z,u)
$$
$$
\dot{z} = \psi(x,z,u)
$$
$$
y = Cx
$$
$$
\zeta = q(x,z)
$$

(2.52)

where $u \in R^P$ is the input, $y \in R^m$ and $\zeta \in R^s$ are measured outputs, $x \in R^P$ and $z \in R^l$ are state vectors and

$$
A = \text{block diag}[A_1,...,A_m], A_i = \begin{bmatrix} 0 & 1 & \ldots & \ldots & 0 \\ 0 & 0 & 1 & \ldots & 0 \\ \vdots & & & & \vdots \\ 0 & \ldots & \ldots & 0 & 1 \\ 0 & \ldots & \ldots & \ldots & 0 \end{bmatrix}_{\rho_i \times \rho_i}
$$

(2.53)

31

$$\beta = \text{block diag}[\beta_1,...,\beta_m], \beta_i = \begin{bmatrix} 0 \\ 0 \\ \vdots \\ 0 \\ 1 \end{bmatrix}_{\rho_i \times 1} \tag{2.54}$$

$$C = \text{block diag}[C_1,...,C_m], C_i = \begin{bmatrix} 1 & 0 & \dots & \dots & 0 \end{bmatrix}_{1 \times \rho_i} \tag{2.55}$$

where $1 \leqslant i \leqslant m$ and $\rho = \rho_1 + ... + \rho_m$ represents m chains of integrators.

Lemma 2.5.4. *[110] In order to estimate the states of the system defined in (2.52) a high-gain observer with the following structure can be designed*

$$\dot{\hat{x}} = A\hat{x} + \beta \phi_0(\hat{x}, \zeta, u) + H(y - C\hat{x}) \tag{2.56}$$

where

$$H = \text{block diag}[H_1,...,H_m], H_i = \begin{bmatrix} \frac{\alpha_1^i}{\varepsilon} \\ \frac{\alpha_2^i}{\varepsilon^2} \\ \dots \\ \frac{\alpha_{\rho_i-1}^i}{\varepsilon^{\rho_i-1}} \\ \frac{\alpha_{\rho_i}^i}{\varepsilon^{\rho_i}} \end{bmatrix}_{\rho_i \times 1} \tag{2.57}$$

The positive constants α_j^i are chosen such that the roots of

$$S^{\rho_i} + \alpha_1^i S^{\rho_i-1} + ... + \alpha_i^{\rho_i-1} S + \alpha_{\rho_j}^i = 0 \tag{2.58}$$

are in the left half-plane for all $i = 1,...,m$ and $\phi_0(x,\zeta,u)$ is a nominal model of $\phi(x,z,u)$. Furthermore, $\phi(x,z,u)$ must be locally Lipschitz in its arguments and globally bounded in x.

Proof. See [110]. □

For the system defined in (2.26) which is linear in the input, (2.52) can be rewritten as follows

$$\dot{x} = Ax + \beta \phi(x, z) + B_1 u$$

$$\dot{z} = \psi(x, z) + B_2 u$$

$$y = Cx \tag{2.59}$$

$$\zeta = q(x, z)$$

where

$$B = \begin{bmatrix} B_1 \\ B_2 \end{bmatrix} \tag{2.60}$$

For the system defined in (2.59) a high-gain observer can be designed with the following structure

$$\dot{\hat{x}} = A\hat{x} + \beta \phi_0(\hat{x}, \zeta) + B_1 u + H(y - C\hat{x}) \tag{2.61}$$

According to Lemma 2.5.4 a high-gain observer can be designed for the nonlinear model of the WMR.

- **Interconnected Observers**

Another approach to design observers for nonlinear systems is to design interconnected observers. Sometimes a system is not in the form for which an observer is available but it can be seen as an interconnection between several subsystems for which an observer can be designed. Then, an observer for each subsystem will be designed. This is shown in Figure 2.4, taken from [1], for a system broken into two subsystems, where Σ_i denotes the ith subsystem for which the observer O_i is designed.

In Chapter 3 also an interconnected observer is designed for the WMR model.
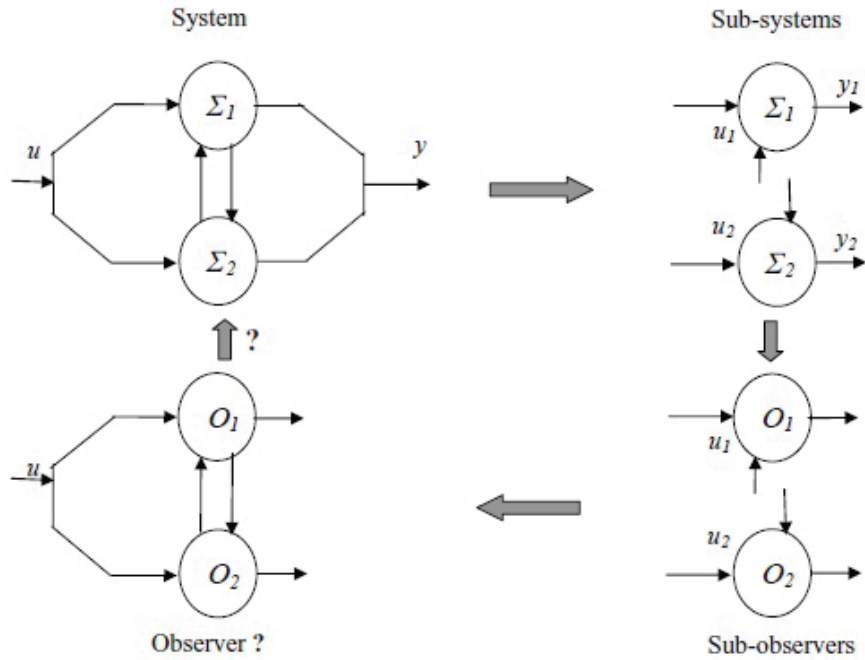
Figure 2.4: Interconnected observers (taken from [1]).

2.6 Summary

In this chapter some general concepts of PWA systems, PWA observer design and some definitions on boundedness and ultimate boundedness are provided. Furthermore, nonlinear observer design techniques are reviewed. This background material will be used in the rest of the thesis.

Chapter 3

Piecewise-Affine Observer Design for a Class of Nonlinear Systems

3.1 Introduction

In this chapter the design of PWA observers for a class of nonlinear systems with a sampled output is studied. The problem of observer design is solved through a convex optimization approach in terms of LMIs. The state estimation error is shown to be ultimately bounded and convergent to a region when a continuous-time PWA observer is applied to a nonlinear system with a sampled output. The state estimation error converges to a region and the size of the region depends on the sampling time and the PWA approximation error. As the sampling time and/or the PWA approximation error decrease, the size of the region decreases. The proof of convergence is broken in two parts. First, the continuous-time PWA observer is applied to the nonlinear continuous-time system and it is proven that the state estimation error is ultimately bounded where the bound is proportional to the upper bound on the PWA approximation error. Then, it is shown that the state estimation error is still convergent when the continuous-time PWA observer is used for state estimation of the nonlinear sampled-data system. Being interested in studying stability of the state estimation error for

sampled-data systems arises from the fact that in real applications the observer is implemented in a computer and the output is only available at sampling instants. Furthermore, stability of the state estimation error in the presence of norm bounded measurement noise is studied in this chapter.

This chapter is organized as follows. In Section 3.2, a class of nonlinear systems and their PWA approximation are represented. Then, the observer which guarantees exponential stability of the state estimation error for the continuous-time PWA approximation of the nonlinear system is presented. Moreover, stability of the state estimation error when the proposed observer is used for state estimation of the nonlinear continuous-time system is studied in Section 3.2. Section 3.3 provides the results on stability of the state estimation error when the observer is applied to the nonlinear system with a sampled output. Then, the results independent of the sampling time and dependent on the sampling time are presented in Section 3.3. In Section 3.4 stability of the state estimation error for the nonlinear system with a sampled output in the presence of norm bounded measurement noise is studied. Section 3.5 contains some numerical examples and simulation results to show the application of the main results. The chapter is closed by a summary and conclusions.

3.2 Piecewise-Affine Observer Design for a Class of Nonlinear Continuous-Time Systems

The following class of nonlinear systems is considered

$$\dot{x}(t) = f(x) + Bu(t)$$
$$y(t) = Cx(t)$$

(3.1)

where $f(x)$ is smooth and nonlinear in one of the states, $x(t) \in R^n$ is the state vector, $u(t) \in R^k$ is the input, $y(t) \in R^l$ is the measured output, B and C are real matrices with appropriate dimensions. In other words, $f(x)$ has the following structure

$$f(x) = \bar{A}x + \bar{f}(x_z)$$

(3.2)

where $\bar{A}$ is a real matrix with appropriate dimensions, $\bar{f}(x_z)$ is the nonlinear term and x_z is the state number z of the system (3.1).

Remark 3.2.1. *Although the class of functions in (3.1) is not the most general form of nonlinear systems, many real systems can be modeled in this form. Some examples of this class of systems are autonomous land vehicles [20], rotorcraft unmanned aerial vehicles [21] and a helicopter pitch model [19].*

To design observers for the system defined in (3.1) a PWA approximation of the form (3.3) is obtained (see [21] for an algorithm to obtain the PWA model),

$$\dot{x}(t) = A_i x(t) + Bu(t) + b_i$$
$$y(t) = Cx(t)$$

(3.3)

for $x \in R_i$, where R_i with $i = 1,..,q$ are slabs and defined as

$$R_i = \{x | d_i < H^T x < d_{i+1}\}$$

(3.4)

or equivalently

$$R_i = \{x | \|E_i x + f_i\| < 1\}$$

(3.5)

where H is a vector of zeros except for one element corresponding to the state x_z that represents the nonlinearity of the system and

$$E_i = \frac{2H^T}{d_{i+1} - d_i}$$

(3.6)

and

$$f_i = \frac{-(d_{i+1} + d_i)}{d_{i+1} - d_i}$$

(3.7)

The PWA observer has the structure as follows [35]

$$\dot{\hat{x}}(t) = A_j \hat{x}(t) + Bu(t) + b_j + L_j C(x(t) - \hat{x}(t))$$
$$\hat{y}(t) = C\hat{x}(t)$$

(3.8)

for $\hat{x} \in R_j$, where L_j, $j = 1,...,q$ are the observer gains.

37

The state estimation error is defined as

$$e(t) = x(t) - \hat{x}(t) \tag{3.9}$$

To show stability of the state estimation error the S-procedure [174], as presented in Lemma 2.3.1, will be used. As explained in Section 2.3, the S-procedure is applied in regions whose projection in the $x_z, \hat{x}_z$ plane are circles.

Before presenting the main results a lemma will be stated. Lemma 3.2.1 is a modified version of the theorem presented in [36] for bimodal PWA systems, where also the S-procedure has been used in a different way. Note that, prior to designing the PWA observer, observability of the PWA system should be checked using the proposed theorems on observability of PWA and hybrid systems [175, 176, 177, 167]. In order to have an observable PWA system the following observability matrices must have full rank.

$$O_i = \begin{bmatrix} C \\ CA_i \\ \vdots \\ CA_i^{n-1} \end{bmatrix} \tag{3.10}$$

$$O_{ij} = \begin{bmatrix} C \\ CA_j \\ CA_iA_j \end{bmatrix} \tag{3.11}$$

for $i, j = 1, ..., q$. Equation (3.10) is regarding the observability of the system in R_i and (3.11) refers to the observability of the system when it goes from R_i to R_j.

Lemma 3.2.1. *For a given $\alpha > 0$ the state estimation error defined in (3.9) regarding the system (3.3) and the observer defined in (3.8), is exponentially stable with a rate of at least α, if there exist $P > 0$, $\lambda_{ij} < 0$ and Y_j with $i, j = 1, ..., q$ verifying*

• for $i = j$

$$A_j^T P - C^T Y_j^T + PA_j - Y_j C + \alpha P \leqslant 0 \tag{3.12}$$

- *for $i \neq j$*

$$\begin{bmatrix} A_j^T P - C^T Y_j^T + PA_j - Y_j C + \alpha P + \lambda_{ij} HH^T & PA_{ij} - \lambda_{ij} HH^T & Pb_{ij} + \lambda_{ij}\beta_j H \\ A_{ij}^T P - \lambda_{ij} HH^T & 2\lambda_{ij} HH^T & -\lambda_{ij}(\beta_j + \gamma_i)H \\ b_{ij}^T P + \lambda_{ij}\beta_j H^T & -\lambda_{ij}(\beta_j + \gamma_i)H^T & \lambda_{ij}(\gamma_i^2 + \beta_j^2 - r_{ij}^2) \end{bmatrix} \leqslant 0$$

(3.13)

where γ_i, β_j and r_{ij} are defined in (2.14), (2.15) and (2.16), respectively and

$$A_{ij} = A_i - A_j \tag{3.14}$$

$$b_{ij} = b_i - b_j \tag{3.15}$$

The observer gains can be obtained by

$$L_j = P^{-1}Y_j \tag{3.16}$$

Proof. According to (3.9) the dynamics of the state estimation error for the system and the observer defined in (3.3) and (3.8) is

$$\dot{e}(t) = (A_j - L_j C)e(t) + (A_i - A_j)x(t) + b_i - b_j \tag{3.17}$$

for $x \in R_i$, $\hat{x} \in R_j$. Equation (3.17) is equivalent to

$$\dot{e}(t) = (A_j - L_j C)e(t) + A_{ij}x(t) + b_{ij} \tag{3.18}$$

where A_{ij} and b_{ij} are defined in (3.14) and (3.15), respectively.

To show stability of the state estimation error the following candidate Lyapunov function is considered.

$$V(t) = e(t)^T Pe(t) \tag{3.19}$$

where $P > 0$. Then, for exponential stability of the state estimation error with a rate of at least $\alpha > 0$, it is sufficient to show

$$\dot{V} = \dot{e}(t)^T Pe(t) + e(t)^T P\dot{e}(t) \leqslant -\alpha e(t)^T Pe(t) \tag{3.20}$$

• for $i = j$

Equation (3.18) leads to

$$\dot{e}(t) = (A_j - L_j C)e(t) \tag{3.21}$$

Replacing (3.21) in (3.20) and substituting $PL_j = Y_j$ in order to have a convex problem yields

$$A_j^T P - C^T Y_j^T + PA_j - Y_j C + \alpha P \leqslant 0 \tag{3.22}$$

which is equivalent to (3.12).

• for $i \neq j$

Replacing (3.18) in (3.20) and writing in matrix form yields the following matrix inequality for $x \in R_i, \hat{x} \in R_j$

$$\begin{bmatrix} e(t) \\ x(t) \\ 1 \end{bmatrix}^T \begin{bmatrix} A_j^T P - C^T L_j^T P + PA_j - PL_j C + \alpha P & PA_{ij} & Pb_{ij} \\ A_{ij}^T P & 0_{n \times n} & 0_{n \times 1} \\ b_{ij}^T P & 0_{1 \times n} & 0 \end{bmatrix} \begin{bmatrix} e(t) \\ x(t) \\ 1 \end{bmatrix} \leqslant 0 \tag{3.23}$$

In order to have a convex problem, all the elements of (3.23) must be linear functions. Therefore, $PL_j = Y_j$ is substituted in (3.23), which leads to

$$\begin{bmatrix} e(t) \\ x(t) \\ 1 \end{bmatrix}^T \begin{bmatrix} A_j^T P - C^T Y_j^T + PA_j - Y_j C + \alpha P & PA_{ij} & Pb_{ij} \\ A_{ij}^T P & 0_{n \times n} & 0_{n \times 1} \\ b_{ij}^T P & 0_{1 \times n} & 0 \end{bmatrix} \begin{bmatrix} e(t) \\ x(t) \\ 1 \end{bmatrix} \leqslant 0 \tag{3.24}$$

Recalling ε_{ij} from Chapter 2,

$$\varepsilon_{ij} = \{x, \hat{x} | \| H^T x - \gamma_i \|^2 + \| H^T \hat{x} - \beta_j \|^2 \leqslant r_{ij}^2 \} \tag{3.25}$$

for $x \in \varepsilon_{ij}$ Equation (3.25) can be rewritten in matrix form as

$$\begin{bmatrix} e(t) \\ x(t) \\ 1 \end{bmatrix}^T \begin{bmatrix} HH^T & -HH^T & \beta_j H \\ -HH^T & 2HH^T & -\beta_j H - \gamma_i H \\ \beta_j H^T & -\beta_j H^T - \gamma_i H^T & \gamma_i^2 + \beta_j^2 - r_{ij}^2 \end{bmatrix} \begin{bmatrix} e(t) \\ x(t) \\ 1 \end{bmatrix} \leqslant 0 \tag{3.26}$$

40

Using Lemma 2.3.1, Equations (3.24), (3.26) and relaxing $R_i \times R_j$ to ε_{ij} leads to

$$
\begin{bmatrix} A_j^T P - C^T Y_j^T + PA_j - Y_j C + \alpha P & PA_{ij} & Pb_{ij} \\ A_{ij}^T P & 0_{n \times n} & 0_{n \times 1} \\ b_{ij}^T P & 0_{1 \times n} & 0 \end{bmatrix} \leqslant
$$

$$
- \lambda_{ij} \begin{bmatrix} HH^T & -HH^T & \beta_j H \\ -HH^T & 2HH^T & -\beta_j H - \gamma_i H \\ \beta_j H^T & -\beta_j H^T - \gamma_i H^T & \gamma_i^2 + \beta_j^2 - r_{ij}^2 \end{bmatrix}
$$

(3.27)

where $\lambda_{ij} < 0$ for $i, j = 1, ..., q$ are scalars. Equation (3.27) is equivalent to (3.13). $\qquad\square$

Remark 3.2.2. *For the circles containing the origin the S-procedure cannot be used. Such cases can only happen when $i = j$. According to Lemma 3.2.1, Equation (3.12) which does not include the S-procedure is used for such cases.*

3.2.1 Stability of the State Estimation Error for the Nonlinear Continuous-Time System

The proposed observer defined in (3.8) with the gains that are obtained from Lemma 3.2.1 is now applied to the nonlinear continuous-time system defined in (3.1). Theorem 3.2.1 provides a result on stability of the state estimation error.

Theorem 3.2.1. *Let*

$$
\delta_{app_i} = f(x) - A_i x - b_i \tag{3.28}
$$

be the PWA approximation error for $x \in R_i$, $\chi_P = \frac{\sigma_{max}(P)}{\sigma_{min}(P)}$ be the condition number of matrix P with $\sigma_{max}(P)$ and $\sigma_{min}(P)$ the maximum and minimum eigenvalues of matrix P, respectively. Assume that there is a solution to the design problem from Lemma 3.2.1. For any $0 < \theta < 1$ define

$$
\mu_\theta = \frac{2 \| \delta_{app_i} \| \chi_P^{\frac{3}{2}}}{\alpha \theta} \tag{3.29}
$$

41

When the PWA observer obtained from Lemma 3.2.1 is applied to the nonlinear continuous-time system defined in (3.1), the state estimation error is globally uniformly ultimately bounded by μ_θ and the trajectories of the state estimation error converge to the set

$$\Omega = \{e | V(e) \leqslant \sigma_{max}(P)v^2\} \tag{3.30}$$

where

$$v = \mu_\theta \chi_P^{-\frac{1}{2}} \tag{3.31}$$

Proof. Using (3.1), (3.8) and (3.9) the dynamics of the state estimation error is as follows

$$\dot{e}(t) = (A_j - L_j C)e(t) + (f(x) - A_j x - b_j) \tag{3.32}$$

for $\hat{x} \in R_j$. Equation (3.32) can be rewritten as

$$\dot{e}(t) = (A_j - L_j C)e(t) + A_{ij}x(t) + b_{ij} + \delta_{app_i} \tag{3.33}$$

for $x \in R_i$, $\hat{x} \in R_j$, where A_{ij}, b_{ij} and δ_{app_i} are defined in (3.14), (3.15) and (3.28), respectively.

- for $i = j$

Equation (3.33) is equivalent to

$$\dot{e}(t) = (A_j - L_j C)e(t) + \delta_{app_i} \tag{3.34}$$

Replacing (3.34) in the derivative of the candidate Lyapunov function defined in (3.19) and using matrix $P > 0$ and observer gains that are designed by (3.12) and calculated by (3.16) yields

$$\dot{V} = e(t)^T [A_j^T P - C^T Y_j^T + PA_j - Y_j C]e(t) + 2e(t)^T P\delta_{app_i} \tag{3.35}$$

- for $i \neq j$

Replacing (3.33) in the derivative of the candidate Lyapunov function defined in (3.19) and using matrix $P > 0$ and observer gains that are designed by (3.13) and calculated

42

by (3.16) yields

$$\dot{V} = \begin{bmatrix} e(t) \\ x(t) \\ 1 \end{bmatrix}^T \begin{bmatrix} A_j^T P - C^T Y_j^T + PA_j - Y_j C & PA_{ij} & Pb_{ij} \\ A_{ij}^T P & 0_{n \times n} & 0_{n \times 1} \\ b_{ij}^T P & 0_{1 \times n} & 0 \end{bmatrix} \begin{bmatrix} e(t) \\ x(t) \\ 1 \end{bmatrix} + 2e(t)^T P\delta_{app_i} \quad (3.36)$$

The rest of the proof is the same for $i = j$ and $i \neq j$. Using Lemma 3.2.1, Equations (3.12) and (3.35) for $i = j$ and (3.24) and (3.36) for $i \neq j$ implies that

$$\dot{V} \leqslant -\alpha e^T P e + 2e^T P \delta_{app_i} \quad (3.37)$$

Since

$$-\alpha e^T(t) P e(t) \leqslant -\alpha \sigma_{min}(P) \| e \|^2 \quad (3.38)$$

and

$$2e^T P \delta_{app_i} \leqslant 2\sigma_{max}(P) \| e \| \| \delta_{app_i} \| \quad (3.39)$$

equation (3.37) can be rewritten as

$$\dot{V} \leqslant -\alpha \sigma_{min}(P) \| e \|^2 + 2\sigma_{max}(P) \| e \| \| \delta_{app_i} \| \quad (3.40)$$

For any $0 < \theta < 1$, adding and subtracting $\alpha \theta \sigma_{min}(P) \| e \|^2$ to (3.40) leads to

$$\dot{V} \leqslant -\alpha(1 - \theta) \sigma_{min}(P) \| e \|^2 - \alpha \theta \sigma_{min}(P) \| e \|^2 + 2\sigma_{max}(P) \| e \| \| \delta_{app_i} \| \quad (3.41)$$

If

$$-\alpha \theta \sigma_{min}(P) \| e \|^2 + 2\sigma_{max}(P) \| e \| \| \delta_{app_i} \| \leqslant 0 \quad (3.42)$$

or alternatively

$$\| e \| \geqslant \frac{2 \| \delta_{app_i} \| \chi_P}{\alpha \theta} \quad (3.43)$$

then (3.41) leads to

$$\dot{V} \leqslant -\alpha(1 - \theta) \sigma_{min}(P) \| e \|^2 \quad (3.44)$$

Since

$$V(e) \leqslant \sigma_{max}(P)\| e \|^2 \qquad (3.45)$$

therefore

$$-\alpha(1-\theta)\sigma_{min}(P)\| e \|^2 \leqslant -\alpha(1-\theta)\chi_P^{-1}V(e) \qquad (3.46)$$

then, (3.44) and (3.43) lead to

$$\dot{V} \leqslant -\alpha(1-\theta)\chi_P^{-1}V(e) \qquad (3.47)$$

Define

$$\Lambda = \{e| \| e \| \leqslant v\} \qquad (3.48)$$

where v is defined in (3.31). According to (3.47) for $e \in R^n \setminus \Lambda$

$$V(e(t)) \leqslant V(e(t_0))e^{-\alpha(1-\theta)\chi_P^{-1}(t-t_0)} \qquad (3.49)$$

Using $\sigma_{min}(P)\| e \|^2 \leqslant V(e) \leqslant \sigma_{max}(P)\| e \|^2$ and (3.49) it can be concluded that for $e \in R^n \setminus \Lambda$

$$\| e(t) \| \leqslant \| e(t_0) \| \chi_P^{\frac{1}{2}}e^{-0.5\alpha(1-\theta)\chi_P^{-1}(t-t_0)} \qquad (3.50)$$

Then according to (3.50) there will be a positive and finite time $t_1 > t_0$ for any $0 < \theta < 1$ such that $e(t_1) \in \Lambda$. Note that $\Lambda \subseteq \Omega$. This can be proved by contradiction. Assume that it is not true that $\Lambda \subseteq \Omega$. Then, there exists at least one $e_* \in \Lambda$ for which $e_*^T Pe_* > \sigma_{max}(P)v^2$, a contradiction because $e_*^T Pe_* \leqslant \sigma_{max}(P)v^2$ for $e_* \in \Lambda$. Since $\dot{V} \leqslant 0$ at the boundary of Ω, Ω is an invariant set for the state estimation error. Consequently, since $e(t_1) \in \Lambda \subseteq \Omega$, then $e(t) \in \Omega$ for all $t \geqslant t_1$ and all $0 < \theta < 1$.

Since for all $t \geqslant t_1$ and all $0 < \theta < 1$ we know that $e(t) \in \Omega$, then according to (3.30)

$$\sigma_{min}(P)\| e \|^2 \leqslant V(e) \leqslant \sigma_{max}(P)v^2 \qquad (3.51)$$

then, (3.51) leads to

$$\| e \| \leqslant \mu_\theta \forall t \geqslant t_1 \qquad (3.52)$$

with μ_θ defined in (3.29).

$$\square$$

Remark 3.2.3. *The size of the region to which the trajectories of the state estimation error converge decreases as the size of the PWA approximation error decreases.*

3.3 Piecewise-Affine Observer Design for a Class of Non-linear Sampled-Data Systems

In this part it is assumed that the output measurements are only available at sampling instants kT, where $T > 0$ is the sampling time. In other words

$$\dot{x}(t) = f(x) + Bu(t)$$
$$y(kT) = Cx(kT) \tag{3.53}$$

The observer now is described as

$$\dot{\hat{x}}(t) = A_j\hat{x}(t) + Bu(t) + b_j + L_jC(x(kT) - \hat{x}(t))$$
$$\hat{y}(t) = C\hat{x}(t) \tag{3.54}$$

The state estimation error dynamics for the continuous-time PWA observer applied to the nonlinear sampled-data system, based on (3.9), (3.53) and (3.54) is

$$\dot{e}(t) = (A_j - L_jC)e(t) + (f(x) - A_jx(t) - b_j) + L_jC(x(t) - x(kT)) \tag{3.55}$$

for $\hat{x} \in R_j$, which is equivalent to

- for $i = j$

$$\dot{e}(t) = (A_j - L_jC)e(t) + \delta_{app_i} + L_jC\bar{\delta}_{Samp} \tag{3.56}$$

- for $i \neq j$

$$\dot{e}(t) = (A_j - L_jC)e(t) + A_{ij}x(t) + b_{ij} + \delta_{app_i} + L_jC\bar{\delta}_{Samp} \tag{3.57}$$

for $x \in R_i$, $\hat{x} \in R_j$, where A_{ij}, b_{ij} and δ_{app_i} are defined in (3.14), (3.15) and (3.28), respectively, and $\bar{\delta}_{Samp}$ is the error due to the sampling defined as

$$\bar{\delta}_{Samp} = x(t) - x(kT) \tag{3.58}$$

Also,

$$\delta_{Samp} = L_j C \bar{\delta}_{Samp} \tag{3.59}$$

Stability of the state estimation error when the continuous-time PWA observer is applied to the nonlinear sampled-data system is studied in the following section.

3.3.1 Stability of the State Estimation Error for the Nonlinear Sampled-Data System

In what follows, two sets of conditions for stability of the state estimation error for the continuous-time PWA observer applied to the nonlinear sampled-data system are provided. In the first part the problem is discussed independently of the sampling time, whereas in the second part conditions dependent on the sampling time are provided for stability of the state estimation error.

Conditions Independent of the Sampling Time

In Theorem 3.3.1 it is stated that the state estimation error is ultimately bounded when the continuous-time PWA observer is applied to the nonlinear sampled-data system.

Theorem 3.3.1. *Let δ_{app_i} and δ_{samp} be as defined in (3.28) and (3.59), respectively, $\chi_P = \frac{\sigma_{max}(P)}{\sigma_{min}(P)}$ be the condition number of matrix P. Assume that there is a solution to the design problem from Lemma 3.2.1. For any $0 < \theta < 1$ define*

$$\eta_\theta = \frac{2(\| \delta_{app_i} \| + \| \delta_{samp} \|)\chi_P^{\frac{3}{2}}}{\alpha\theta} \tag{3.60}$$

When the PWA observer obtained from Lemma 3.2.1 is applied to the nonlinear sampled-data system, the state estimation error of the nonlinear sampled-data system defined in

46

(3.53) is globally uniformly ultimately bounded by η_θ and the trajectories of the state estimation error converge to the set

$$\Sigma = \{e|V(e) \leqslant \sigma_{max}(P)\zeta^2\} \tag{3.61}$$

where

$$\zeta = \eta_\theta \chi_P^{-\frac{1}{2}} \tag{3.62}$$

Proof. The proof of Theorem 3.3.1 is the same as the proof of Theorem 3.2.1 with $\| \delta_{app_i} \|$ replaced by $\| \delta_{app_i} \| + \| \delta_{samp} \|$ because

$$\| \delta_{app_i} + \delta_{samp} \| \leqslant \| \delta_{app_i} \| + \| \delta_{samp} \| \tag{3.63}$$

$\square$

Remark 3.3.1. *Applying the continuous-time PWA observer to the nonlinear sampled-data system, the state estimation error converges to a region and the size of the region depends on the sampling error and the PWA approximation error. The size of the region decreases as the PWA approximation error and/or the sampling error decrease. Since sampling error depends on the deviation of the continuous-time state from the last measured state during the sampling interval, changes in the size of the region after convergence of the state estimation error, depends on the changes of the state at each sampling interval. Though, the state estimation error is ultimately bounded with the bound presented in (3.60).*

Conditions Dependent on the Sampling Time

In Theorem 3.3.2 convergence of the state estimation error for the nonlinear sampled-data system with conditions dependent on the sampling time is discussed.

Theorem 3.3.2. *Let δ_{app_i} and δ_{samp} be as defined in (3.28) and (3.59), respectively, $\chi_P = \frac{\sigma_{max}(P)}{\sigma_{min}(P)}$ be the condition number of matrix P. Furthermore,*

$$A = max_{i=1,...,q} \| A_i \| \tag{3.64}$$

$$b = max_{i=1,...,q} \| b_i \| \tag{3.65}$$

$$\| B \| = \bar{B} \tag{3.66}$$

$$\| C \| = \bar{C} \tag{3.67}$$

$$\| u \| \leqslant U \tag{3.68}$$

$$L = max_{j=1,...,q} \| L_j \| \tag{3.69}$$

Assume that there is a solution to the design problem from Lemma 3.2.1. For any $0 < \theta < 1$

define

$$\rho_\theta = \frac{2\chi_P^{\frac{3}{2}}}{\alpha\theta}(\| \delta_{app_i} \| + L\bar{C}T[AX(k,T) + \bar{B}U + b]) \tag{3.70}$$

When the PWA observer obtained from Lemma 3.2.1 is applied to the nonlinear sampled-data system, the state estimation error is globally uniformly bounded by ρ_θ and the trajectories of the state estimation error converge to the set

$$\Pi = \{e | V(e) \leqslant \sigma_{max}(P)\xi^2\} \tag{3.71}$$

where

$$\xi = \rho_\theta \chi_P^{-\frac{1}{2}} \tag{3.72}$$

Proof. Integrating (3.3) for $t \in [kT, (k+1)T]$ yields [139]

$$x(t) - x(kT) = \int_{kT}^{t} A_i(\tau)x(\tau)d\tau + \int_{kT}^{t} B(\tau)u(\tau)d\tau + \int_{kT}^{t} b_i(\tau)d\tau \tag{3.73}$$

Equation (3.73) is rewritten as

$$\| x(t) - x(kT) \| \leqslant A \int_{kT}^{t} \| x(\tau) \| d\tau + (t - kT)[\bar{B}U + b] \tag{3.74}$$

Since all possible dynamics in a PWA system are affine, finite escape times cannot occur when the coefficients of each affine system are uniformly bounded and therefore there will be a finite constant

$$X(k,T) = sup_{kT \leqslant t \leqslant kT+T} \| x(t) \| \tag{3.75}$$

such that

$$\| x(t) \|_{kT \leqslant t \leqslant kT+T} \leqslant X(k,T) \tag{3.76}$$

For (3.74), the highest possible bound is the one corresponding to $t = (k+1)T$ which leads to

$$\| x(t) - x(kT) \| \leqslant ATX(k,T) + T[\bar{B}U + b] \tag{3.77}$$

On the other hand (3.59) leads to

$$\| \delta_{Samp} \| \leqslant L\bar{C} \| x(t) - x(kT) \| \tag{3.78}$$

Equations (3.77) and (3.78)

$$\| \delta_{Samp} \| \leqslant L\bar{C}(ATX(k,T) + T[\bar{B}U + b]) \tag{3.79}$$

which using the results of Theorem 3.3.1 leads to

$$\| e \| \leqslant \frac{2\chi_P^{\frac{3}{2}}}{\alpha\theta}(\| \delta_{app_i} \| + L\bar{C}T[AX(k,T) + \bar{B}U + b]) \tag{3.80}$$

$\square$

Remark 3.3.2. *The continuous-time PWA observer defined in (3.8) can be used for state estimation of the nonlinear sampled-data system defined in (3.53). The state estimation error converges to a region and the size of the region depends on the sampling time and the PWA approximation error. The size of the region decreases as the sampling time and/or the PWA approximation error decrease. This is illustrated in Figure 3.1.*
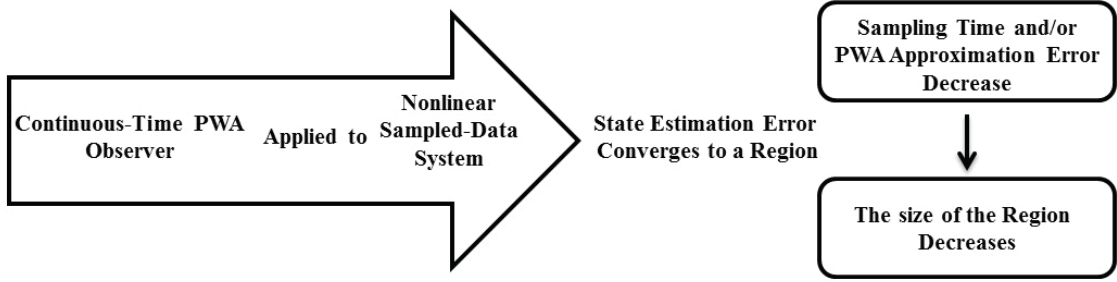
Figure 3.1: PWA Observer Design for a Class of Nonlinear Sampled-Data Systems.

3.4 Piecewise-Affine Observer Design for a Class of Nonlinear Sampled-Data Systems in the Presence of Norm Bounded Measurement Noise

In this part it is assumed that measurement noise exists in the nonlinear sampled-data system. The objective is to implement the continuous-time PWA observer that is designed for the noise free situation on the nonlinear sampled-data system in the presence of measurement noise.

The following structure is considered for the system

$$
\dot{x}(t) = f(x) + Bu(t)
$$
$$
y(kT) = Cx(kT) + v
$$
(3.81)

where v is the measurement noise and it is assumed to be norm bounded. In other words, the noise has a known upper bound.

For the system defined in (3.81) the PWA observer has the following structure

$$
\dot{\hat{x}}(t) = A_j\hat{x}(t) + Bu(t) + b_j + L_j(Cx(kT) + v - C\hat{x}(t))
$$
$$
\hat{y}(t) = C\hat{x}(t)
$$
(3.82)

In Theorem 3.4.1 it is shown that when the continuous-time PWA observer (3.82) is applied to the system defined in (3.81), the state estimation error is still convergent. In other words, the continuous-time PWA observer is robust to norm bounded measurement noise.

50

Theorem 3.4.1. *Let δ_{app_i} and δ_{samp} be as defined in (3.28) and (3.59), respectively, $\chi_P = \frac{\sigma_{max}(P)}{\sigma_{min}(P)}$ be the condition number of matrix P. Assume that there exists $\kappa > 0$ such that the noise term v from (3.81) satisfies $\| v \| < \kappa$. Suppose that there is a solution to the design problem from Lemma 3.2.1. For any $0 < \theta < 1$ define*

$$\vartheta_\theta = \frac{2(\| \delta_{app_i} \| + \| \delta_{samp} \| + L\kappa)\chi_P^{\frac{3}{2}}}{\alpha\theta} \tag{3.83}$$

When the PWA observer obtained from Lemma 3.2.1 is applied to the nonlinear sampled-data system in the presence of norm bounded measurement noise, the state estimation error is globally uniformly ultimately bounded by ϑ_θ and the trajectories of the state estimation error converge to the set

$$S = \{e|V(e) \leqslant \sigma_{max}(P)\phi^2\} \tag{3.84}$$

where

$$\phi = \vartheta_\theta \chi_P^{-\frac{1}{2}} \tag{3.85}$$

Proof. The dynamics of the state estimation error for the system defined in (3.81) and observer defined in (3.82) is as follows

$$\dot{e}(t) = (A_j - L_jC)e(t) + f(x) - A_jx - b_j + L_jC(x - x(kT)) - L_jv \tag{3.86}$$

for $\hat{x} \in R_j$, which is equivalent to

- for $i = j$

$$\dot{e}(t) = (A_j - L_jC)e(t) + \delta_{app_i} + \delta_{Samp} - L_jv \tag{3.87}$$

- for $i \neq j$

$$\dot{e}(t) = (A_j - L_jC)e(t) + A_{ij}x(t) + b_{ij} + \delta_{app_i} + \delta_{Samp} - L_jv \tag{3.88}$$

where A_{ij}, b_{ij}, δ_{app_i} and δ_{Samp} are defined in (3.14), (3.15), (3.28) and (3.59), respectively.

The following inequality is obtained for the derivative of the candidate Lyapunov function defined in (3.19) using Lemma 3.2.1, Equations (3.12) and (3.87) for $i = j$ and (3.24) and (3.88) for $i \neq j$

$$\dot{V} \leqslant -\alpha e^T P e + 2 e^T P \delta_{app_j} + 2 e^T P \delta_{Samp} - 2 e^T P L_j v \qquad (3.89)$$

Using (3.69) and

$$\| v \| < \kappa \qquad (3.90)$$

leads to

$$-2 e^T P L_j v \leqslant 2 \| e \| \sigma_{max}(P) L \kappa \qquad (3.91)$$

The rest of the proof is the same as the proof of Theorem 3.2.1 with $\| \delta_{app_i} \|$ replaced by $\| \delta_{app_i} \| + \| \delta_{samp} \| + L\kappa$.

$\square$

Remark 3.4.1. *The continuous-time PWA observer can be used for state estimation of the nonlinear sampled-data system with norm bounded measurement noise yielding a convergent state estimation error. The trajectories of the state estimation error converge to a region. The size of the region depends on the PWA approximation error, sampling time and the size of the bound on the norm of the noise.*

In Table 3.4 the results of the proposed theorems on ultimate bound of the state estimation error are compared.

System	Bound on the State Estimation Error
Nonlinear Continuous-Time System	$\dfrac{2\|\delta_{app_i}\|\chi_P^{\frac{3}{2}}}{\alpha\theta}$
Nonlinear Sampled-Data System (Independent of the Sampling Time)	$\dfrac{2(\|\delta_{app_i}\|+\|\delta_{samp}\|)\chi_P^{\frac{3}{2}}}{\alpha\theta}$
Nonlinear Sampled-Data System (Dependent on the Sampling Time)	$\dfrac{2\chi_P^{\frac{3}{2}}}{\alpha\theta}(\| \delta_{app_i} \| + L\bar{C}T[AX(k,T)+\bar{B}U+b])$
Nonlinear Sampled-Data System with Measurement Noise	$\dfrac{2(\|\delta_{app_i}\|+\|\delta_{samp}\|+L\kappa)\chi_P^{\frac{3}{2}}}{\alpha\theta}$
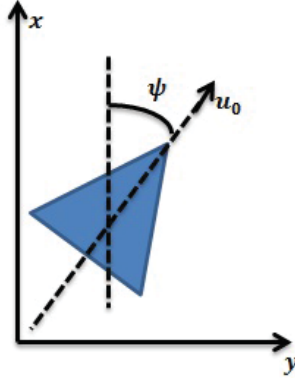
Figure 3.2: WMR schematic.

3.5 Numerical Example

In this section a numerical example with simulation results is provided to show the application of the main results.

Example 3.5.1. *Wheeled Mobile Robot (WMR):*

In this example a dynamical model of a WMR is presented [20, 125]. The nonlinear state space equations are

$$\dot{y} = u_0 \sin \psi$$

$$\dot{\psi} = R \tag{3.92}$$

$$\dot{R} = \frac{M}{I}$$

where ψ is the heading angle with time derivative R, y is the signed distance of the cart to the x axis and M is the torque and it is the input to the system. The constant velocity is $u_0 = 1\frac{m}{s}$ and the moment of inertia is $I = 1kg.m^2$. In Figure 3.2 the schematic model of the WMR is provided.

The system dynamics are described as

$$\begin{bmatrix} \dot{y} \\ \dot{\psi} \\ \dot{R} \end{bmatrix} = \begin{bmatrix} 0 & 0 & 0 \\ 0 & 0 & 1 \\ 0 & 0 & 0 \end{bmatrix} \begin{bmatrix} y \\ \psi \\ R \end{bmatrix} + \begin{bmatrix} \sin \psi \\ 0 \\ 0 \end{bmatrix} + \begin{bmatrix} 0 \\ 0 \\ 1 \end{bmatrix} M \tag{3.93}$$
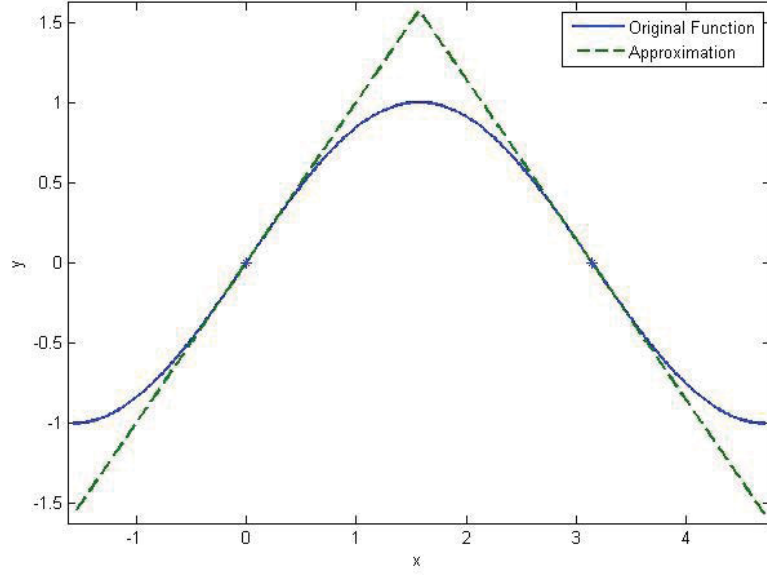
Figure 3.3: PWA approximation of "$\sin \psi$".

In this example the nonlinear term is $\sin \psi$ which is approximated for $\psi \in (-\frac{\pi}{2}, \frac{3\pi}{2})$ by two lines as illustrated in Figure 3.3. The bimodal PWA approximation of the system is obtained by the following state space partitioning [21]

$$R_1 = \{x \in R^3 | \psi \in (-\frac{\pi}{2}, \frac{\pi}{2})\} \tag{3.94}$$

$$R_2 = \{x \in R^3 | \psi \in (\frac{\pi}{2}, \frac{3\pi}{2})\} \tag{3.95}$$

as follows

$\forall x \in R_1$

$$\begin{bmatrix} \dot{y} \\ \dot{\psi} \\ \dot{R} \end{bmatrix} = \begin{bmatrix} 0 & 1 & 0 \\ 0 & 0 & 1 \\ 0 & 0 & 0 \end{bmatrix} \begin{bmatrix} y \\ \psi \\ R \end{bmatrix} + \begin{bmatrix} 0 \\ 0 \\ 0 \end{bmatrix} + \begin{bmatrix} 0 \\ 0 \\ 1 \end{bmatrix} M \tag{3.96}$$

$\forall x \in R_2$

$$\begin{bmatrix} \dot{y} \\ \dot{\psi} \\ \dot{R} \end{bmatrix} = \begin{bmatrix} 0 & -0.6366 & 0 \\ 0 & 0 & 1 \\ 0 & 0 & 0 \end{bmatrix} \begin{bmatrix} y \\ \psi \\ R \end{bmatrix} + \begin{bmatrix} 2 \\ 0 \\ 0 \end{bmatrix} + \begin{bmatrix} 0 \\ 0 \\ 1 \end{bmatrix} M \tag{3.97}$$

$$C = \begin{bmatrix} 1 & 0 & 0 \\ 0 & 1 & 0 \end{bmatrix} \tag{3.98}$$

In order to have an observable system the following observability matrices must have full rank.

$$O_1 = \begin{bmatrix} C \\ CA_1 \\ CA_1A_1 \end{bmatrix} = \begin{bmatrix} 1 & 0 & 0 \\ 0 & 1 & 0 \\ 0 & 1 & 0 \\ 0 & 0 & 1 \\ 0 & 0 & 1 \\ 0 & 0 & 0 \end{bmatrix} \tag{3.99}$$

$$O_2 = \begin{bmatrix} C \\ CA_2 \\ CA_2A_2 \end{bmatrix} = \begin{bmatrix} 1 & 0 & 0 \\ 0 & 1 & 0 \\ 0 & -0.6366 & 0 \\ 0 & 0 & 1 \\ 0 & 0 & -0.6366 \\ 0 & 0 & 0 \end{bmatrix} \tag{3.100}$$

$$O_{12} = \begin{bmatrix} C \\ CA_2 \\ CA_1A_2 \end{bmatrix} = \begin{bmatrix} 1 & 0 & 0 \\ 0 & 1 & 0 \\ 0 & -0.6366 & 0 \\ 0 & 0 & 1 \\ 0 & 0 & 1 \\ 0 & 0 & 0 \end{bmatrix} \tag{3.101}$$

55

$$O_{21} = \begin{bmatrix} C \\ CA_1 \\ CA_2A_1 \end{bmatrix} = \begin{bmatrix} 1 & 0 & 0 \\ 0 & 1 & 0 \\ 0 & 1 & 0 \\ 0 & 0 & 1 \\ 0 & 0 & -0.6366 \\ 0 & 0 & 0 \end{bmatrix} \qquad (3.102)$$

Since, O_1, O_2, O_{12} and O_{21} have full rank, the PWA system is observable.

The LMIs defined in Lemma 3.2.1 are solved using SeDuMi [171] and YALMIP [172] in MATLAB. By considering $\alpha = 4.041$ the following parameters are obtained,

$$L_1 = \begin{bmatrix} 625.6122 & -643.1309 \\ -12.4697 & 18.3164 \\ -35.1906 & 67.4576 \end{bmatrix} \qquad (3.103)$$

$$L_2 = \begin{bmatrix} 636.5618 & -643.3714 \\ -12.6996 & 18.3232 \\ -35.8737 & 67.5422 \end{bmatrix} \qquad (3.104)$$

The initial conditions are considered such that the system and the observer are in different regions at the initial time.

$$x_0 = \begin{bmatrix} 0.5 & \frac{3\pi}{4} & 0.1 \end{bmatrix}^T \qquad (3.105)$$

$$\hat{x}_0 = \begin{bmatrix} 0 & 0 & 0 \end{bmatrix}^T \qquad (3.106)$$

At first, the PWA observer is applied to the nonlinear continuous-time system. Figures 3.4, 3.5 and 3.6 show the estimation and the estimation errors of the position y, heading angle ψ and heading angle rate R, respectively. All the states are estimated correctly after a short time. In other words, state estimation errors have converged to zero after a few seconds.

Figure 3.7 illustrates the regions related to the PWA approximation in which the observer is operating. Table 3.1 summarizes the results of the state estimation for the nonlinear continuous-time system.
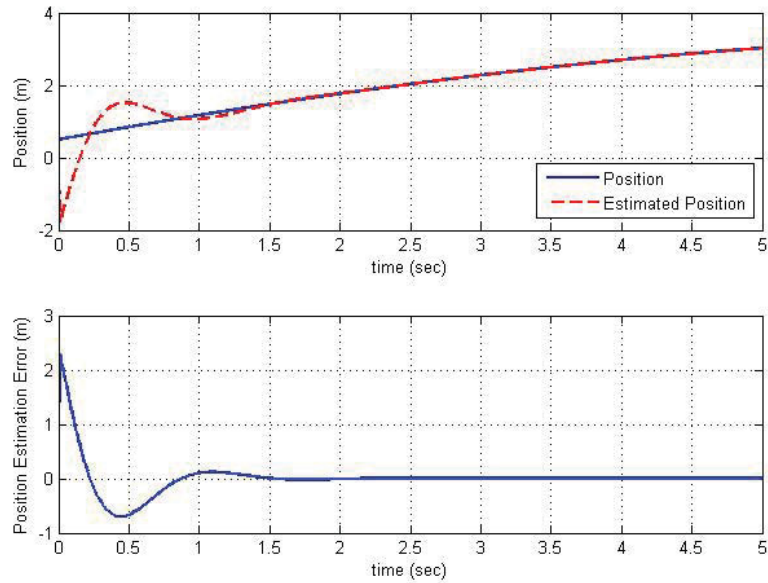
Figure 3.4: Estimation and estimation error of the position "*y*" of the nonlinear continuous-time system, using PWA observer.
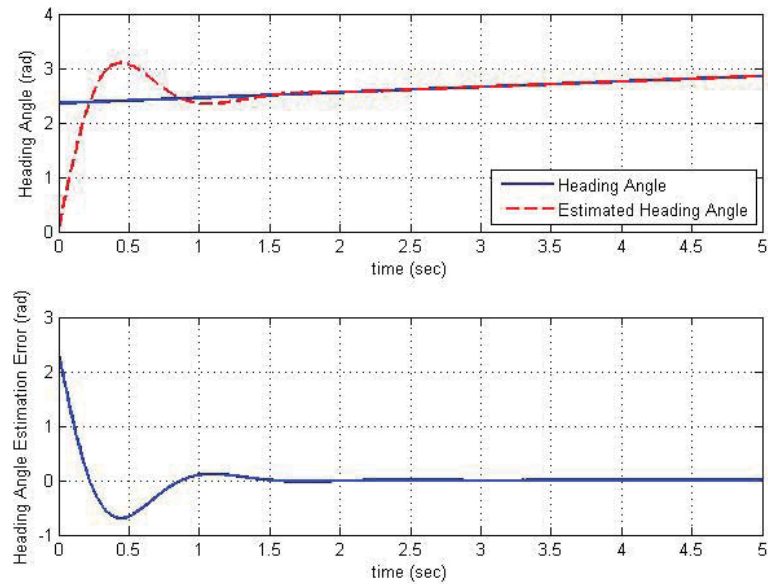
Figure 3.5: Estimation and estimation error of the heading angle "ψ" of the nonlinear continuous-time system, using PWA observer.

57
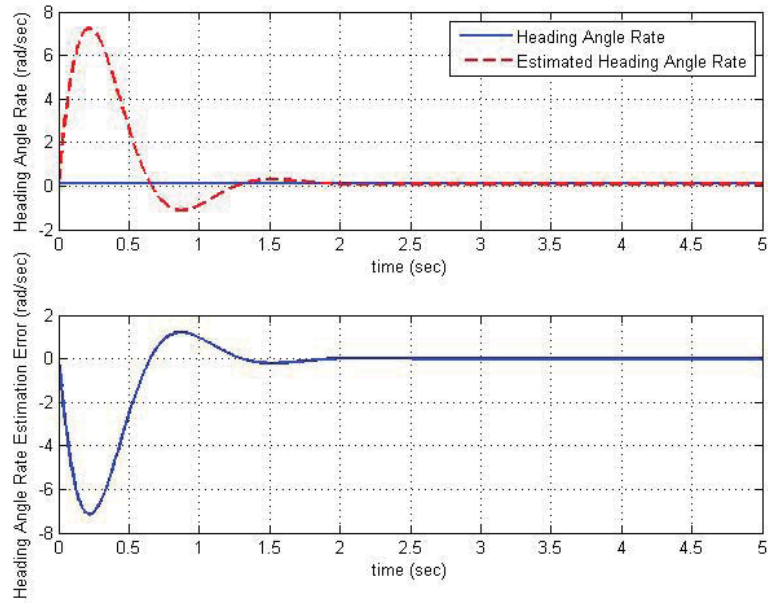
Figure 3.6: Estimation and estimation error of the heading angle rate "R" of the nonlinear continuous-time system, using PWA observer.

Then, the observer is applied to the nonlinear sampled-data system with sampling time $T = 0.2s$. The estimations and the state estimation errors of the nonlinear sampled-data system are shown in Figures 3.8, 3.9 and 3.10. As expected, the state estimation errors have converged to small regions after a short time. In other words, the state estimation errors are ultimately bounded. This continuous the results of the theorems which indicated that the state estimation error is ultimately bounded when the PWA observer is applied to the nonlinear sampled-data system.

Table 3.2 shows the results of the state estimation for the nonlinear sampled-data WMR Model.

Then a sampling time $T = 0.1s$ is considered for the nonlinear sampled-data system and white Gaussian noise with variance $\delta = 0.01$ is added to the output. Using a saturation block, the generated white Gaussian noise is norm bounded. Figure 3.11 shows the state estimation errors for the nonlinear sampled-data system in the presence of measurement noise. The state estimation errors have converged to small regions around zero. As proven, the proposed observer is robust to norm bounded measurement noise. Table 3.3 contains
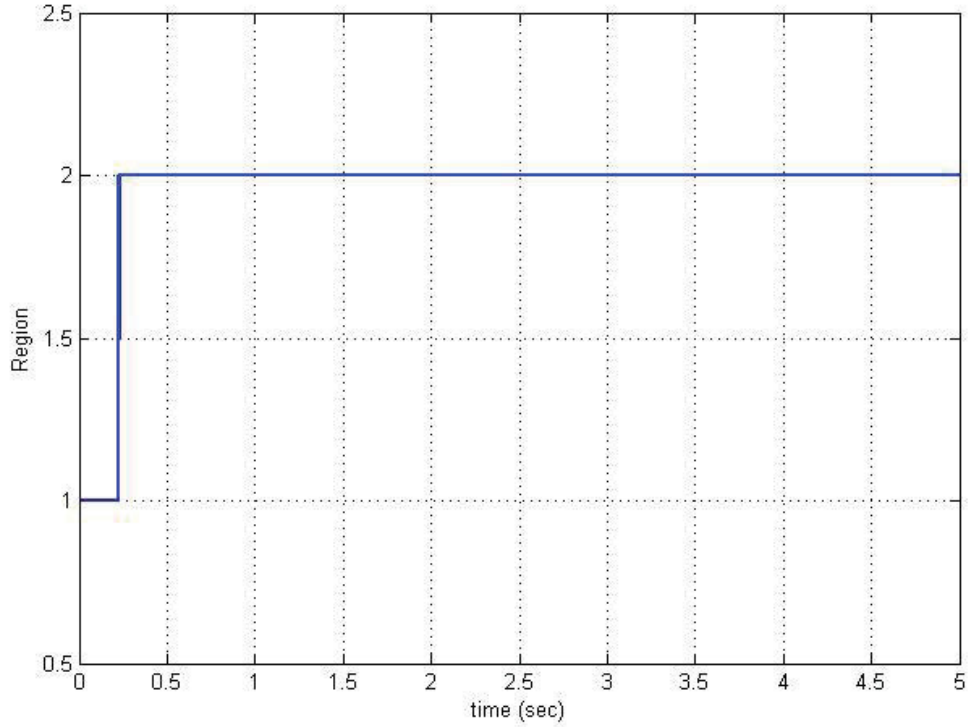
Figure 3.7: PWA regions in which the observer is operating.

the results of the state estimation for the nonlinear sampled-data system in the presence of measurement noise.

In what follows several nonlinear observers which are presented in Section 2.5 are applied to the nonlinear model of the WMR and the results of the state estimation are provided. All the observer gains are designed such that $1 \leqslant t_s \leqslant 3$ for the position, $3 \leqslant t_s \leqslant 4$ for the heading angle and $3 \leqslant t_s \leqslant 4$ for the heading angle rate, where t_s defines the time at which the state estimation error reaches its steady state value. For all the observers three experiments, as performed for the PWA observer, are done: applying the observer to the nonlinear continuous-time system, applying the observer to the nonlinear system with sampled output ($T = 0.2s$) and applying the observer to the nonlinear sampled-data system with measurement noise ($T = 0.1s$ and $\delta = 0.01$). The initial conditions are considered the same as the PWA observer implementation. Tables 3.1, 3.2 and 3.3 summarize the results of the state estimation for different observers.
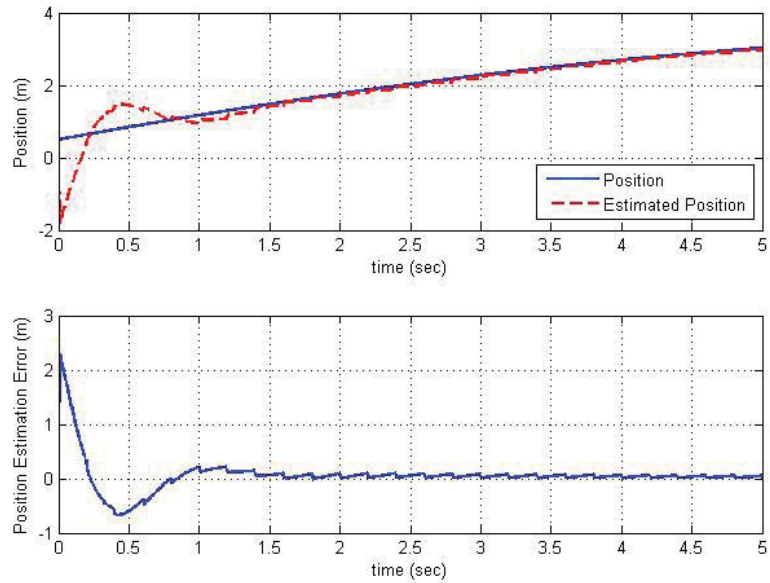
Figure 3.8: Estimation and estimation error of the position "*y*" of the nonlinear sampled-data system ($T = 0.2s$), using PWA observer.
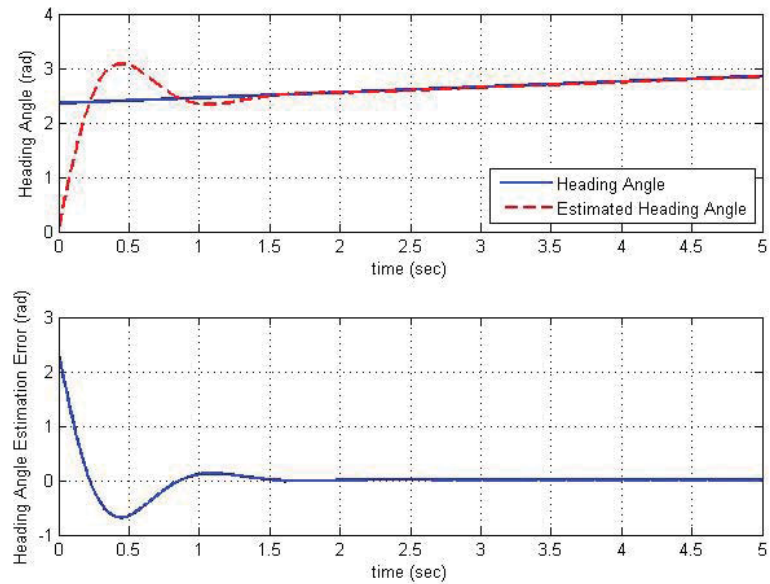
Figure 3.9: Estimation and estimation error of the heading angle "ψ" of the nonlinear sampled-data system ($T = 0.2s$), using PWA observer.
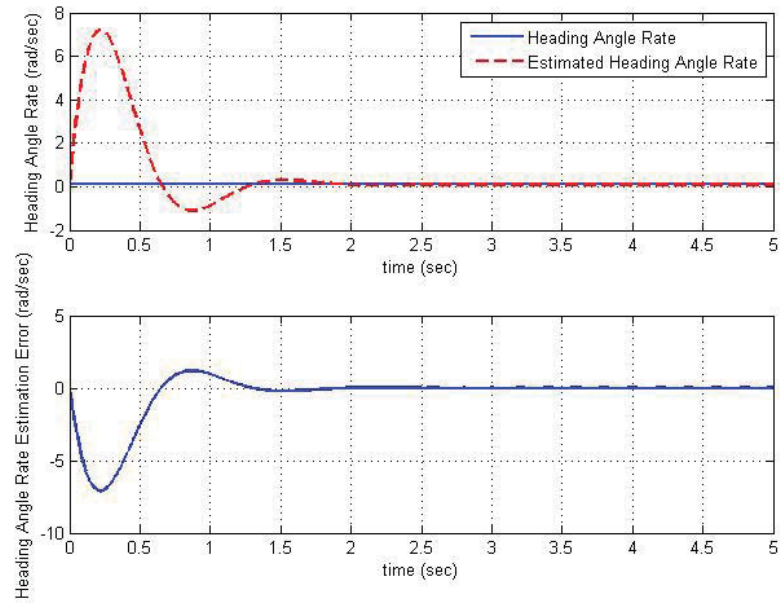
Figure 3.10: Estimation and estimation error of heading angle rate "R" of the nonlinear sampled-data system ($T = 0.2s$), using PWA observer.
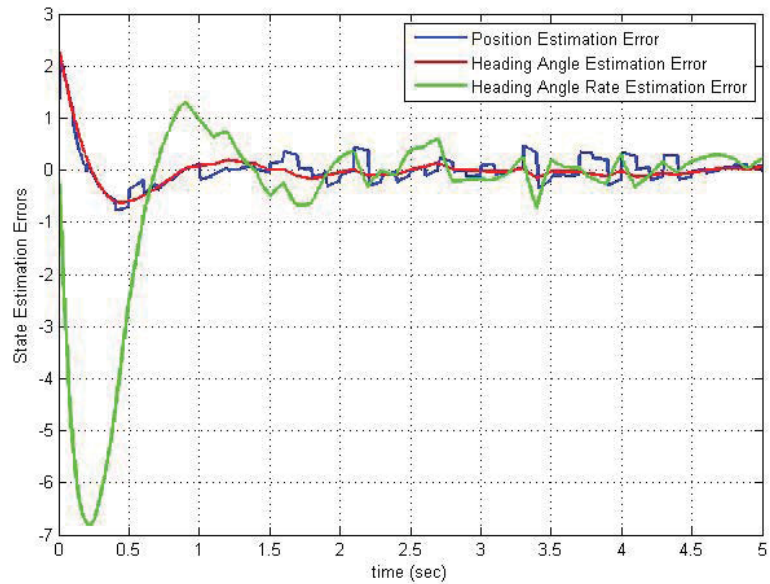
Figure 3.11: State estimation errors for the nonlinear sampled-data system in the presence of norm bounded white Gaussian measurement noise, using PWA observer.

- **Nonlinear Observer With Output Injection**

In this part according to the material presented in Section 2.5 a nonlinear observer with output injection is designed for the nonlinear model of the WMR.

Since the pair (A, C) is observable, placing the eigenvalues of $A - LC$ at $[-400; -4 + 4i; -4 - 4i]$, the observer gain L can be calculated, where

$$A = \begin{bmatrix} 0 & 0 & 0 \\ 0 & 0 & 1 \\ 0 & 0 & 0 \end{bmatrix} \tag{3.107}$$

The poles of $A - LC$ are placed such that the speed of convergence of the nonlinear observer is as desired. The observer gain is as follows

$$L = \begin{bmatrix} 398.758 & 30.9828 \\ 16.0338 & 9.242 \\ 146.1509 & 43.4553 \end{bmatrix} \tag{3.108}$$

Figures 3.12, 3.13 and 3.14 show the estimations and the estimation errors for position, heading angle and heading angle rate of the nonlinear continuous-time WMR system, respectively. All three states are estimated correctly after a few seconds and the state estimation errors have converged to small regions around zero.

The results of the state estimation for the nonlinear sampled-data system are plotted in Figures 3.15, 3.16 and 3.17. As depicted in Figures 3.15, 3.16 and 3.17 the estimation errors of the position y, heading angle ψ and heading angle rate R have converged after a few seconds.

Figure 3.18 shows the state estimation errors when the nonlinear observer with output injection is applied to the WMR nonlinear sampled-data model in the presence of measurement noise.

The results show that state estimation errors converge when the nonlinear observer with output injection is applied to the nonlinear model of the WMR.

- **Sliding Mode Observer**
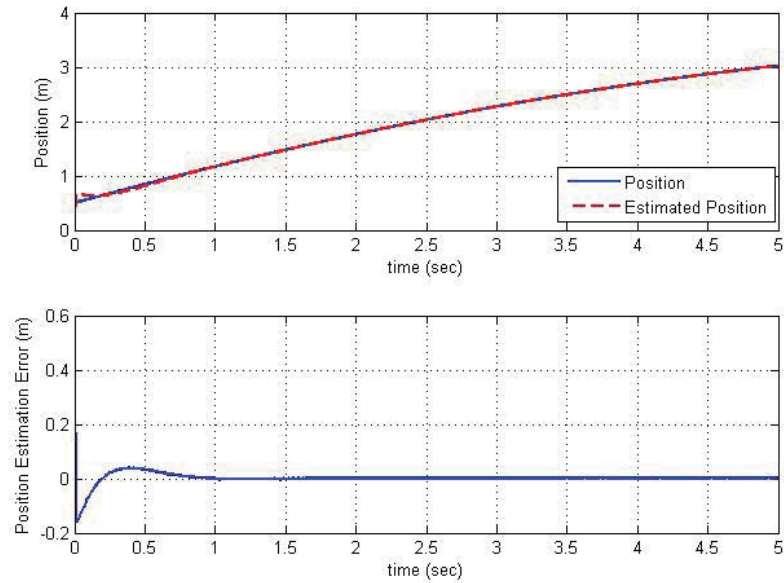
Figure 3.12: Estimation and estimation error of the position "y" of the nonlinear continuous-time system, using nonlinear observer with output injection.
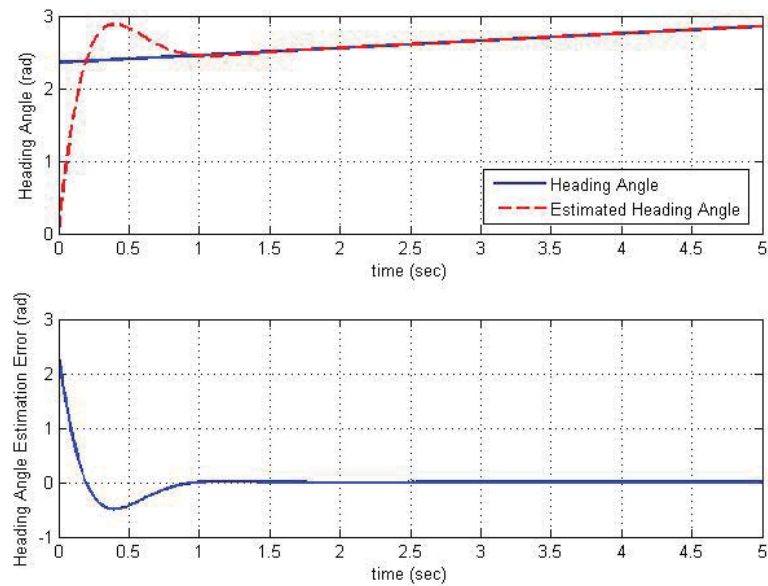
Figure 3.13: Estimation and estimation error of heading angle "ψ" of the nonlinear continuous-time system, using nonlinear observer with output injection.

63
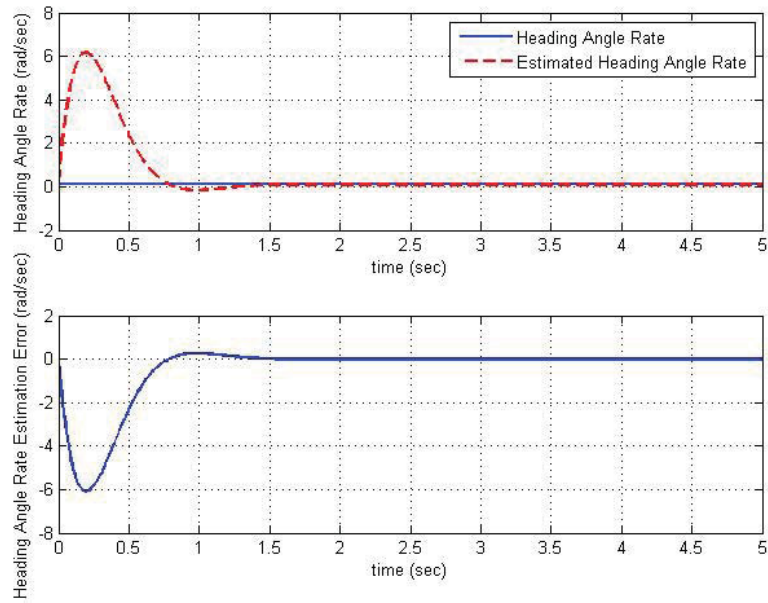
Figure 3.14: Estimation and estimation error of heading angle rate "R" of the nonlinear continuous-time system, using nonlinear observer with output injection.
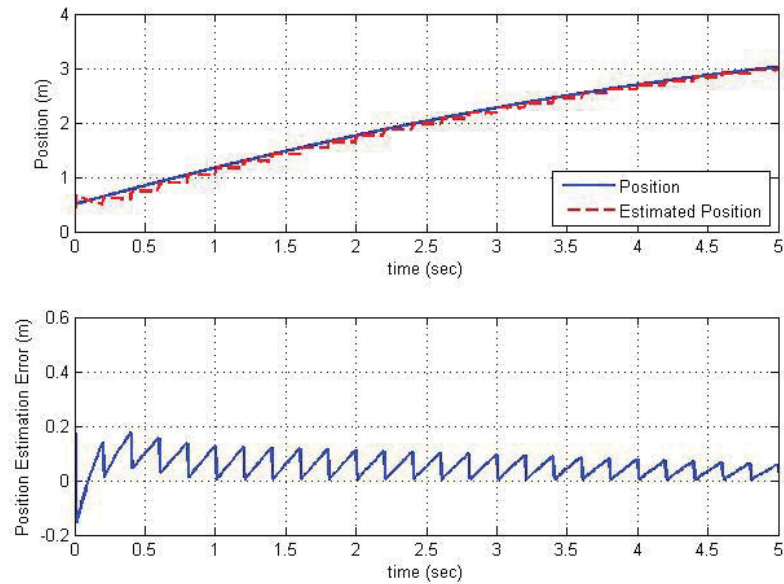
Figure 3.15: Estimation and estimation error of the position "y" of the nonlinear sampled-data system ($T = 0.2s$), using nonlinear observer with output injection.
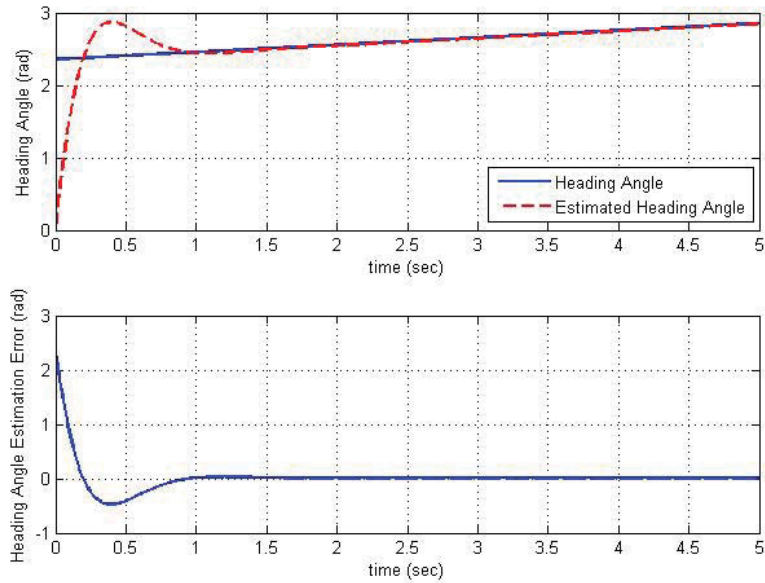
Figure 3.16: Estimation and estimation error of the heading angle "ψ" of the nonlinear sampled-data system ($T = 0.2s$), using nonlinear observer with output injection.
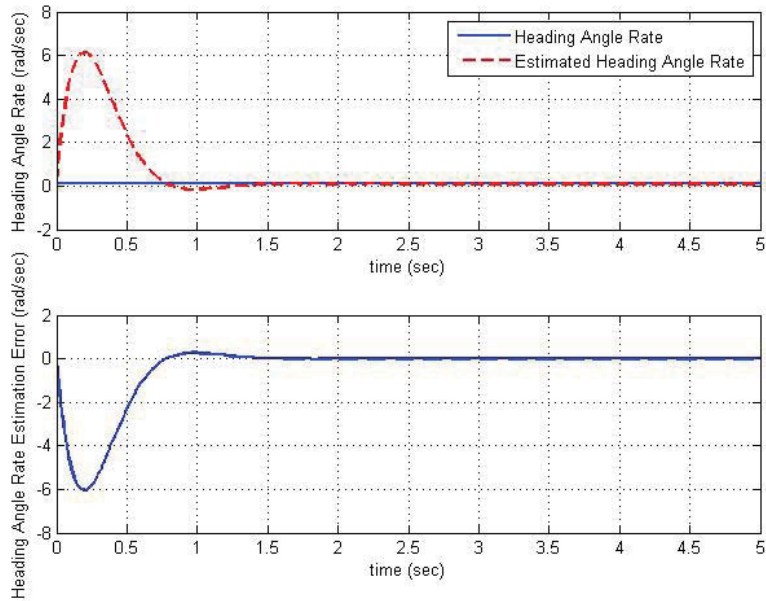
Figure 3.17: Estimation and estimation error of the heading angle rate "R" of the nonlinear sampled-data system ($T = 0.2s$), using nonlinear observer with output injection.
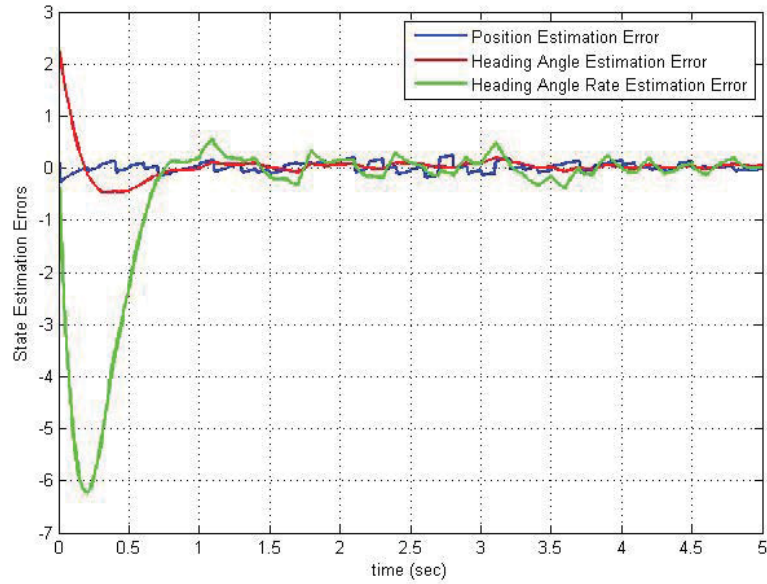
Figure 3.18: State estimation errors for the nonlinear sampled-data system in the presence of norm bounded white Gaussian measurement noise, using nonlinear observer with output injection.

For the nonlinear system defined in (3.92) a sliding mode observer can be designed using the approach provided in Section 2.5 with the following structure

$$\dot{\hat{\psi}} = \hat{R} + \lambda_1 Sign(\psi - \hat{\psi})$$

$$\dot{\hat{R}} = u + \lambda_2 Sign(\lambda_1 Sign(\psi - \hat{\psi})) \tag{3.109}$$

$$\hat{y} = \sin \psi + \lambda_3 Sign(y - \hat{y})$$

where $\lambda_1 = 1$, $\lambda_2 = 5$ and $\lambda_3 = 8$ are considered.

The results of the estimation for the position, heading angle and heading angle rate of the continuous-time nonlinear system are provided in Figures 3.19, 3.20 and 3.21, respectively.

The results of the state estimation for the nonlinear sampled-data system are provided in Figures 3.22, 3.23 and 3.24.

Figure 3.25 shows the state estimation error for the nonlinear sampled-data WMR in the presence of measurement noise.

The results show that the state estimation errors are ultimately bounded when the

66
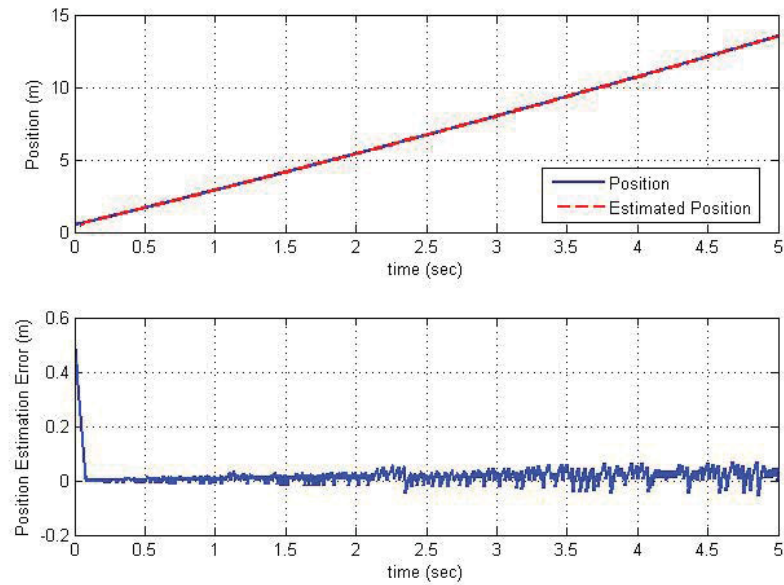
Figure 3.19: Estimation and estimation error of the position "*y*" of the continuous-time nonlinear system, using sliding mode observer.
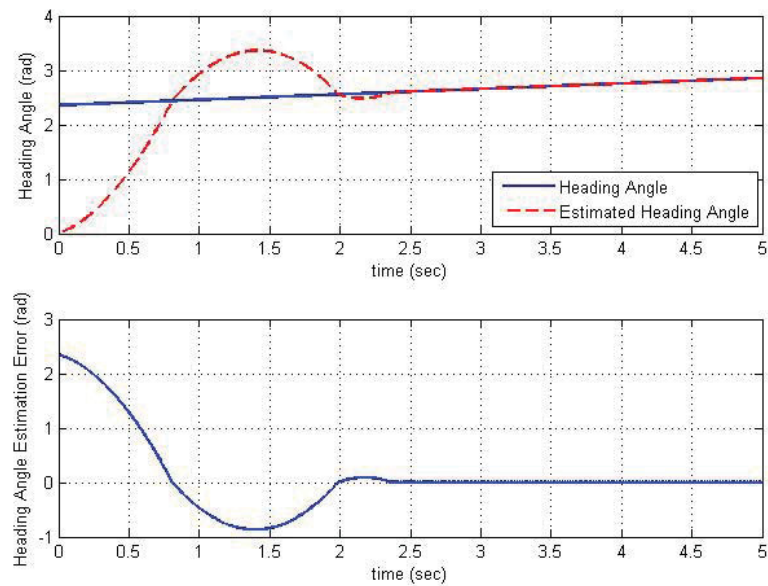
Figure 3.20: Estimation and estimation error of the heading angle "ψ" of the continuous-time nonlinear system, using sliding mode observer.
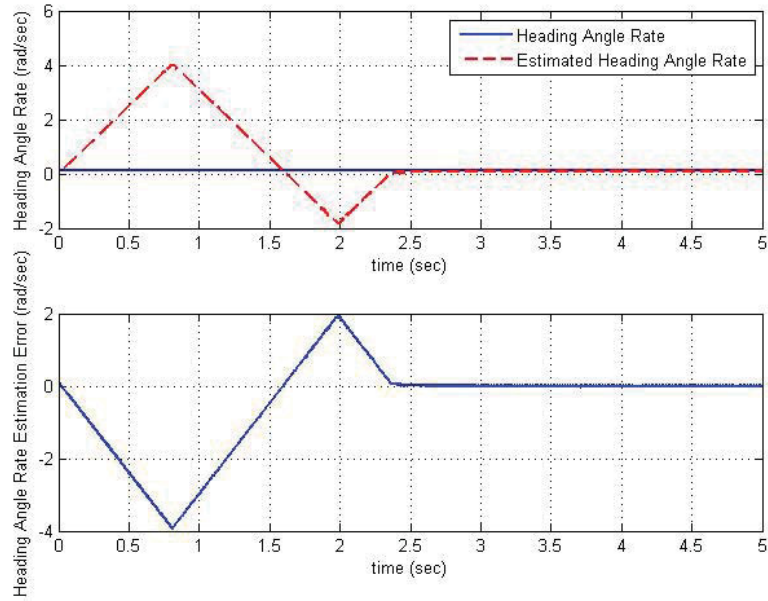
Figure 3.21: Estimation and estimation error of the heading angle "*R*" of the continuous-time nonlinear system, using sliding mode observer.
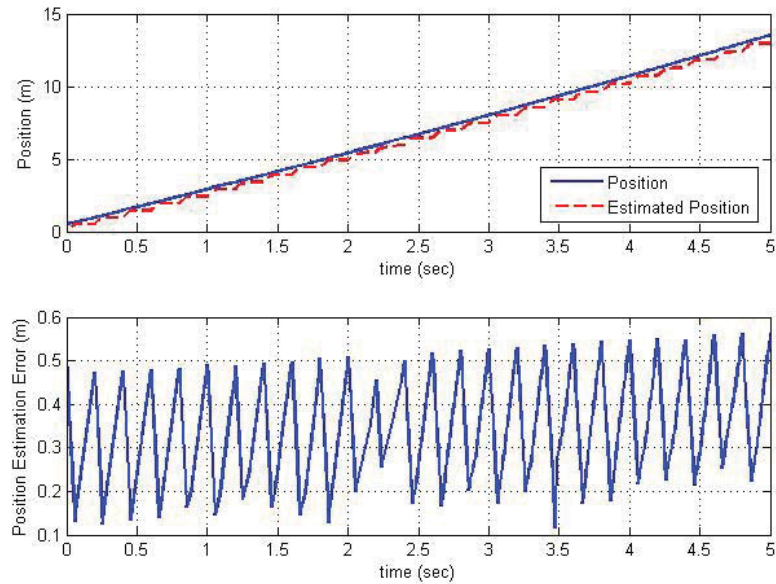
Figure 3.22: Estimation and estimation error of the position "*y*" of the nonlinear sampled-data system ($T = 0.2s$), using sliding mode observer.
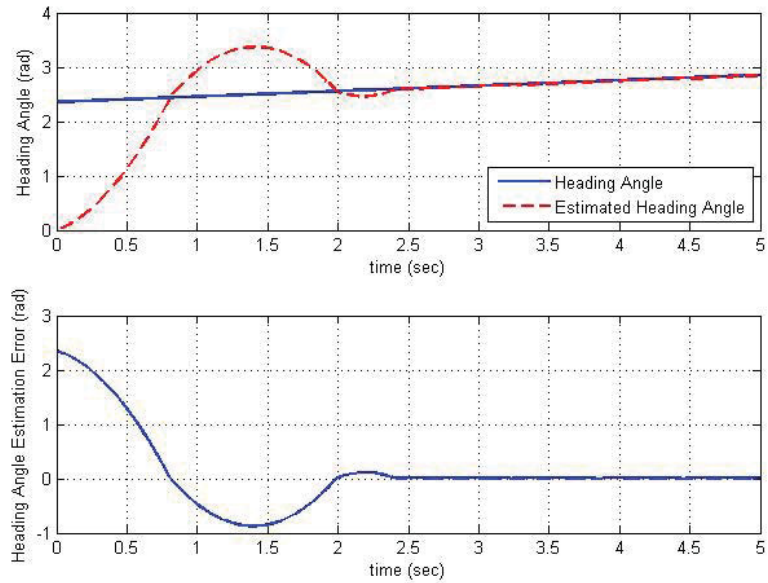
Figure 3.23: Estimation and estimation error of the heading angle "ψ" of the nonlinear sampled-data system ($T = 0.2s$), using sliding mode observer.
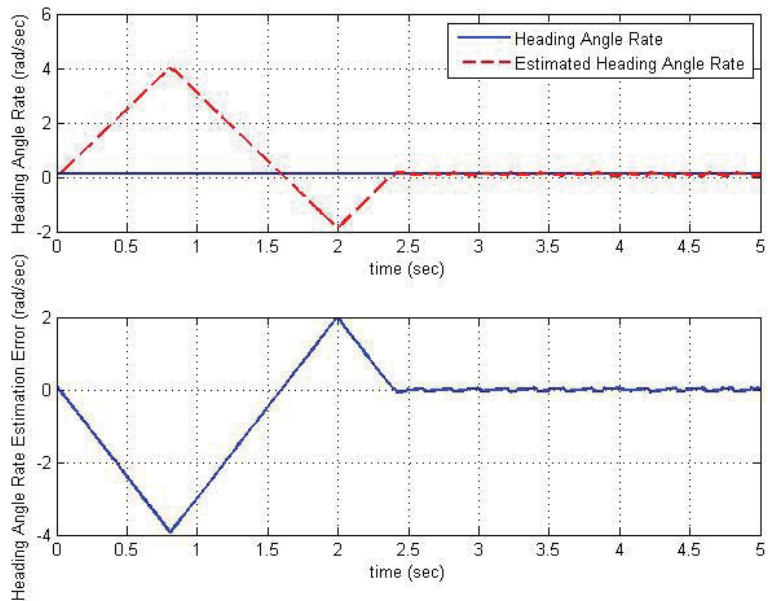
Figure 3.24: Estimation and estimation error of the heading angle "R" of the nonlinear sampled-data system ($T = 0.2s$), using sliding mode observer.
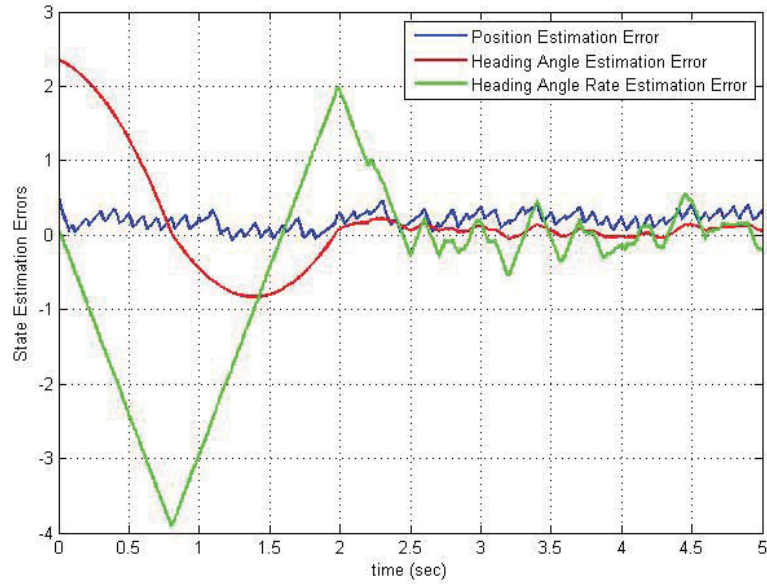
Figure 3.25: State estimation errors for the nonlinear sampled-data system in the presence of norm bounded white Gaussian measurement noise, using sliding mode observer.

sliding mode observer is applied to the nonlinear model of the WMR.

- **High-Gain Observer**

The nonlinear model of the WMR defined in (3.92) can be written in the following form for which a high-gain observer can be designed based on the method represented in Section 2.5.

$$
\begin{bmatrix} \dot{\psi} \\ \dot{R} \end{bmatrix} = \begin{bmatrix} 0 & 1 \\ 0 & 0 \end{bmatrix} \begin{bmatrix} \psi \\ R \end{bmatrix} + \begin{bmatrix} 0 \\ 1 \end{bmatrix} u
$$

$$
\dot{y} = \sin \psi
$$

$$
\zeta_1 = \begin{bmatrix} 1 & 0 \end{bmatrix} \begin{bmatrix} \psi \\ R \end{bmatrix}
$$

$$
\zeta_2 = y
$$
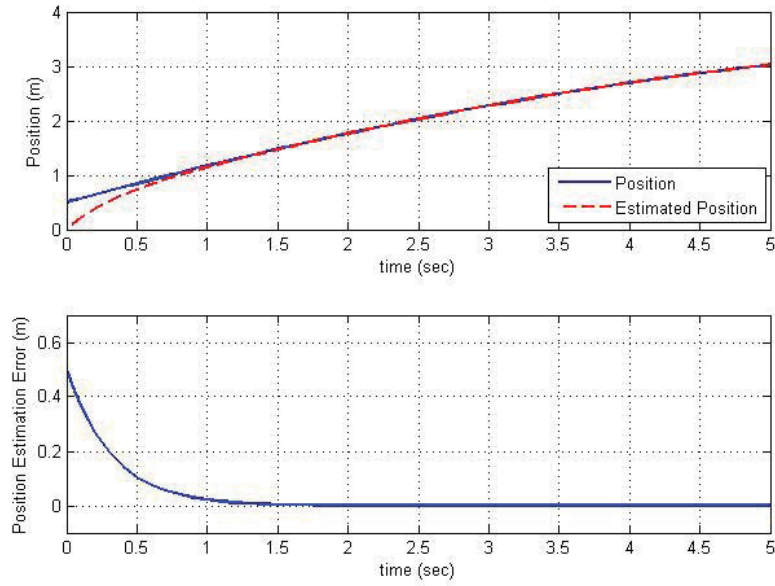
(3.110)

Figure 3.26: Estimation and estimation error of the position "*y*" of the continuous-time nonlinear system, using high-gain observer.

For the system defined in (3.110) a high-gain observer can be designed as follows

$$
\begin{bmatrix} \dot{\hat{\psi}} \\ \dot{\hat{R}} \end{bmatrix} = \begin{bmatrix} 0 & 1 \\ 0 & 0 \end{bmatrix} \begin{bmatrix} \hat{\psi} \\ \hat{R} \end{bmatrix} + \begin{bmatrix} 0 \\ 1 \end{bmatrix} u + H_1(\psi - \hat{\psi})
$$

(3.111)

$$
\hat{y} = \sin \psi + H_2(y - \hat{y})
$$

where

$$
H_1 = \begin{bmatrix} \dfrac{\alpha_1}{\varepsilon} \\ \dfrac{\alpha_2}{\varepsilon^2} \end{bmatrix}
$$

(3.112)

and

$$
H_2 = \frac{\alpha_3}{\varepsilon}
$$

(3.113)

with

$$
\varepsilon = 0.8, \alpha_1 = 5, \alpha_2 = 6, \alpha_3 = 2.5
$$

(3.114)

Figures 3.26, 3.27 and 3.28 show the estimation and the state estimation errors of the position, the heading angle and the heading angle rate of the continuous-time nonlinear system, respectively.

71
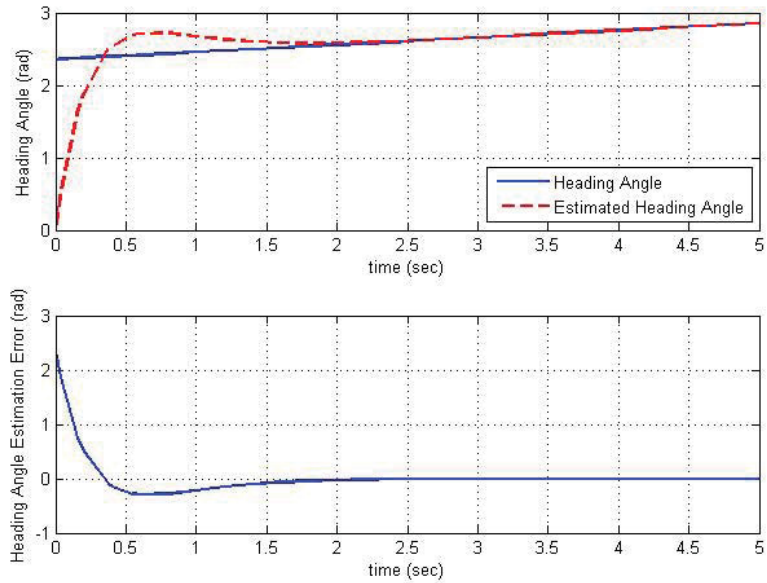
Figure 3.27: Estimation and estimation error of the heading angle "ψ" of the continuous-time nonlinear system, using high-gain observer.
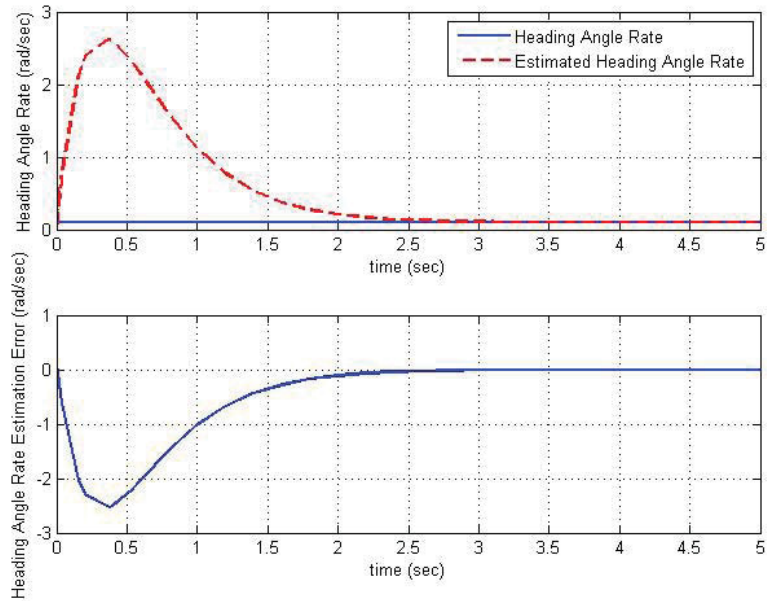
Figure 3.28: Estimation and estimation error of the heading angle rate "R" of the continuous-time nonlinear system, using high-gain observer.

72
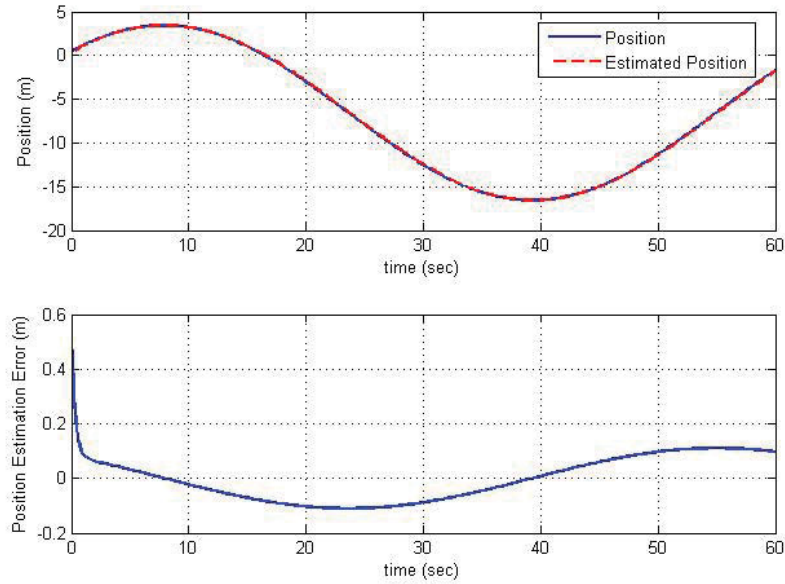
Figure 3.29: Estimation and estimation error of the position "*y*" of the nonlinear sampled-data system ($T = 0.2s$), using high-gain observer.

The results of the estimation of the position, the heading angle and the heading angle rate of the nonlinear sampled-data system are shown in Figures 3.29, 3.30 and 3.31, respectively. Figure 3.29 is plotted for $t = 60s$ to show the small region around zero to which the position estimation error has converged.

The position estimation error, the heading angle estimation error and the heading angle rate estimation error of the nonlinear sampled-data system in the presence of measurement noise are shown in Figure 3.32.

The state estimation errors are ultimately bounded when the high-gain observer is applied to the nonlinear model of the WMR.

● **Backstepping Observer**

To design a backstepping observer for the nonlinear model of the WMR defined in (3.92), according to the approach provided in Section 2.5 the system should be broken into
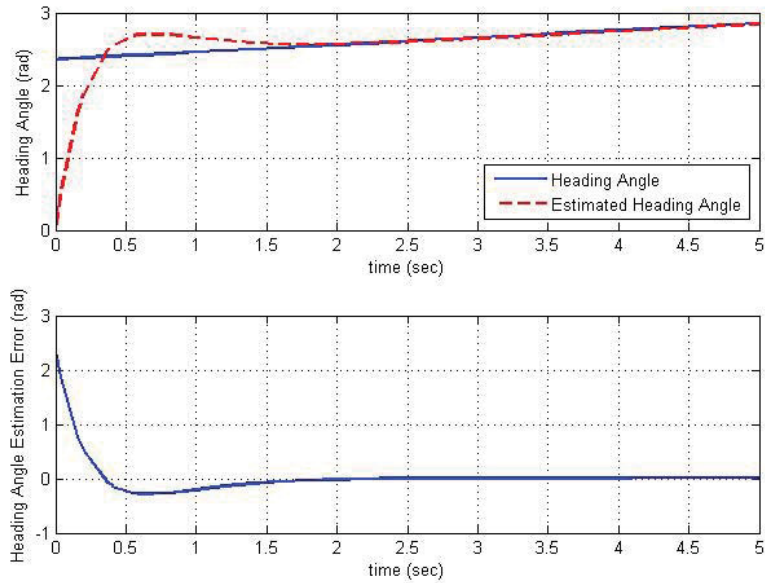
Figure 3.30: Estimation and estimation error of the heading angle "ψ" of the nonlinear sampled-data system ($T = 0.2s$), using high-gain observer.
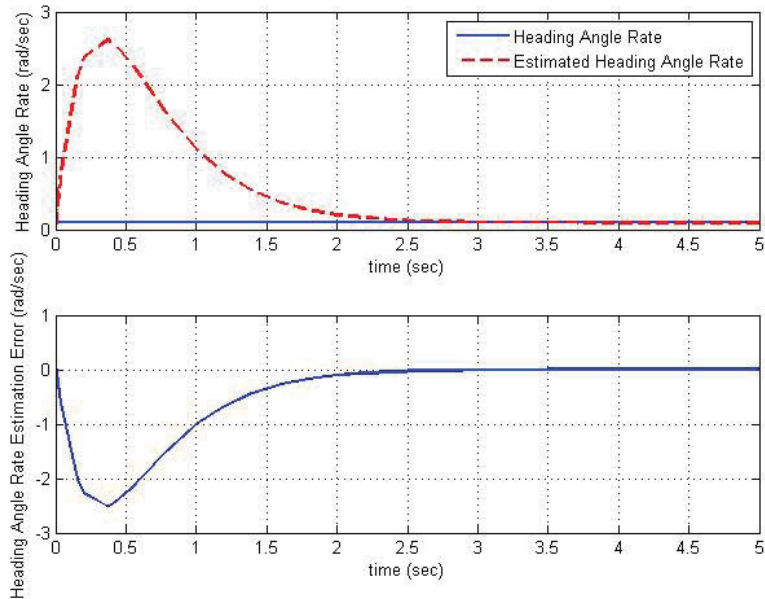
Figure 3.31: Estimation and estimation error of the heading angle rate "R" of the nonlinear sampled-data system ($T = 0.2s$), using high-gain observer.
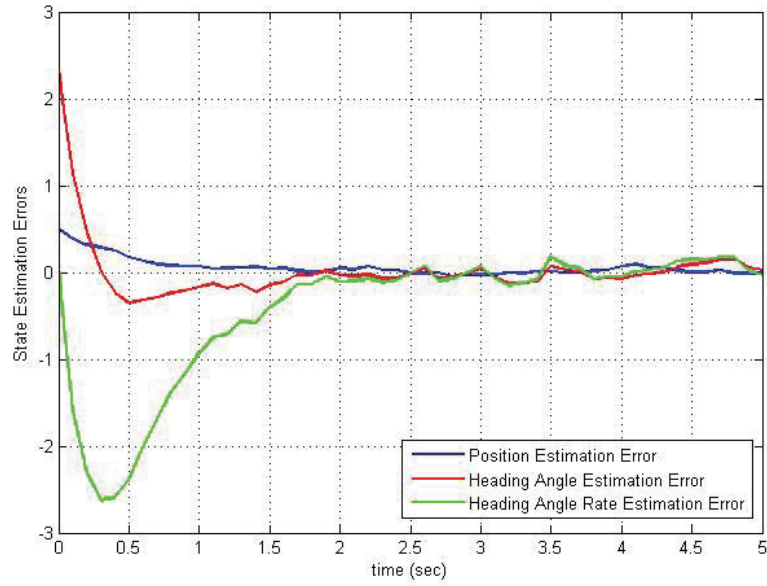
Figure 3.32: State Estimation Errors for the nonlinear sampled-data system in the presence of norm bounded white Gaussian measurement noise, using high-gain observer.

two single-input subsystems as follows

$$
\begin{bmatrix} \dot{\psi} \\ \dot{R} \end{bmatrix} = \begin{bmatrix} 0 & 1 \\ 0 & 0 \end{bmatrix} \begin{bmatrix} \psi \\ R \end{bmatrix} + \begin{bmatrix} 0 \\ u \end{bmatrix}
$$

$$
\dot{y} = \sin \psi \tag{3.115}
$$

$$
\zeta_1 = \psi
$$

$$
\zeta_2 = y
$$

The system (3.115) is equivalent to

$$
\begin{bmatrix} \dot{Z}_{1,1} \\ \dot{Z}_{1,2} \end{bmatrix} = \begin{bmatrix} 0 & 1 \\ 0 & 0 \end{bmatrix} \begin{bmatrix} Z_{1,1} \\ Z_{1,2} \end{bmatrix} + \begin{bmatrix} 0 \\ u \end{bmatrix}
$$

$$
\dot{Z}_{2,1} = \sin \zeta_1 \tag{3.116}
$$

$$
\zeta_1 = Z_{1,1}
$$

$$
\zeta_2 = Z_{2,1}
$$

where $Z_{1,1} = \psi$, and $Z_{1,2} = R$ and $Z_{2,1} = y$.

75

For the system defined in (3.116) a backstepping observer can be designed with the following structure

$$
\begin{bmatrix} \dot{\hat{Z}}_{1,1} \\ \dot{\hat{Z}}_{1,2} \end{bmatrix} = \begin{bmatrix} 0 & 1 \\ 0 & 0 \end{bmatrix} \begin{bmatrix} \hat{Z}_{1,1} \\ \hat{Z}_{1,2} \end{bmatrix} + \begin{bmatrix} 0 \\ u \end{bmatrix} + \begin{bmatrix} \phi_{1,1}(\hat{Z}_{1,1}, \hat{Z}_{1,2})(Z_{1,1} - \hat{Z}_{1,1}) \\ \phi_{1,2}(\hat{Z}_{1,1}, \hat{Z}_{1,2})(Z_{1,1} - \hat{Z}_{1,1}) \end{bmatrix} \tag{3.117}
$$

$$
\dot{\hat{Z}}_{2,1} = \sin \zeta_1 + \phi_{2,1}(\hat{Z}_{2,1})(Z_{2,1} - \hat{Z}_{2,1})
$$

According to (2.48), (2.49) and the Appendix

$$
\phi_{1,1} = C_2 + C_1
$$

$$
\phi_{1,2} = 1 + C_1 + C_2 \tag{3.118}
$$

$$
\phi_{2,1} = C_1
$$

where

$$
C_1 = 2, C_2 = 3 \tag{3.119}
$$

The results of the estimation and estimation errors of the position, heading angle and the heading angle rate of the continuous-time nonlinear system are shown in Figures 3.33, 3.34 and 3.35, respectively.

Figures 3.36, 3.37 and 3.38 show the estimations and estimation errors of the position, the heading angle and the heading angle rate of the nonlinear sampled-data system, respectively. Figure 3.36 is plotted for $t = 80s$ to show the small region around zero to which the position estimation error has converged.

Fiure 3.39 shows the state estimation errors when the backstepping observer is applied to the nonlinear sampled-data model of the WMR in the presence of measurement noise. The state estimation errors are convergent and ultimately bounded.

• **Interconnected Observers**

The nonlinear system defined in (3.92) can be broken into two subsystems as follows

$$
\Sigma_1 : \begin{cases} \begin{bmatrix} \dot{\psi} \\ \dot{R} \end{bmatrix} = \begin{bmatrix} 0 & 1 \\ 0 & 0 \end{bmatrix} \begin{bmatrix} \psi \\ R \end{bmatrix} + \begin{bmatrix} 0 \\ u \end{bmatrix} \\ \\ \zeta_1 = \psi \end{cases} \tag{3.120}
$$

76
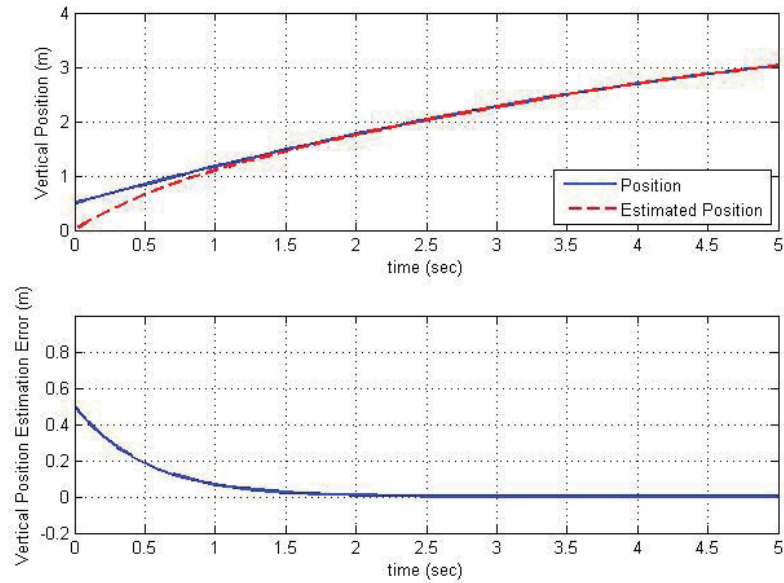
Figure 3.33: Estimation and estimation error of the position "y" of the continuous-time nonlinear system, using backstepping observer.
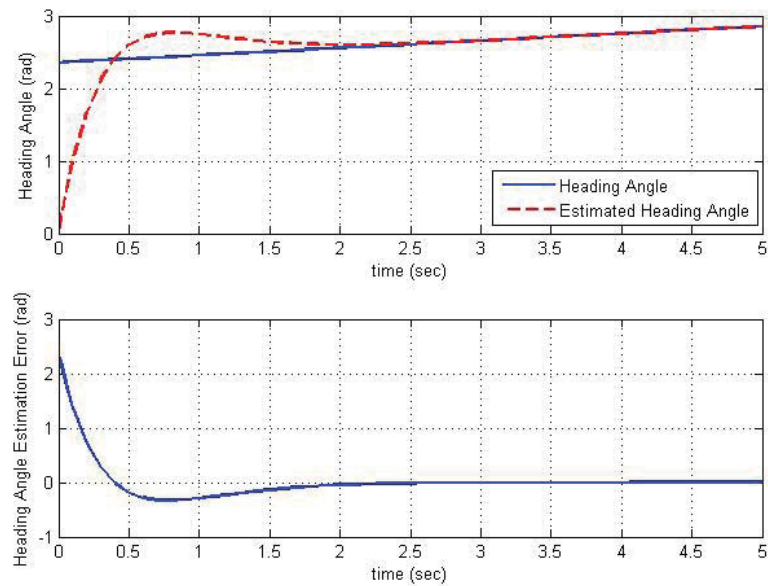
Figure 3.34: Estimation and estimation error of the heading angle "ψ" of the continuous-time nonlinear system, using backstepping observer.
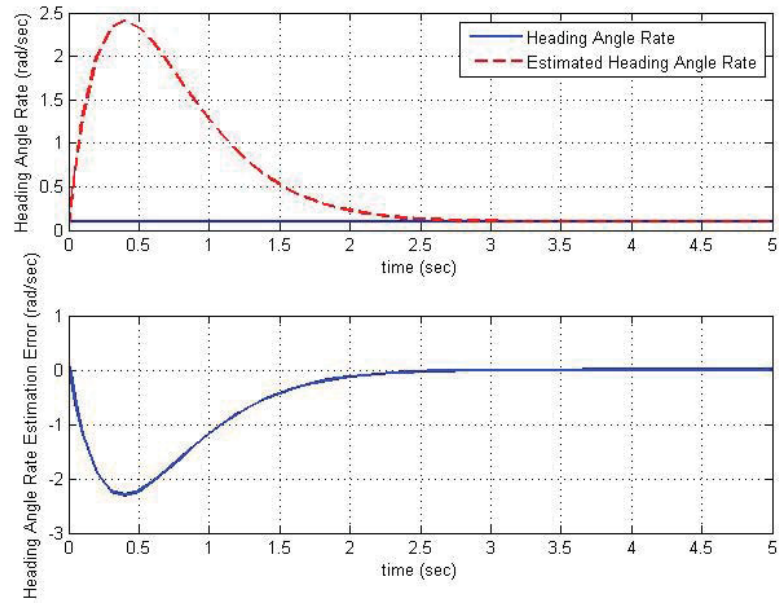
Figure 3.35: Estimation and estimation error of the heading angle rate "*R*" of the continuous-time nonlinear system, using backstepping observer.
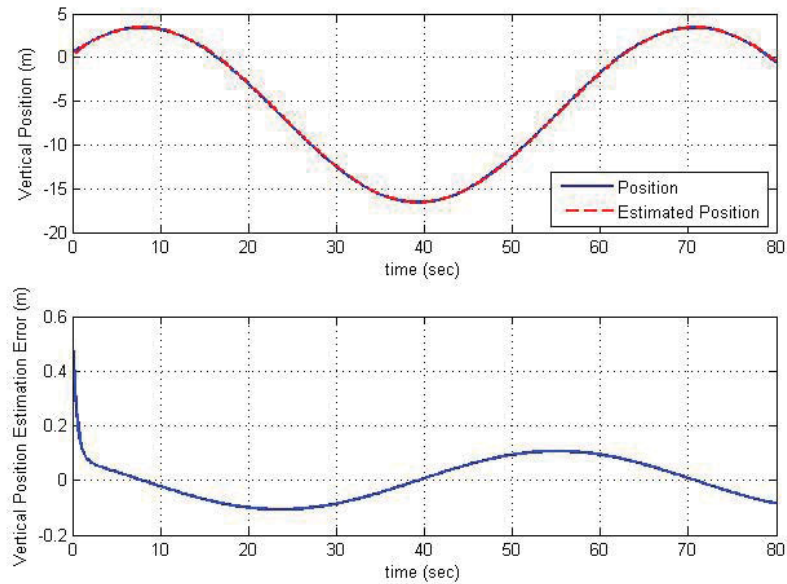
Figure 3.36: Estimation and estimation error of the position "*y*" of the nonlinear sampled-data system ($T = 0.2s$), using backstepping observer.
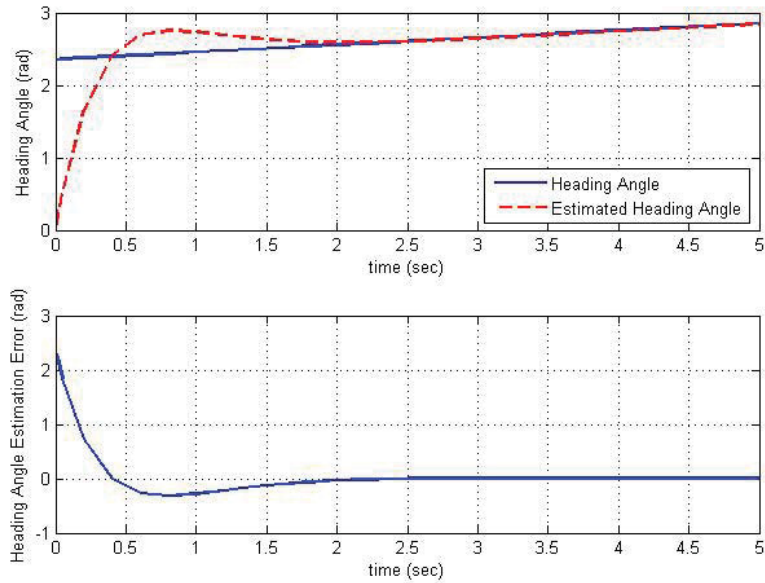
Figure 3.37: Estimation and estimation error of the heading angle "ψ" of the nonlinear sampled-data system ($T = 0.2s$), using backstepping observer.
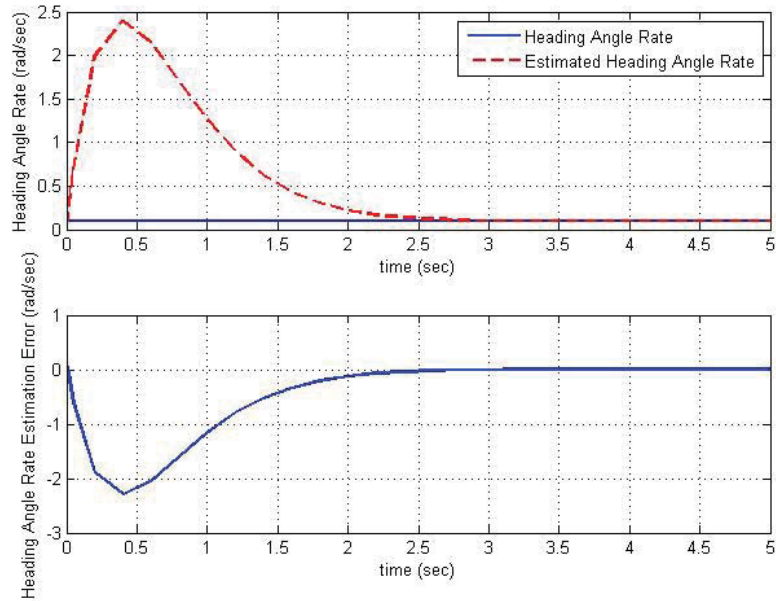
Figure 3.38: Estimation and estimation error of the heading angle rate "R" of the nonlinear sampled-data system ($T = 0.2s$), using backstepping observer.
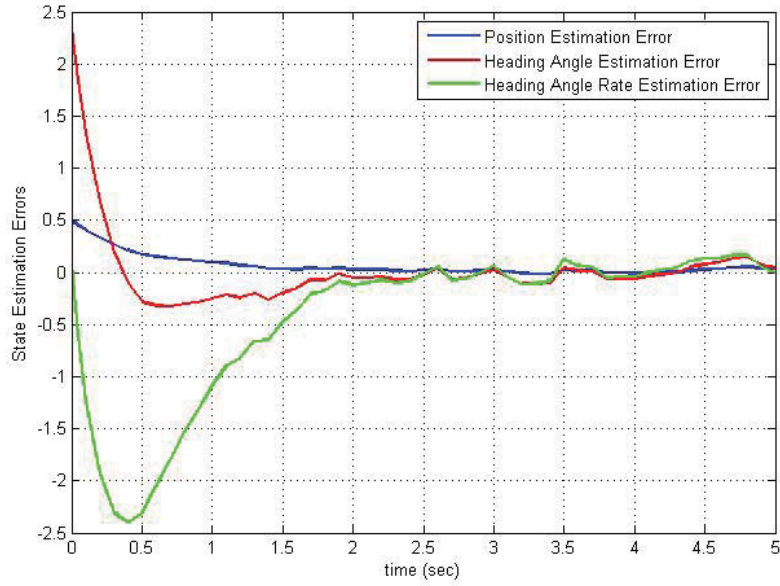
Figure 3.39: State estimation errors of the nonlinear sampled-Data system in the presence of norm bounded white Gaussian measurement noise, using backstepping observer.

and

$$\Sigma_2 : \begin{cases} \dot{y} = \sin \zeta_1 \\ \\ \zeta_2 = y \end{cases} \tag{3.121}$$

where the output of the first subsystem is the input to the second subsystem. For each of Σ_1 and Σ_2 observers can be designed. The gains of the observers are designed by placing the eigenvalues of $A - L_1 C$ at $[-4; -3]$ as follows

$$L_1 = \begin{bmatrix} 7 \\ 12 \end{bmatrix}, L_2 = 2.5 \tag{3.122}$$

where L_1 and L_2 are the observer gains for Σ_1 and Σ_2, respectively.

The results of the estimation and estimation error of the position, the heading angle and the heading angle rate of the continuous-time nonlinear system are shown in Figures 3.40, 3.41 and 3.42, respectively.

Figures 3.43, 3.44 and 3.45 show the estimation and the estimation errors of the position, the heading angle and the heading angle rate of the nonlinear sampled-data WMR,
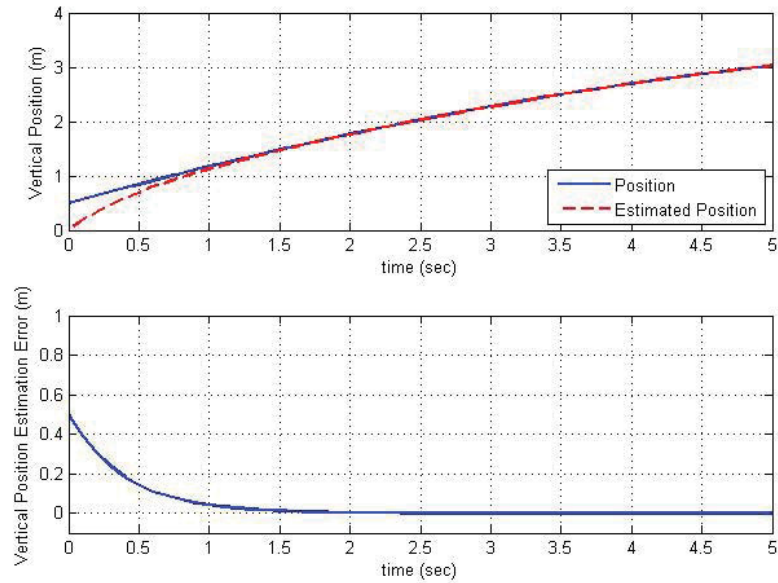
Figure 3.40: Estimation and estimation error of the position "y" of the continuous-time nonlinear system, using interconnected observer.
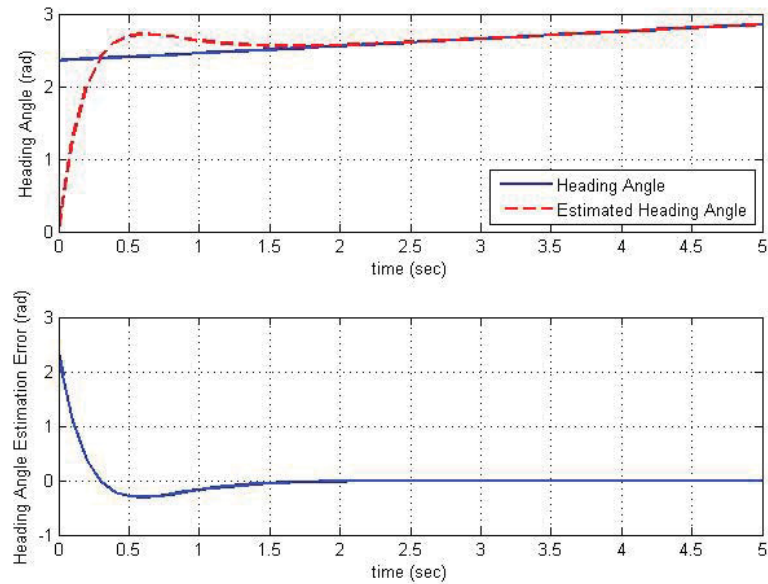
Figure 3.41: Estimation and estimation error of the heading angle "ψ" of the continuous-time nonlinear system, using interconnected observer.
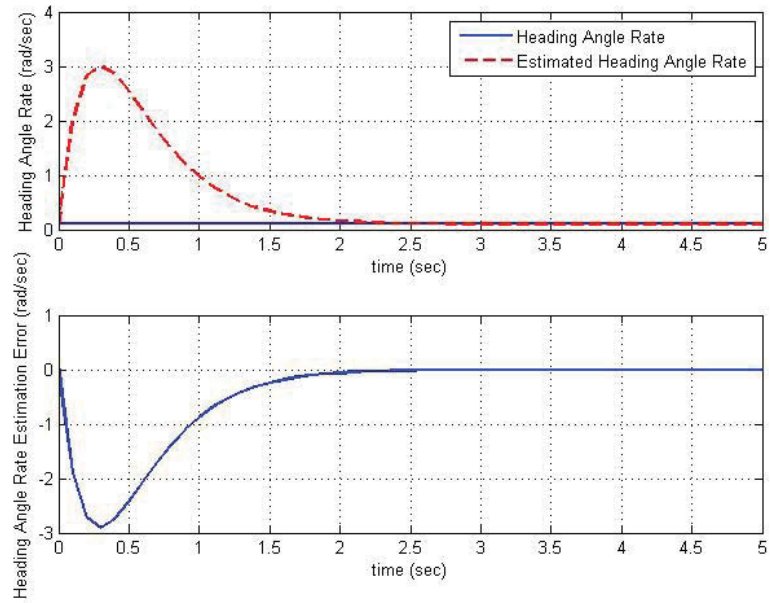
Figure 3.42: Estimation and estimation error of the heading angle rate "*R*" of the continuous-time nonlinear system, using interconnected observer.

respectively. Figure 3.43 is plotted for $t = 80s$ to show the small region around zero to which the position estimation error has converged.

The state estimation errors of the nonlinear sampled-data system in the presence of measurement noise are shown in Figure 3.46.

The interconnected observer is able to estimate the states of the nonlinear WMR system with convergent state estimation errors.

Tables 3.1, 3.2 and 3.3 summarize the results of the state estimation error for different observers for the nonlinear continuous-time system, nonlinear sampled-data system and nonlinear sampled-data system in the presence of measurement noise, respectively. The results are concluded after performing the experiments for different initial conditions. The parameters e_{max} and e_{rms} have been commonly used to evaluate the performance of the observers in transient and steady state, respectively [96, 178]. In this table e_{max} shows the maximum value for the estimation error in the transient time, and e_{rms} is the root mean
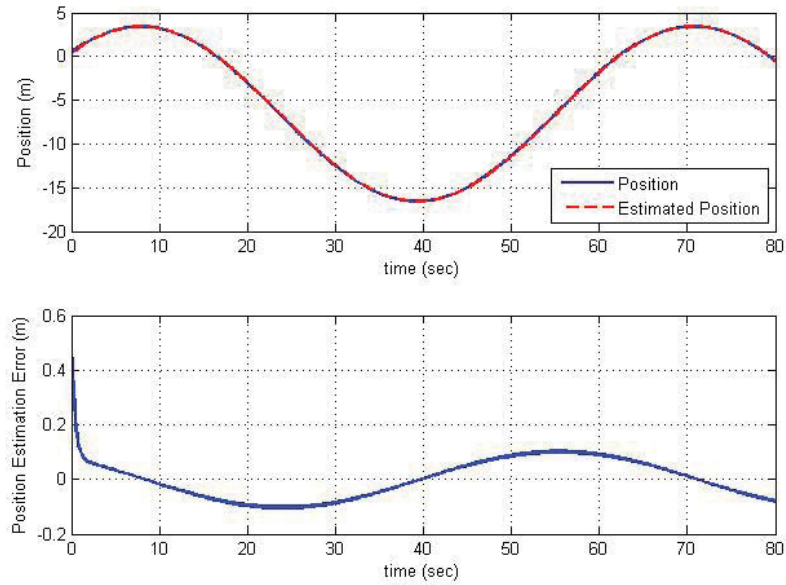
Figure 3.43: Estimation and estimation error of the position "*y*" of the nonlinear sampled-data system ($T = 0.2s$), using interconnected observer.
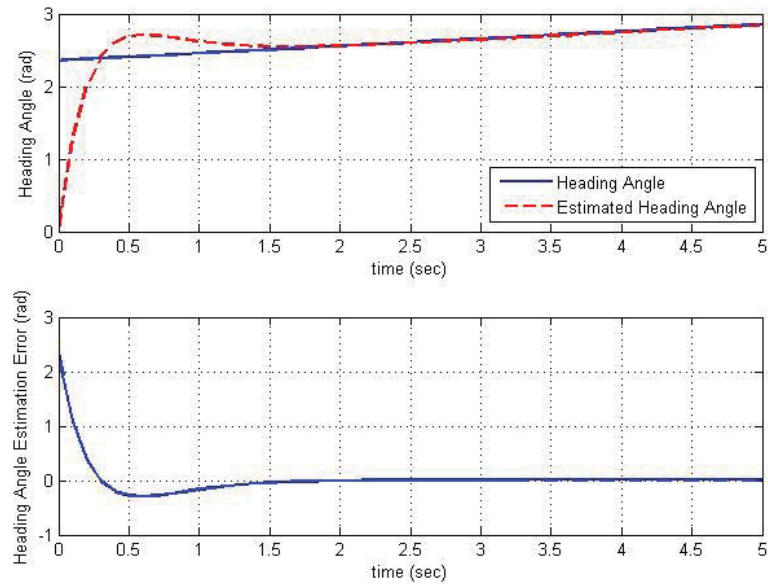
Figure 3.44: Estimation and estimation error of the heading angle "ψ" of the nonlinear sampled-data system ($T = 0.2s$), using interconnected observer.
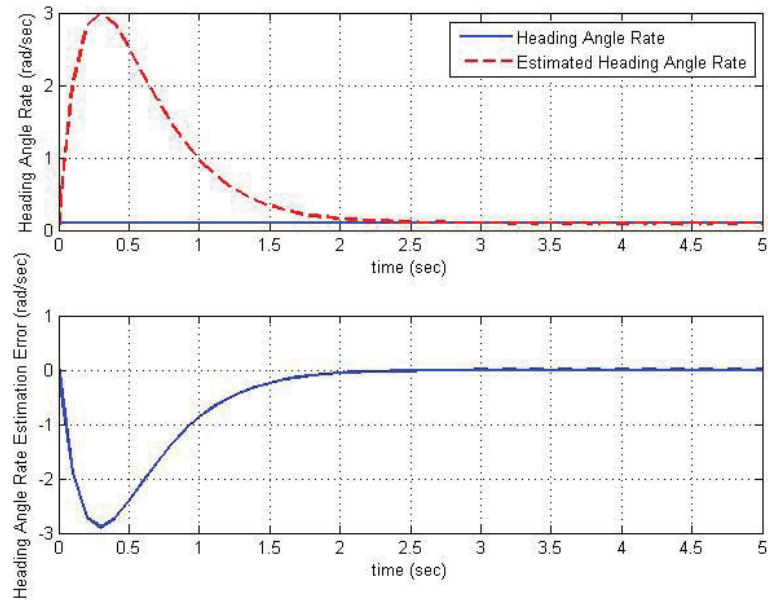
Figure 3.45: Estimation and estimation error of the heading angle rate "R" of the nonlinear sampled-data system ($T = 0.2s$), using interconnected observer.
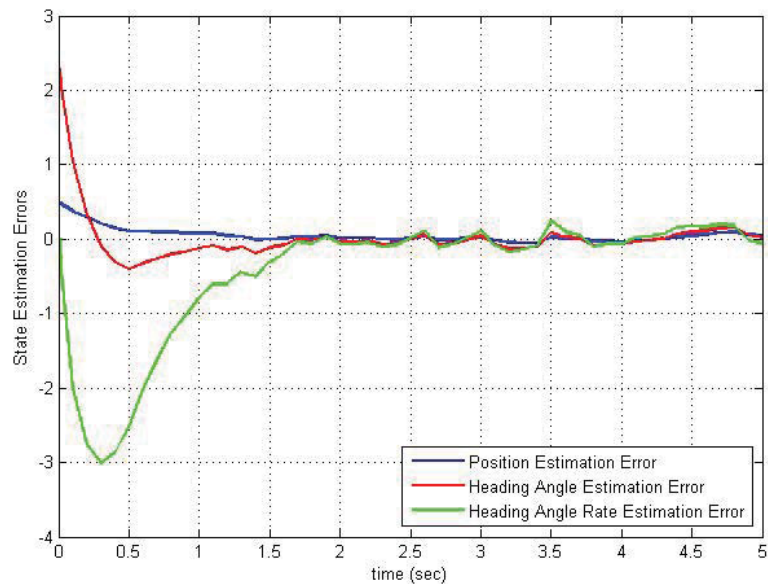
Figure 3.46: State estimation errors for the nonlinear sampled-data system in the presence of norm bounded white Gaussian measurement noise, using interconnected observer.

square error and is defined as

$$e_{rms} = \sqrt{\frac{1}{n}(e_1^2 + ... + e_n^2)} \tag{3.123}$$

where e_1 denotes the state estimation error at the time that the state estimation error reaches its steady state value (t_s) and e_n is the error at the final time (t_n). In other words e_{rms} is calculated by ignoring the transient data and uses the data starting from t_s to the end.

Note that for the position y and the heading angle ψ the maximum error in the transient (e_{max}) occurs at the initial condition and therefore it is not provided in the table.

Observers	Transient Performance (e_{max})	Steady State Performance (e_{rms})		
	R	y	ψ	R
PWA	7.1461	0.0014	0.00016	0.00088
Sliding Mode	3.9421	0.0061	0.00081	0.0041
Backstepping	2.308	0.0004	0.000016	0.000065
High-Gain	2.5335	0.0003	0.00022	0.0001
Output Injection	6.0806	0.0015	0.00006	0.0011
Interconnected	2.9071	0.00022	0.00011	0.00025

Table 3.1: Different observers implemented on the nonlinear continuous-time WMR model.

Observers	Transient Performance (e_{max})	Steady State Performance (e_{rms})		
	R	y	ψ	R
PWA	7.1062	0.0444	0.0101	0.0052
Sliding Mode	3.9314	0.3247	0.0123	0.035
Backstepping	2.2956	0.0708	0.0116	0.0023
High-Gain	2.5125	0.0777	0.012	0.003
Output Injection	6.045	0.0828	0.0101	0.0097
Interconnected	2.8963	0.0677	0.0106	0.0032

Table 3.2: Different observers implemented on the nonlinear sampled-data ($T = 0.2s$) WMR model.

● **Robustness**

In order to compare the robustness of the implemented observers for the case that the output is sampled and in the presence of measurement noise, the following parameters which are related to the relative change of the estimation error are defined. Relative change

Observers	Transient Performance (e_{max})	Steady State Performance (e_{rms})		
	R	y	ψ	R
PWA	6.8145	0.1071	0.0724	0.2263
Sliding Mode	3.9111	0.2118	0.087	0.2646
Backstepping	2.3997	0.0463	0.0619	0.0749
High-Gain	2.6248	0.0442	0.0655	0.0866
Output Injection	6.2288	0.1474	0.0749	0.2507
Interconnected	3.014	0.0492	0.0682	0.1002

Table 3.3: Different observers implemented on the nonlinear sampled-data ($T = 0.1s$) WMR model in the presence of measurement noise ($\delta = 0.01$).

can be used to evaluate the robustness of the observers [179, 180, 181] as

$$e_s = \frac{e_2 - e_1}{e_1} \tag{3.124}$$

where e_1 is the state estimation error (e_{rms} at steady state) of the nonlinear continuous-time system and e_2 is the state estimation error (e_{rms} at steady state) of the nonlinear system with sampled output with sampling time $T = 0.2s$ and

$$e_n = \frac{e_3 - e_1}{e_1} \tag{3.125}$$

where e_3 is the state estimation error (e_{rms} at steady state) of the sampled-data nonlinear system in the presence of measurement noise with variance $\delta = 0.01$ and sampling time $T = 0.1s$.

Table 3.4 summarizes the results for the position y of the WMR for different observers.

Observer	e_s	e_n
PWA	30.7143	75.5
Sliding Mode	52.2295	33.7213
Backstepping	171.83	112.02
Nonlinear Observer With Output Injection	54.2	97.26667
Interconnected	299.66	217.5
High-Gain	266.6081	151.2301

Table 3.4: State estimation of the position with different observers.

Table 3.5 summarizes the results for the heading angle of the WMR for different observers.

Observer	e_s	e_n
PWA	62.125	320.2638
Sliding Mode	14.2085	106.5721
Backstepping	711.92	3803.3
Nonlinear Observer With Output Injection	166.582	1241.8
Interconnected	95.84	622.11
High-Gain	53.5455	391.16

Table 3.5: State estimation of the heading angle with different observers.

Table 3.6 summarizes the results for the heading angle rate of the WMR for different observers.

Observer	e_s	e_n
PWA	4.9091	256.1591
Sliding Mode	7.5366	63.5366
Backstepping	34.18	1145
Nonlinear Observer With Output Injection	7.8182	226.9091
Interconnected	11.89	402.69
High-Gain	25.39	761.05

Table 3.6: State estimation of the heading angle rate with different observers.

- **Comparison**

All the nonlinear observers that are applied to the WMR model are able to estimate the states of the nonlinear continuous-time system, nonlinear system with a sampled output and nonlinear sampled-data system in the presence of measurement noise with convergent state estimation errors. The PWA observer which is designed for a PWA approximation of the nonlinear system is also able to estimate the states of the system with convergent state estimation error. The state estimation error is still bounded when the output is only available at sampling times and in the presence of measurement noise. In the transient, the PWA observer has a large overshoot for the position estimation error in comparison with other observers. However, the steady state behavior which is defined by e_{rms} is almost the same for all the proposed observers except that the sliding mode observer has a large value for e_{rms} when estimating the position and the heading angle. Moreover, the position estimation error of the sliding mode observer becomes unstable for the gains that yield

lower speed of convergence.

The values of e_s and e_n show that for the position, estimation error of the interconnected observer, the high-gain observer and the backstepping observer have the most increase in the presence of perturbations (sampled-output and measurement noise). Therefore, these observers are less robust to the perturbations than the nonlinear observer with output injection, sliding mode observer and PWA observer.

For the Heading angle the backstepping observer, interconnected observer and nonlinear observer with output injection are the ones with larger values for e_s and e_n. Then, the high-gain observer has the largest value for e_s and e_n. The PWA observer and the sliding-mode observer show the most robustness to the perturbations.

For the heading angle rate, the most and the least robust observers are almost the same as the one for heading angle. The backstepping observer, high-gain observer, nonlinear observer with output injection and interconnected observer are the ones with larger values for e_s and e_n which means they are less robust to the perturbation than the sliding mode observer and the PWA observer.

To conclude, the PWA observer and the sliding mode observer are more robust to perturbations (sampled output and measurement noise). The interconnected observer, backstepping observer, high-gain observer and the nonlinear observer with output injection show less robustness in the presence of measurement noise and in the case that the output is sampled.

The PWA observer is based on a convex optimization approach which can be solved easily using available software packages. The overall performance, robustness and scalability of PWA observer makes this method an alternative approach to design observers for nonlinear systems.

3.6 Summary

In this section a continuous-time PWA observer is designed for a class of nonlinear sampled-data systems. The observer design is based on the PWA approximation of the continuous-time nonlinear system. It is proven that the proposed observer can be used for state estimation of the nonlinear sampled-data system yielding a convergent and ultimately bounded state estimation error. It is shown that the state estimation error converges to a region. The size of the region depends on the PWA approximation error and the sampling time. As the PWA approximation error and/or the sampling time decrease the size of the region decreases. Moreover, it is proven that despite the fact that the presence of the measurement noise is not considered in the design step, the state estimation error of the proposed observer is ultimately bounded in the presence of norm bounded measurement noise. The ultimate bound is proportional to the upper bound on the perturbation terms (approximation error, sampling error, sampling time and noise). This shows the robustness of the proposed observer. Some examples were solved in this chapter and the simulation results showed the application of the proposed theorems.

Chapter 4

Wheeled Mobile Robot Experimental Results

4.1 Introduction

The problem of PWA observer design for a PWA approximation of a class of nonlinear sampled-data systems in the presence of measurement noise is addressed in this thesis. In this chapter, the proposed observer is applied to an experimental setup of a WMR available at the HYCONS Laboratory of Concordia University. The dynamics of the WMR are in the class of nonlinear systems studied in this thesis. Due to the sampling times of the sensors, the output is only available at sampling instants. Therefore, this system is considered a sampled-data system. In addition, the data from the WMR contains measurement noise and this makes the WMR a suitable system for validating the theorems proposed in this thesis.

The WMR modeling and dynamic equations of the WMR are presented in Section 4.2. It is followed by a description of the wireless communication, electronics and sensors of the WMR in Section 4.3. Then, the proposed observer is implemented on the WMR and the results of the state estimation are provided in Section 4.4. The chapter is closed by a
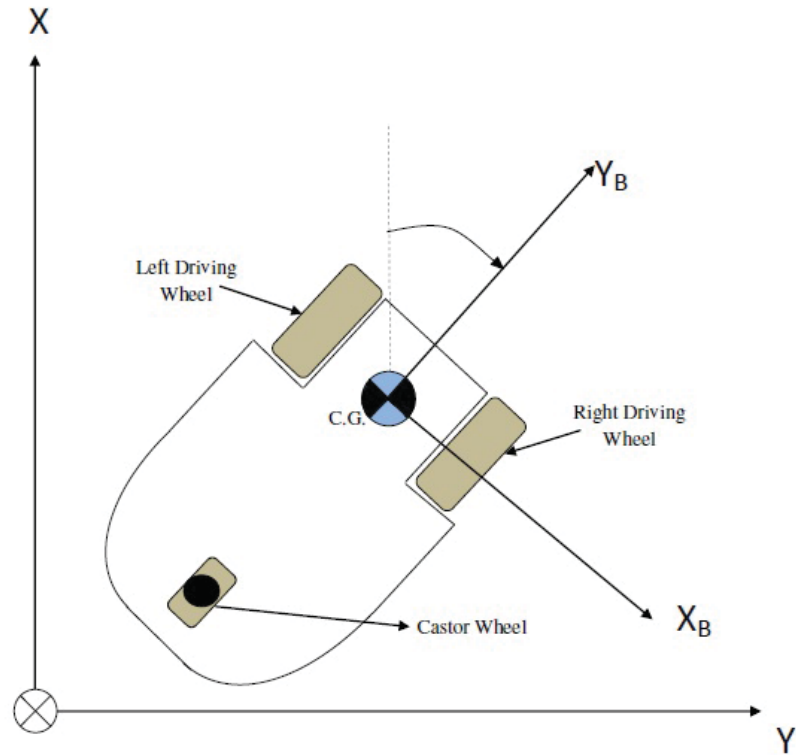
Figure 4.1: WMR schematic [2].

brief summary in Section 4.5.

4.2 Wheeled Mobile Robot Modeling

Figures 4.1 and 4.2 show the schematic and experimental setup of the WMR available at the HYCONS Laboratory of Concordia University, respectively.

The dynamic equations of the WMR are as follows

$$\dot{y} = u_0 sin \psi$$

$$\dot{\psi} = R$$

$$\dot{R} = \frac{M}{I}$$

(4.1)

where y is the signed distance to the x axis, ψ is the heading angle and R is the heading angle rate of the WMR. There exist two inputs for the WMR system: velocity and torque.

91
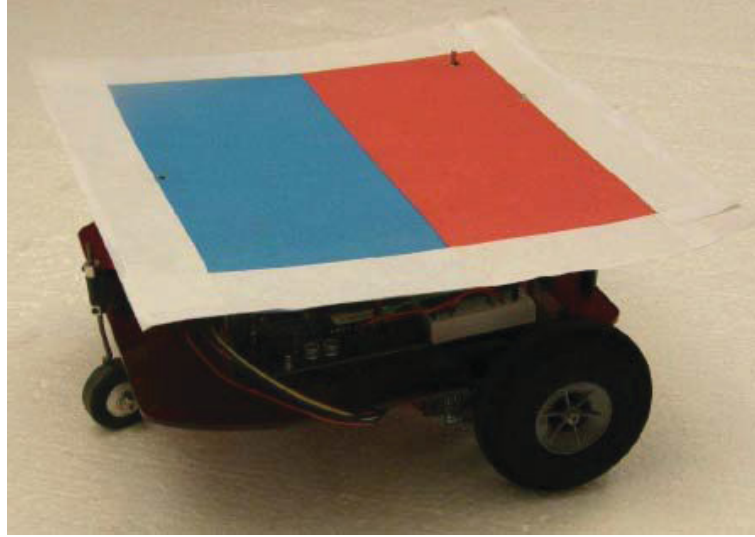
Figure 4.2: Experimental setup of the WMR available at the HYCONS Laboratory of Concordia University [2].

The torque input is defined by M and the forward velocity u_0 is assumed to be constant. Therefore, only one input is considered in the model of the system.

The constant velocity $u_0 = 0.04\frac{m}{s}$ is measured for this system. The moment of inertia I is calculated from data. Table 4.1 and Figure 4.3 show the data used for identification of the moment of inertia I. Different steering inputs are given to the WMR. It turns around and the period is measured. The data from Table 4.1 is approximated by a linear function as shown in Figure 4.3. According to Figure 4.3, the slope of the line is $\frac{1}{I} = 0.1154\frac{1}{kg.m^2}$ and as a result, the moment of inertia is $I = 8.6655 kg.m^2$.

Steering Input (PWM)	Period T_p (sec)	$\psi = \frac{2\pi}{T_p}$
0	0	0
2	13.8	0.4553
4	8.6	0.7306
6	7.2	0.8727
8	5.7	1.1023
10	4.7	1.3368
12	4.3	1.4612
14	3.9	1.6111
16	3.6	1.7453
18	3.5	1.7956

Table 4.1: WMR Data.
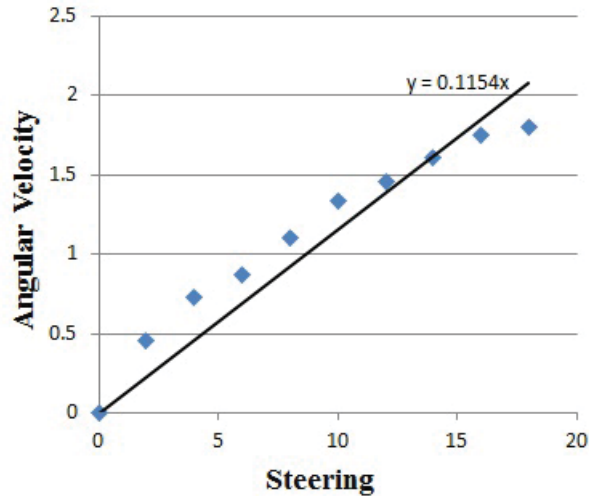
Figure 4.3: Moment of inertia identification.

4.3   Wireless Communication, Electronics and Sensors

The experimental setup of the WMR located at the HYCONS Laboratory of Concordia University consists of the WMR, two Xbee wireless communication modules, one Arduino Atmega328 board, one camera, one battery and a server computer. As shown in Figure 4.1, the WMR has two driving wheels and a castor wheel. It has two DC motors for generating torque as the input of the two driving wheels.

Sending commands to the WMR is performed through wireless communication. In this system, Xbee is used for wireless communication. Xbee is a Commercial-Off-The-Shelf (COTS) hardware that uses the ZigBee standard [182, 183]. The ZigBee standard features a good compromise of low power consumption and long distance range [182, 184]. Two Xbee modules are used for sending the commands from the computer and receiving the commands by the WMR. The first Xbee is connected to the computer and the second one is installed on the WMR. One of the advantages of Xbee is its low weight and small size which makes it suitable for using on the WMR. Figures 4.4 and 4.5 show the Xbees connected to the computer and implemented on the WMR, respectively.

An Arduino Mega Board that is shown in Figure 4.6 is used on the WMR to process the commands received by the Xbee. The Arduino Mega Board is a powerful, open source

Figure 4.4: Xbee connected to the server computer.

Figure 4.5: Xbee on the WMR.

and low cost board [182]. It features a platform development environment on C++ with several libraries [182]. Moreover, the Arduino Mega has many digital input/output and analog pins that can be used for tests and further development. For example, adding new sensors or actuators.

To measure the horizontal position x and the vertical position y of the WMR, a camera is mounted on the workspace and is connected to the computer. The camera gives the position by digital image processing [185]. Two markers (red and blue) are placed on the WMR which are the center of the red rectangle and the blue rectangle shown in Figure 4.2. The camera captures images and these images are processed in the server computer running Matlab/Simulink in real-time using the RTsync Blockset [182, 186]. The captured images are processed by a custom S-function block that is running code written in C++ using the OpenCV library to identify the markers and output the positions x and y of the

94
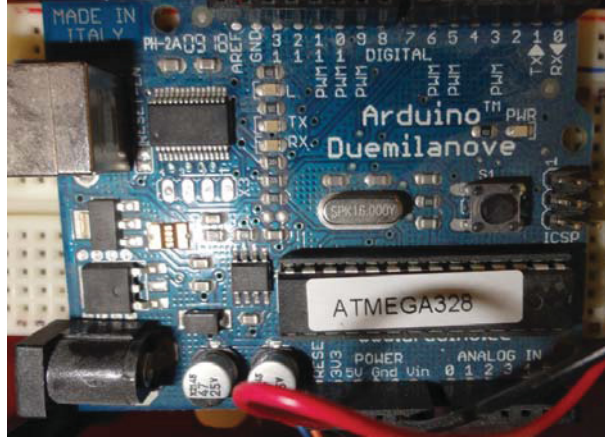
Figure 4.6: Arduino Mega board.

WMR [182, 187]. Figure 4.7 shows the camera used in this experiment.

The images captured by the camera contain noise. Noise exists in any electronic device that transmits or receives a signal. Image noise is a random change in brightness or color information in images and is considered electronic noise [41]. One of the common types of image noise is white Gaussian noise [41].

The heading angle ψ is calculated by using the information from the horizontal position x and the vertical position y, as follows

$$\psi = \arctan(\frac{Y_R - Y_B}{X_R - X_B}) \tag{4.2}$$

where Y_R, Y_B, X_R and X_B are the vertical position of the red marker, vertical position of the blue marker, horizontal position of the red marker and horizontal position of the blue marker, respectively.

There is no sensor on the WMR to measure the heading angle rate. One is able to have information about all the states of the system by implementing the observer on the WMR setup.

All the data are processed in the server computer using MATLAB and a MEX file written in C++. The commands from the server computer are sent through Xbee wireless communication to the Arduino Mega board installed on the WMR, which is connected to the DC motors.

Figure 4.7: Camera used for image processing.

The power required for the motors, Arduino Mega board and Xbee wireless communication is provided by a rechargeable Lithium-ion Polymer (LiPo) battery shown in Figure 4.8. In order to recharge the battery a Turnigy Accucell-6 charger 9 should be used, which is shown in Figure 4.9.

Figure 4.10 illustrates the communication of each part of the system with other parts.

4.4 Implementation of the Continuous-Time Piecewise-Affine Observer on the Wheeled Mobile Robot

In this section an observer is designed and implemented on the WMR. The method of observer design is based on the theorems proposed in Chapter 3. Before presenting the results of the state estimation, the model of the WMR is validated using the data from the

Figure 4.8: Lipo battery.

WMR experimental setup.

In order to perform the model validation, the same input and the same constant forward velocity are considered for the experimental setup and the Simulink model of the WMR and the outputs are compared. Moreover, both systems have started from the same initial conditions.

Figures 4.11 and 4.12 depict the comparative studies related to the outputs (the position and the heading angle) of the real system and the simulation model.

The e_{rms} between these results as defined in (3.123) are provided in Table 4.2 which are small errors and validate the WMR modeling.

State	e_{rms}
y (m)	0.0095
ψ (rad)	0.1148

Table 4.2: Model Validation.

Now, an observer is designed to estimate the states of the WMR. In order to design the observer, a PWA approximation of the nonlinear system defined in (4.1) is obtained as follows

Figure 4.9: Turnigy Accucell-6 charger 9.

$$\forall X \in R_1$$

$$
\begin{bmatrix} \dot{y} \\ \dot{\psi} \\ \dot{R} \end{bmatrix} = \begin{bmatrix} 0 & 0.04 & 0 \\ 0 & 0 & 1 \\ 0 & 0 & 0 \end{bmatrix} \begin{bmatrix} y \\ \psi \\ R \end{bmatrix} + \begin{bmatrix} 0 \\ 0 \\ 0 \end{bmatrix} + \begin{bmatrix} 0 \\ 0 \\ 0.1154 \end{bmatrix} M
$$

(4.3)

$$\forall X \in R_2$$

$$
\begin{bmatrix} \dot{y} \\ \dot{\psi} \\ \dot{R} \end{bmatrix} = \begin{bmatrix} 0 & -0.025 & 0 \\ 0 & 0 & 1 \\ 0 & 0 & 0 \end{bmatrix} \begin{bmatrix} y \\ \psi \\ R \end{bmatrix} + \begin{bmatrix} 0.08 \\ 0 \\ 0 \end{bmatrix} + \begin{bmatrix} 0 \\ 0 \\ 0.1154 \end{bmatrix} M
$$

where $X = [y; \psi; R]$ and R_1 and R_2 are defined in (3.94) and (3.95), respectively. Since the position y is measured and the heading angel ψ can be obtained using (4.2), the output is given by $y = CX$ where

$$
C = \begin{bmatrix} 1 & 0 & 0 \\ 0 & 1 & 0 \end{bmatrix}
$$

(4.4)

98
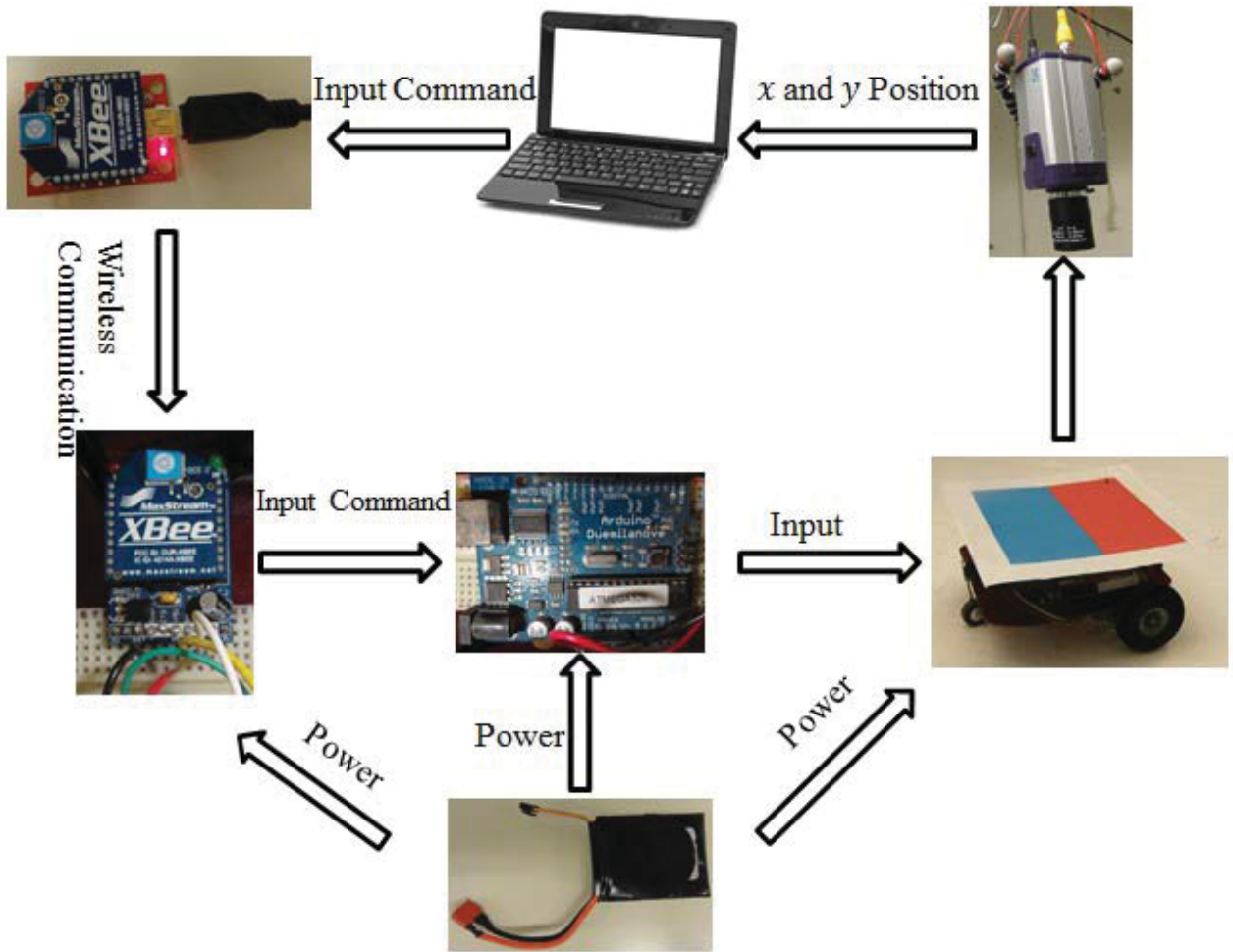
Figure 4.10: Structure of the experimental setup.
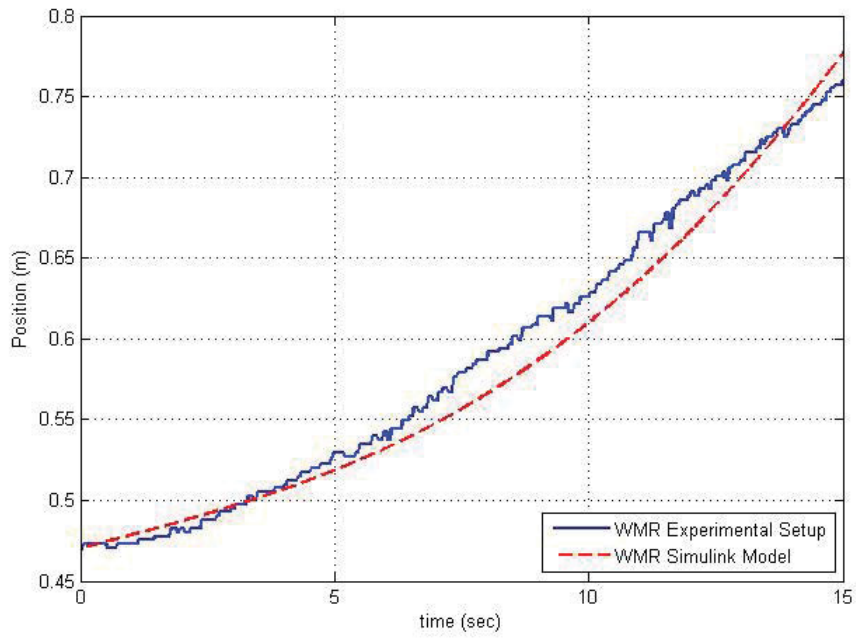
Figure 4.11: Position of the WMR experimental setup and the simulation model.
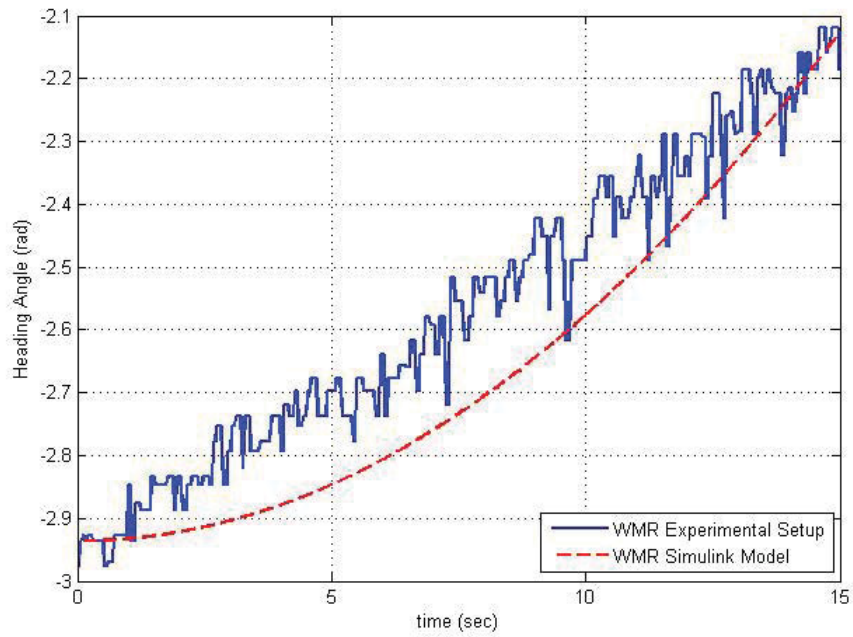
Figure 4.12: Heading Angle of the WMR experimental setup and the simulation model.

100

The LMIs defined in Lemma 3.2.1 are solved for this system using SeDuMi [171] and YALMIP [172] in MATLAB. By considering $\alpha = 1.67$ the following observer gains are obtained,

$$L_1 = \begin{bmatrix} 105.6599 & -132.1558 \\ -6.7757 & 11.0076 \\ -8.0716 & 21.3562 \end{bmatrix} \tag{4.5}$$

$$L_2 = \begin{bmatrix} 107.0414 & -132.0185 \\ -6.8648 & 10.9962 \\ -8.1904 & 21.3366 \end{bmatrix} \tag{4.6}$$

By placing the WMR in a random position of the workspace, the initial conditions of the system are unknown and the initial conditions of the observer are set to

$$\hat{x}_0 = \begin{bmatrix} 0 & 0 & 0 \end{bmatrix}^T \tag{4.7}$$

The observer is implemented in the computer and applied to the WMR experimental setup. The experiments are performed for the open loop system which means no controller is implemented on the system. The WMR turns around and moves while the camera captures images and by using digital image processing the output is given to the observer. The observer performs the state estimation online based on the information from the image processing and the input. Also, simulations are performed for this observer and the results are provided.

In Figure 4.13 the position y measured by the camera and the estimated position, which is obtained by the observer are plotted. Although the real value and the estimated value are different at the initial time, after a short time the estimated position has converged to the real value of the position.

The heading angle ψ calculated by the information from the camera and the estimated heading angle, which is obtained by the observer are depicted in Figure 4.14. The values of the real heading angle and the estimated heading angle are different at the initial time, but after a few seconds the estimated value has converged to the real value.
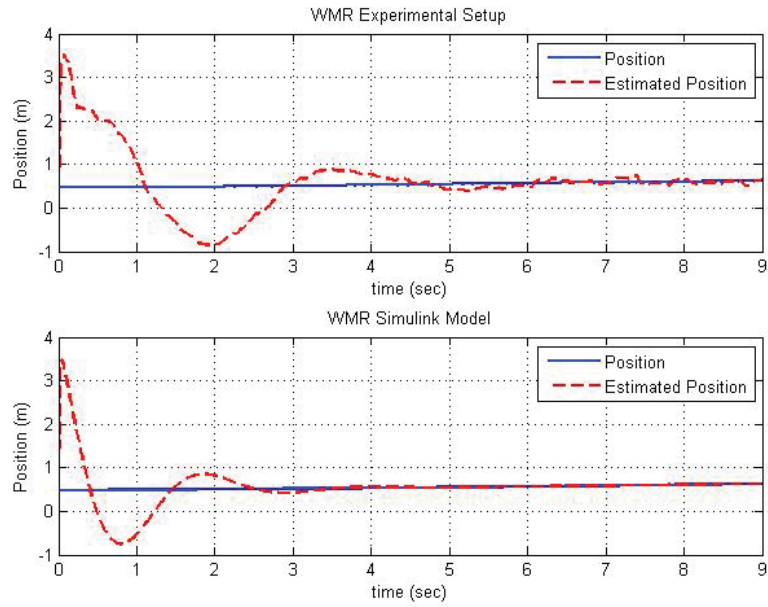
Figure 4.13: Position "*y*" estimation of the WMR, using a PWA observer.
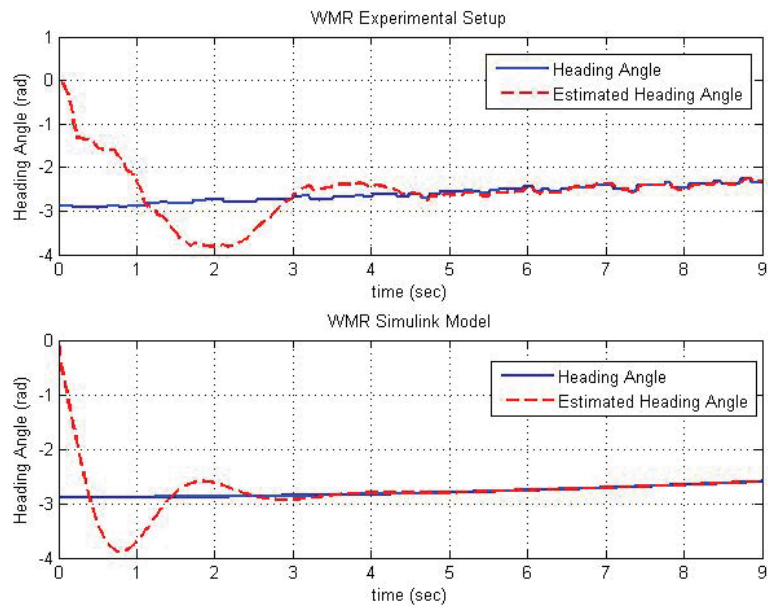
Figure 4.14: Heading angle "*ψ*" estimation of the WMR, using a PWA observer.

102
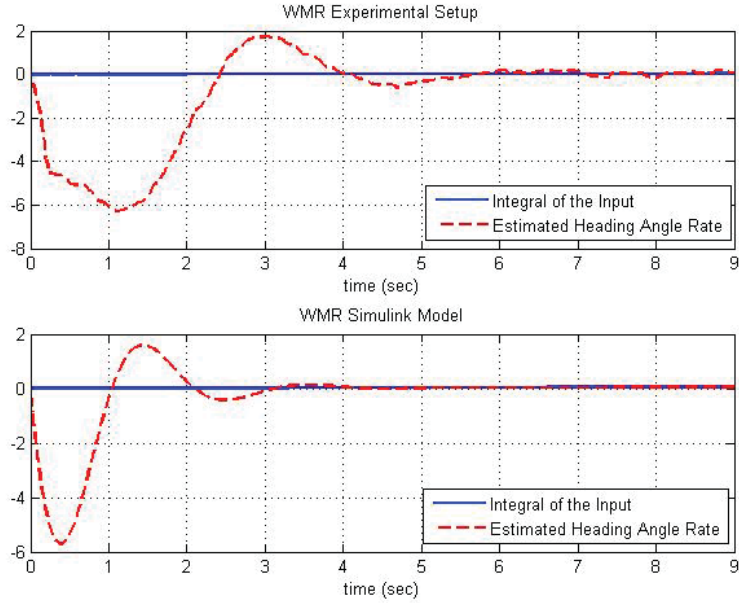
Figure 4.15: Heading angle rate "R" estimation of the WMR, using a PWA observer.

Figure 4.15 shows the estimation of the heading angle rate R. Since the heading angle rate is not being measured, there is no real value to compare with the estimated value. However, since the obtained result needs to be validated, the following equation is considered,

$$\dot{R} = \frac{M}{I} \tag{4.8}$$

which means integrating $\frac{M}{I}$, yields the heading angle rate. Therefore, to validate the results, the estimated value of the heading angle rate is compared to the integral of the $\frac{M}{I}$. Figure 4.15 shows that the heading angle rate is estimated correctly.

Using a zero order hold the output of the system is then sampled with the sampling time $T = 0.2s$ and the results of the state estimation are provided in Figures 4.16, 4.17 and 4.18. It is shown that the estimated values of the position, heading angle and heading angle rate have converged to small regions around the real values.

Then, in order to experiment the performance of the PWA observer for larger sampling times, the data given to the observer is sampled with the sampling time $T = 0.9s$ and the results of the state estimation are provided in Figures 4.19, 4.20 and 4.21. Figures 4.19,
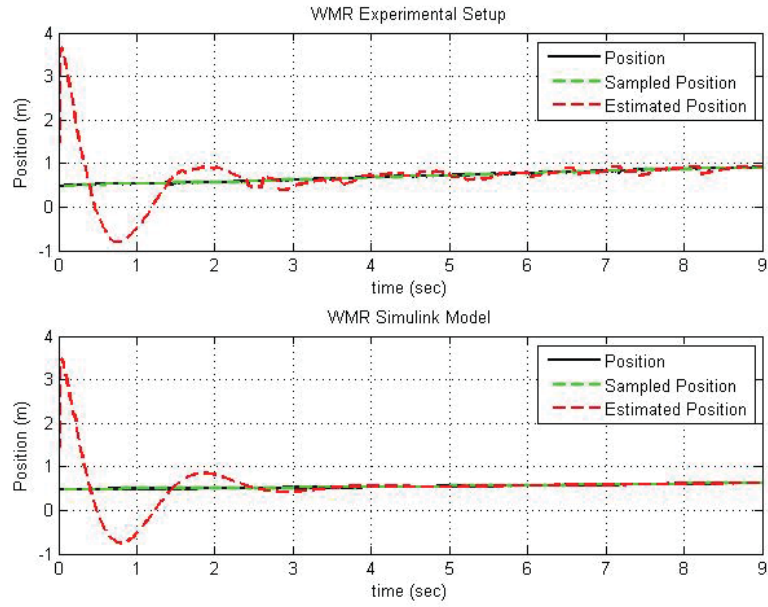
Figure 4.16: Position "*y*" estimation of the WMR sampled-data ($T = 0.2s$), using a PWA observer.
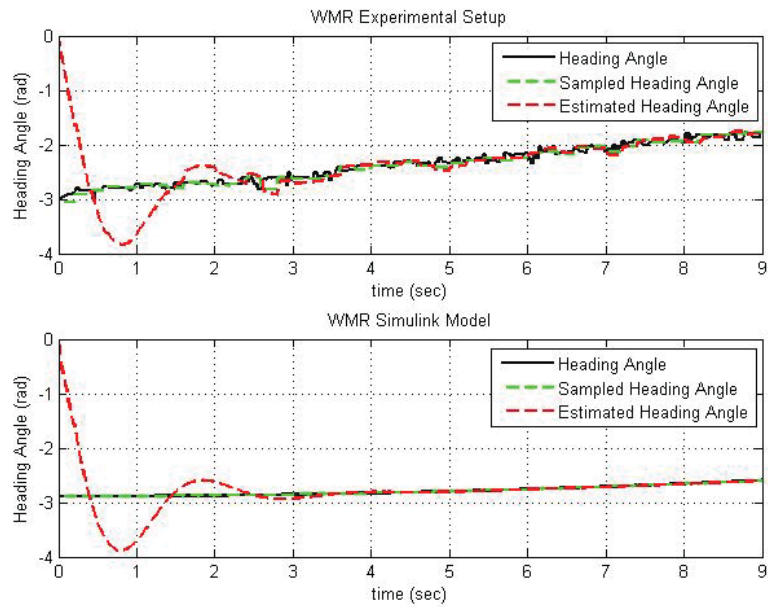
Figure 4.17: Heading angle "ψ" estimation of the WMR sampled-data ($T = 0.2s$), using a PWA observer.
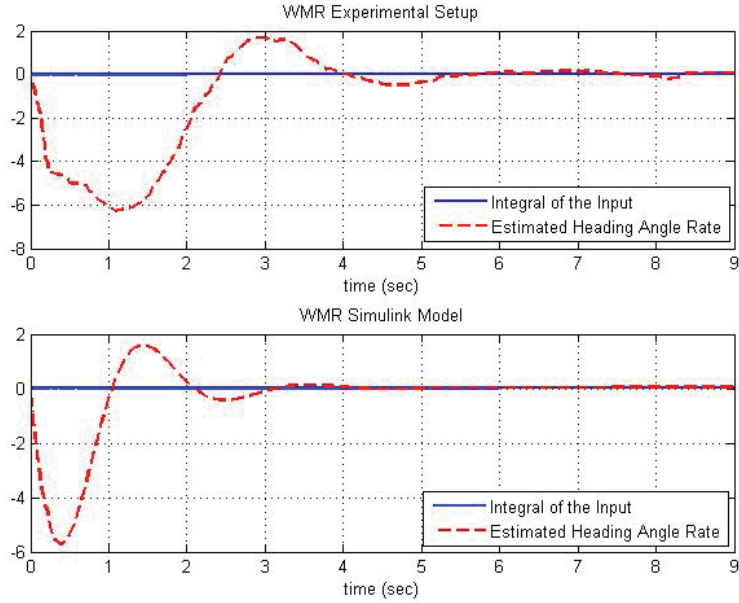
Figure 4.18: Heading angle rate "R" estimation of the WMR sampled-data ($T = 0.2s$), using a PWA observer.

4.20 and 4.21 show that the estimated values of the position, the heading angle and the heading angle rate have converged to small regions around the real values.

Now, all the nonlinear observers that are studied in Chapter 3 are implemented on the system. In the practical implementation the gains of the observers are designed such that $t_s \leqslant 3$. The conclusions are drawn after performing the experiments for different initial conditions. Also, in order to evaluate the performance of the observers for larger sampling times the sampling time $T = 0.2s$ is considered for the outputs and experiments are performed. Since, noise already exists in the system it is not possible to compare the observers in aspect of robustness to the noise as done in Chapter 3. However, all the observers are compared based on their steady state performance and transient performance. All the results are summarized in Tables 4.3 and 4.4 and then compared.

• **Backstepping Observer**

In this part, the backstepping observer is implemented on the WMR. The results of the state estimation are shown in Figures 4.22, 4.23 and 4.24. All the states are estimated correctly after a short time and the state estimation errors have converged.
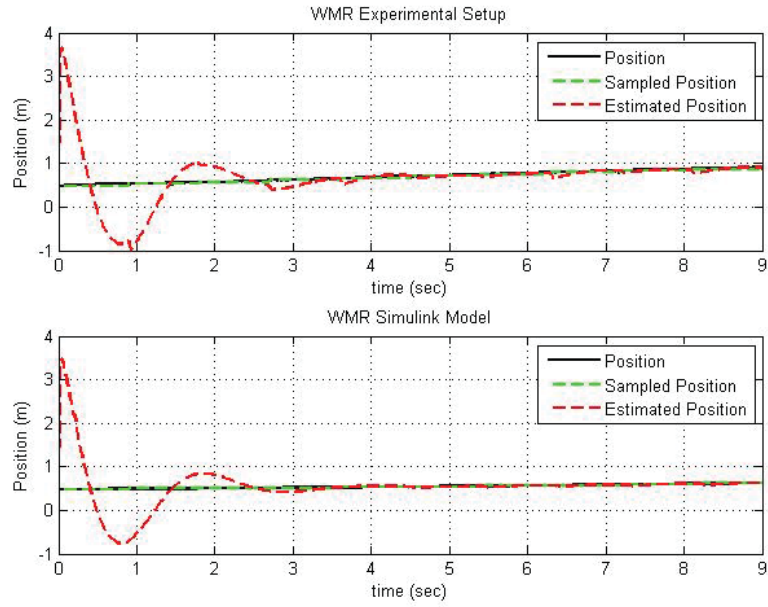
Figure 4.19: Position "y" estimation of the WMR sampled-data ($T = 0.9s$), using a PWA observer.
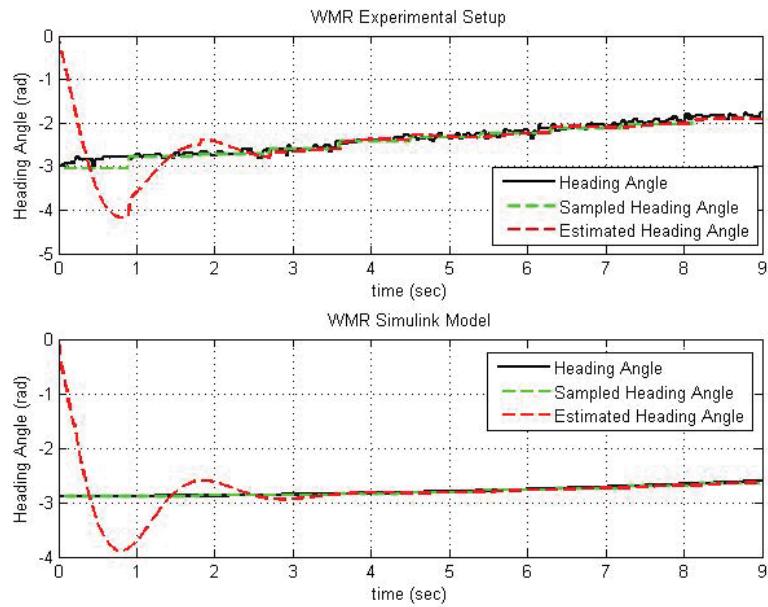
Figure 4.20: Heading angle "ψ" estimation of the WMR sampled-data ($T = 0.9s$), using a PWA observer.
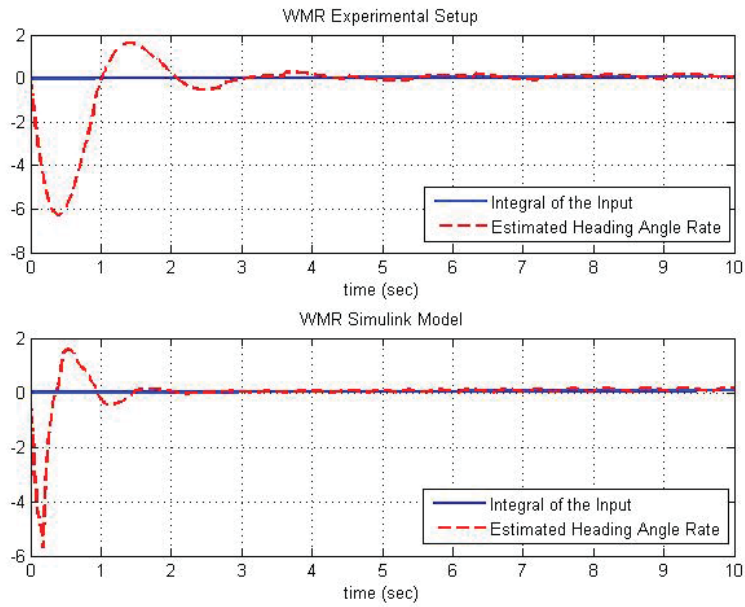
Figure 4.21: Heading angle rate "R" estimation of the WMR sampled-data ($T = 0.9s$), using a PWA observer.
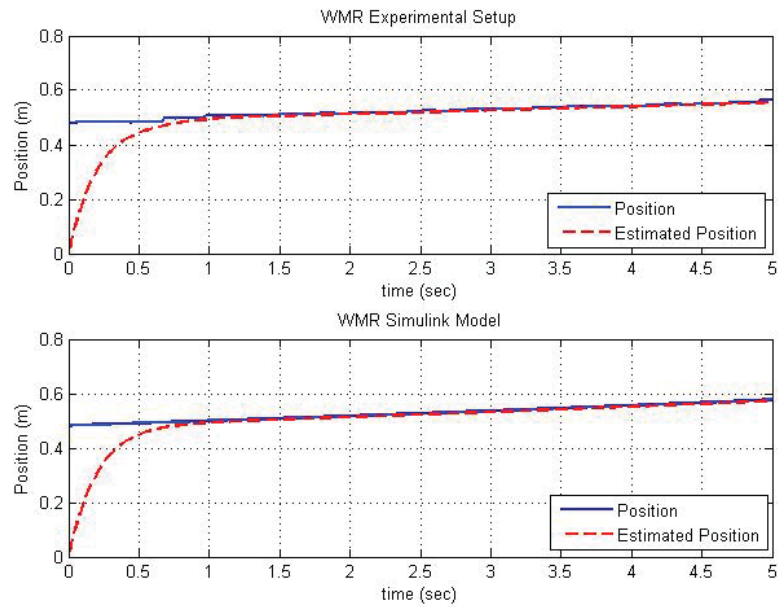
Figure 4.22: Position "y" estimation of the WMR, using a backstepping observer.
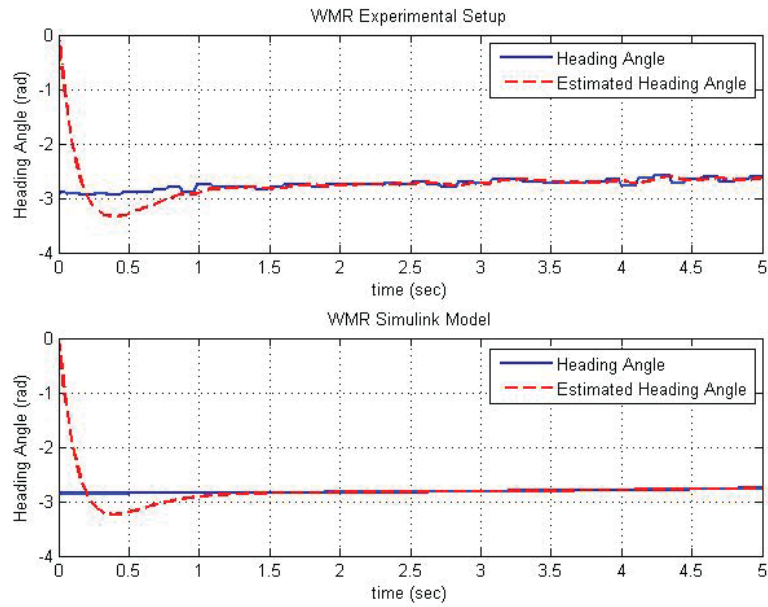
Figure 4.23: Heading angle "ψ" estimation of the WMR, using a backstepping observer.
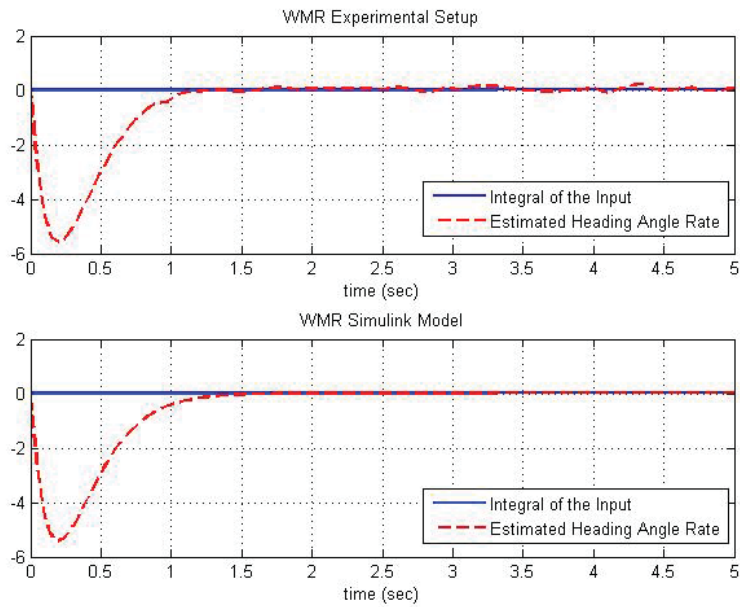
Figure 4.24: Heading angle rate "R" estimation of the WMR, using a backstepping observer.

108
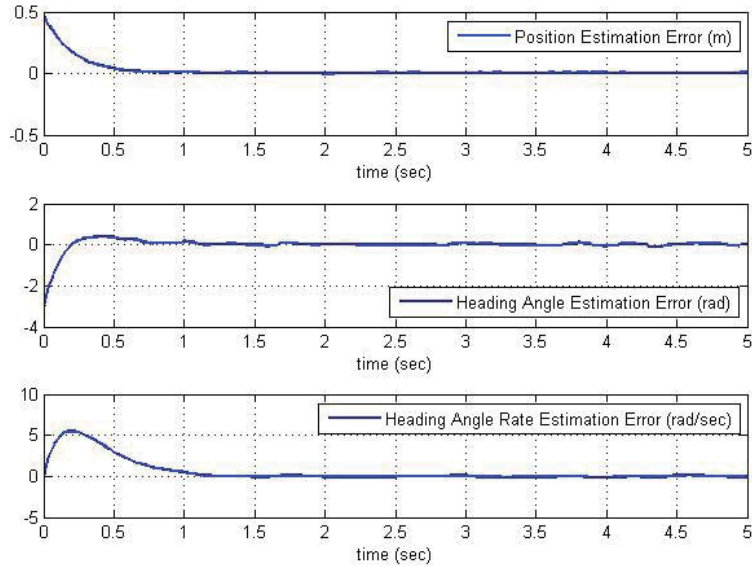
Figure 4.25: State estimation errors of real setup of the WMR sampled-data ($T = 0.2s$) experimental setup, using a backstepping observer.

The output of the system is sampled with sampling time $T = 0.2s$ and the state estimation errors are plotted in Figure 4.25.

- **Sliding Mode Observer**

The sliding mode observer is applied to the WMR system. The chattering phenomenon occurs and it is not possible to execute the real-time program. Therefore, the *sign* functions are changed to *saturation* function and the results of the state estimation are provided in Figures 4.26, 4.27 and 4.28.

In this part the sampling time $T = 0.2s$ is considered for the output of the system. The state estimation errors are shown in Figure 4.29.

- **Interconnected Observer**

In this part the interconnected observer is implemented on the WMR. The results of the estimation and estimation error of the position, the heading angle and the heading angle rate are shown in Figures 4.30, 4.31 and 4.32, respectively.

In this part the output of the system is sampled with sampling time $T = 0.2s$. The state estimation errors are shown in Figure 4.33.

109
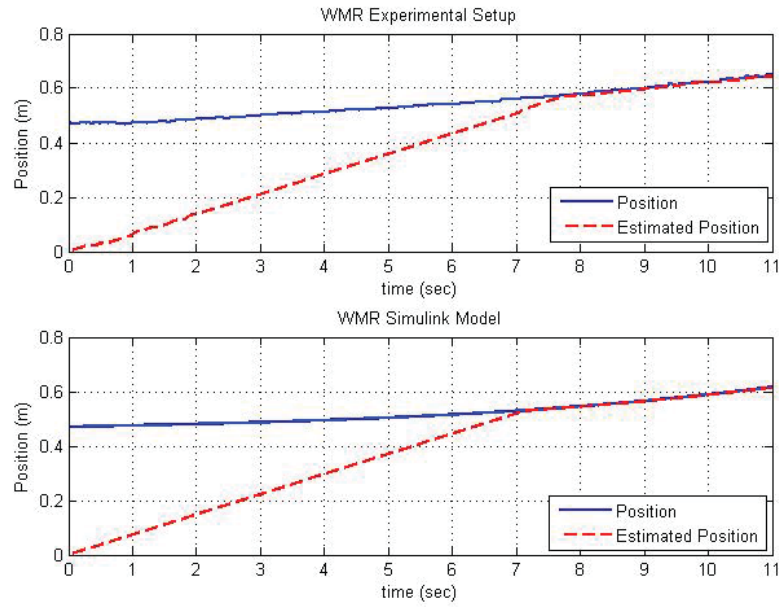
Figure 4.26: Position "y" estimation of the WMR, using a sliding mode observer.
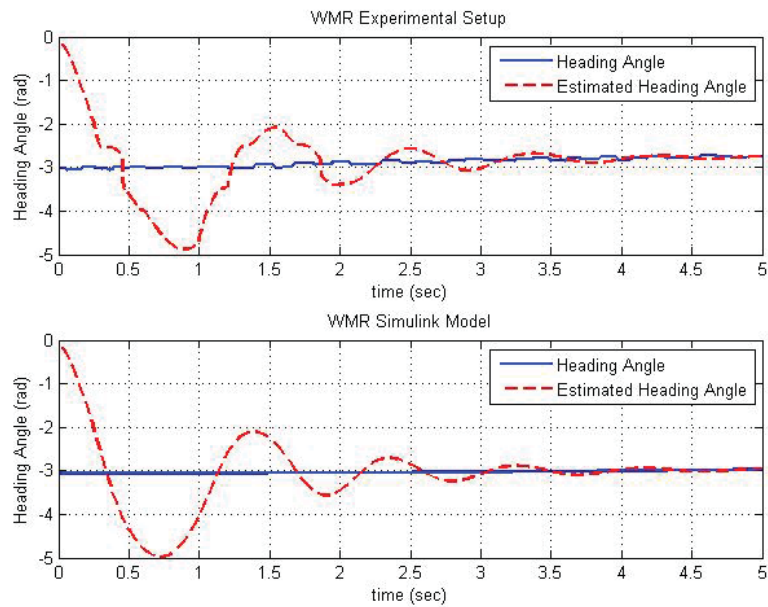
Figure 4.27: Heading angle "ψ" estimation of the WMR, using a sliding mode observer.
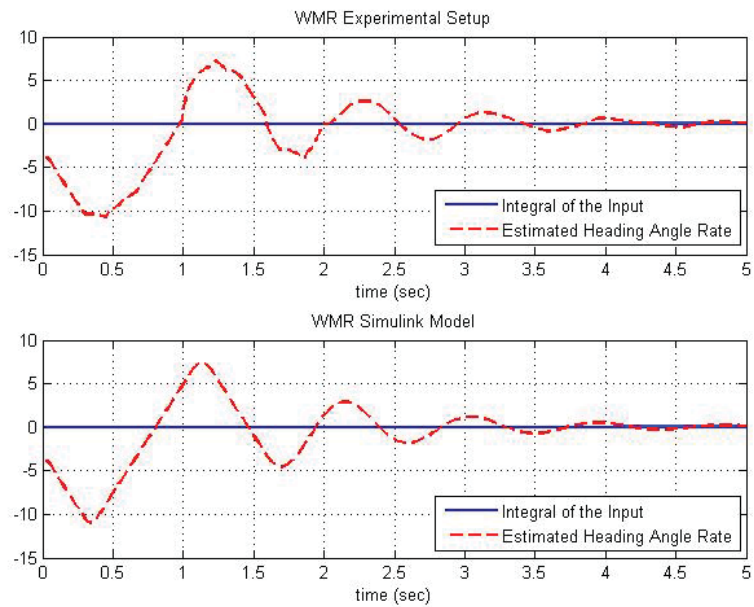
Figure 4.28: Heading angle rate "R" estimation of the WMR, using a sliding mode observer.
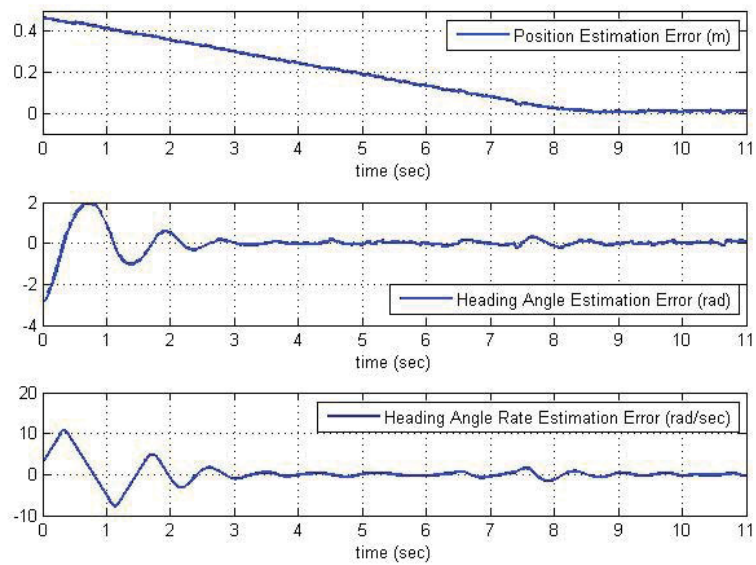
Figure 4.29: State estimation errors of real setup of the WMR sampled-data ($T = 0.2s$) experimental setup, using a sliding mode observer.
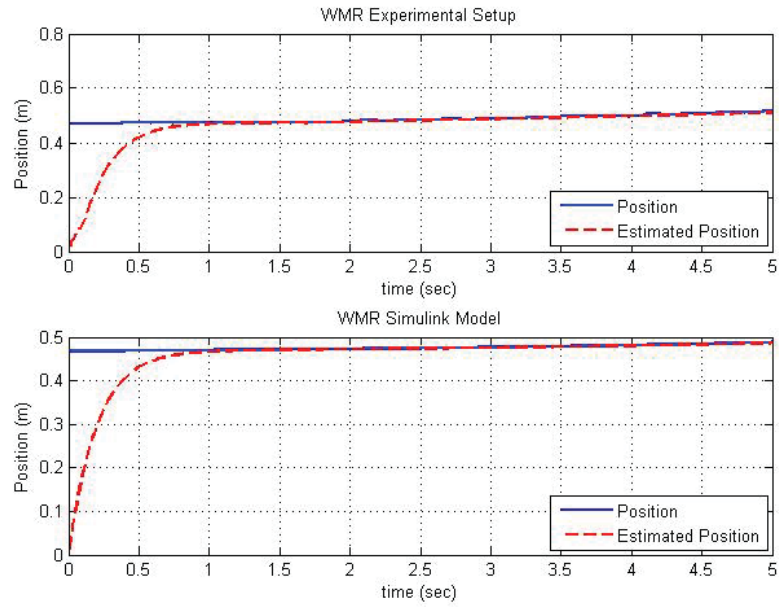
Figure 4.30: Position "*y*" estimation of the WMR, using an interconnected observer.
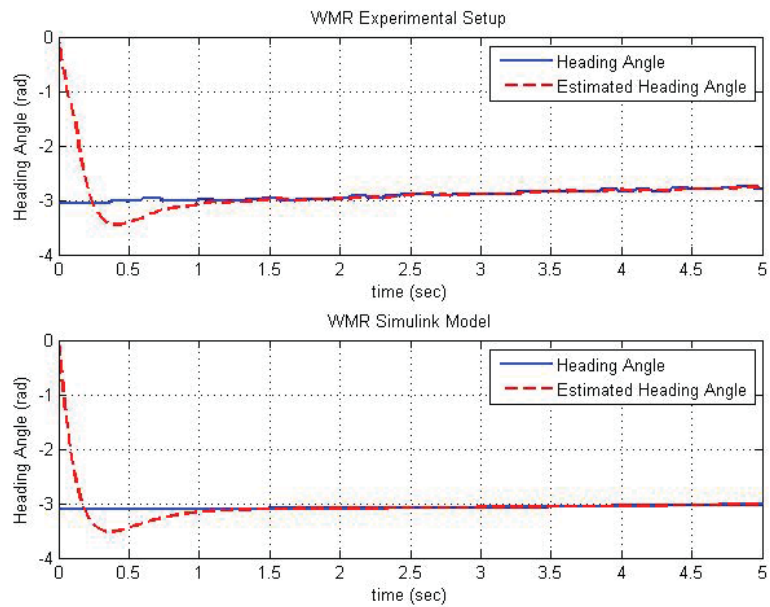
Figure 4.31: Heading angle "ψ" estimation of the WMR, using an interconnected observer.
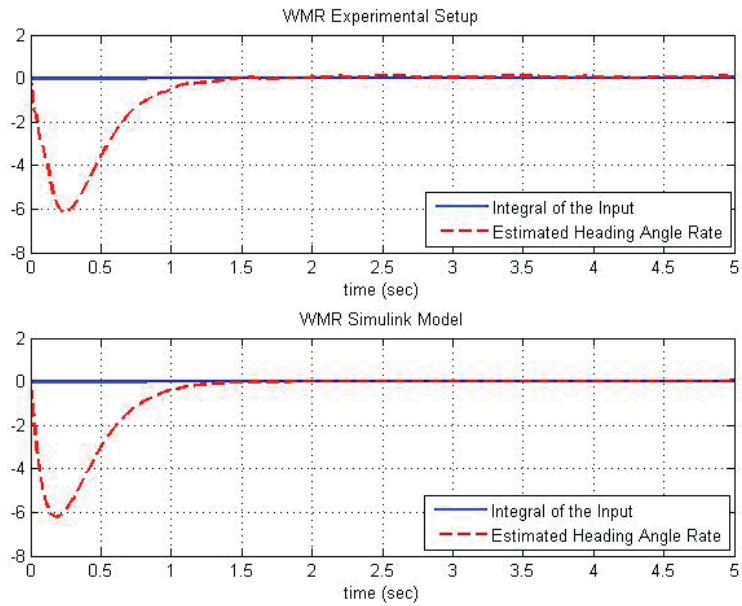
Figure 4.32: Heading angle rate "*R*" estimation of the WMR, using an interconnected observer.
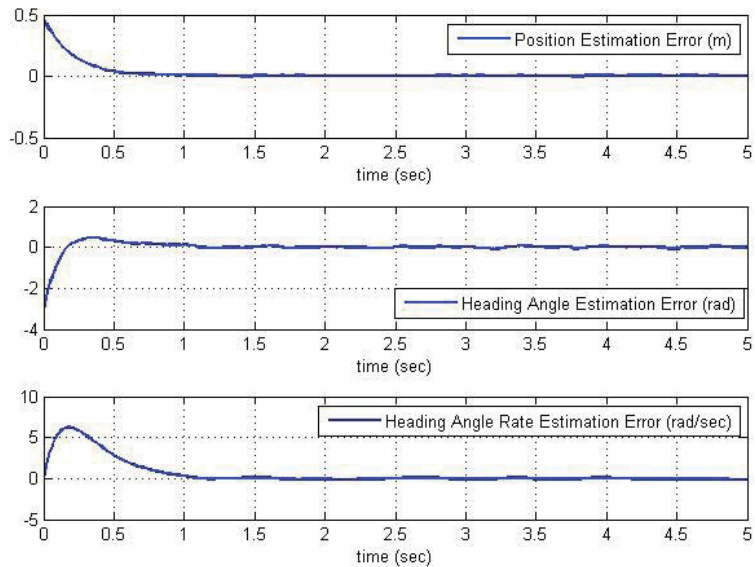
Figure 4.33: State estimation errors of real setup of the WMR sampled-data ($T = 0.2s$) experimental setup, using an interconnected observer.
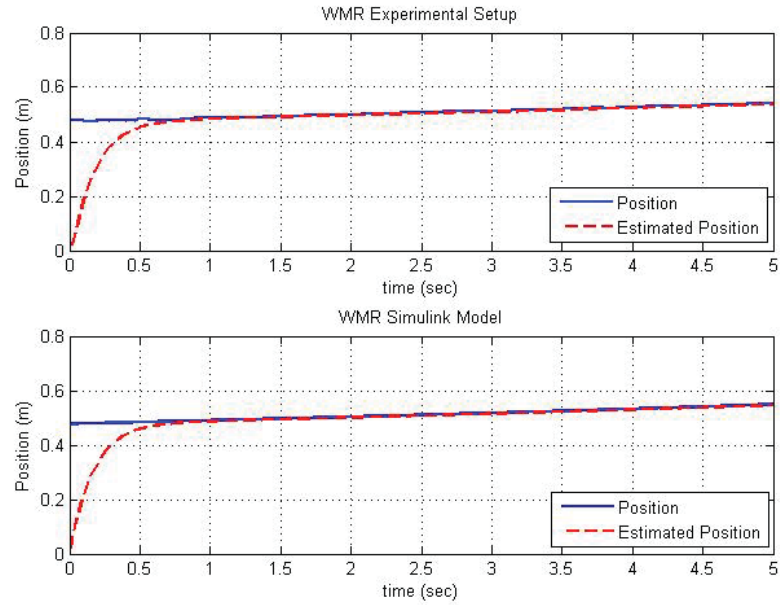
Figure 4.34: Position "*y*" estimation of the WMR, using a nonlinear observer with output injection.

- **Nonlinear Observer With Output Injection**

The nonlinear observer with output injection is applied to the WMR system and the results of the state estimation are shown in Figures 4.34, 4.35 and 4.36.

The sampling time $T = 0.2s$ is considered for the output of the system. The position estimation error, the heading angle estimation error and the heading angle rate estimation error are shown in Figure 4.37.

- **High-Gain Observer**

In this part the high-gain observer is implemented on the WMR. The estimation and estimation error of the position, the heading angle and the heading angle rate are shown in Figures 4.38, 4.39 and 4.40, respectively.

In this part the sampling time $T = 0.2s$ is considered for the output of the system and the state estimation errors are shown in Figure 4.41.

- **Piecewise-Affine Observer**

In this part a PWA observer is designed such that it yields the desired speed of convergence for the state estimation errors ($t_s \leqslant 3$) to be comparable with other nonlinear

114
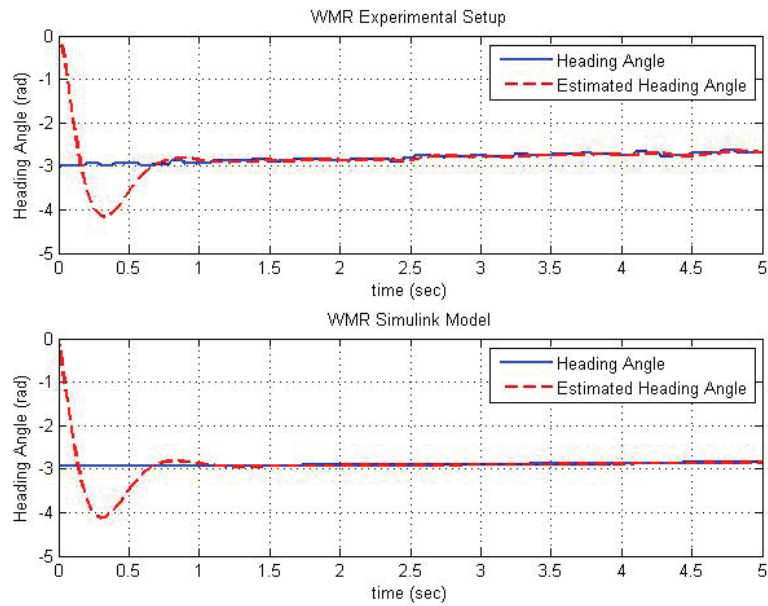
Figure 4.35: Heading angle "ψ" estimation of the WMR, using a nonlinear observer with output injection.
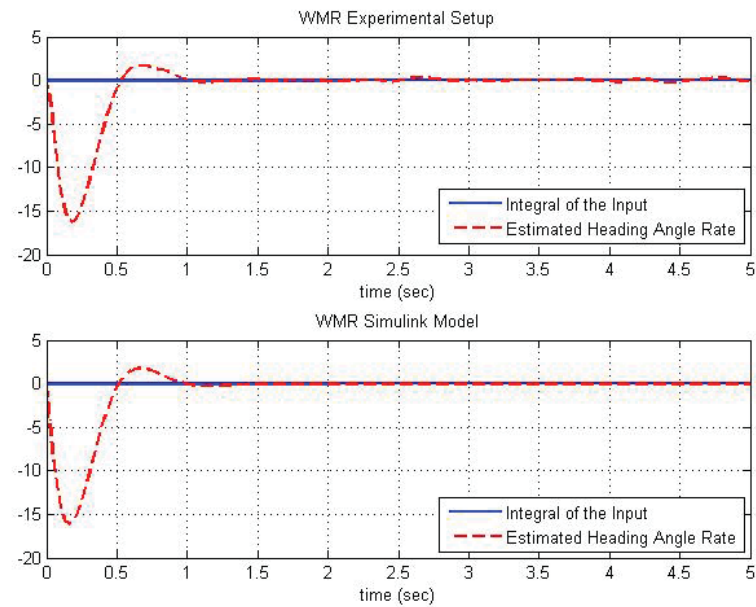
Figure 4.36: Heading angle rate "R" estimation of the WMR, using a nonlinear observer with output injection.
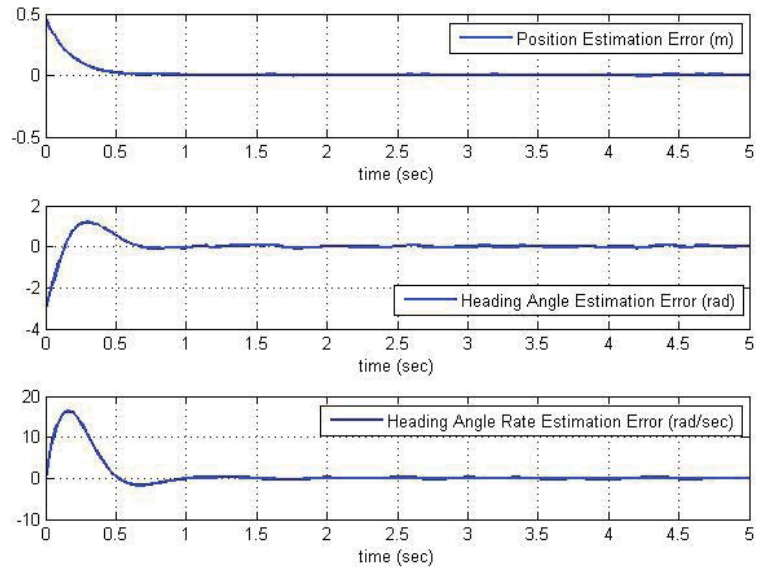
Figure 4.37: State estimation errors of real setup of the WMR sampled-data ($T = 0.2s$) experimental setup, using nonlinear observer with output injection.
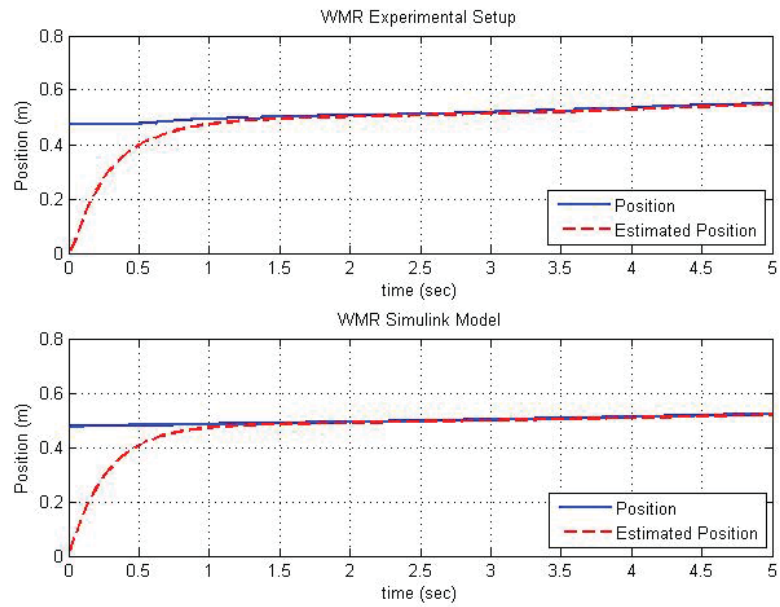
Figure 4.38: Heading angle "ψ" estimation of the WMR, using high-gain observer.
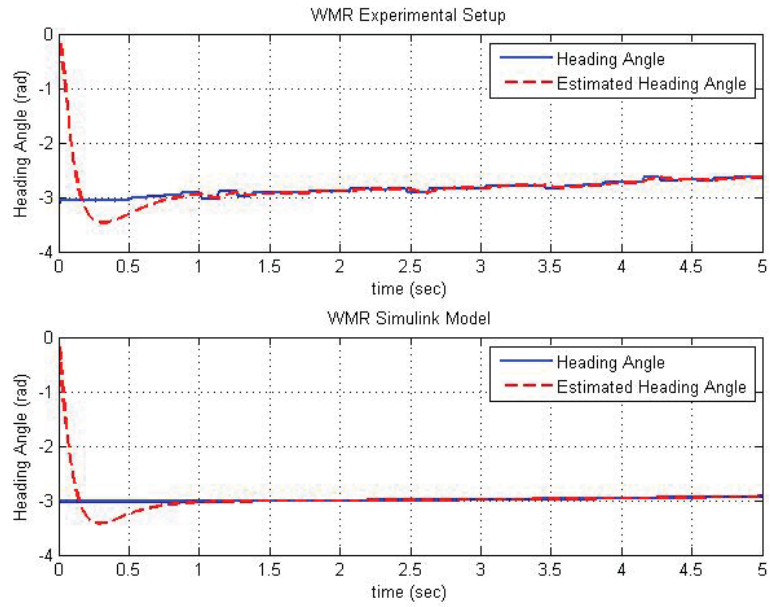
Figure 4.39: Heading angle "ψ" estimation of the WMR, using high-gain observer.
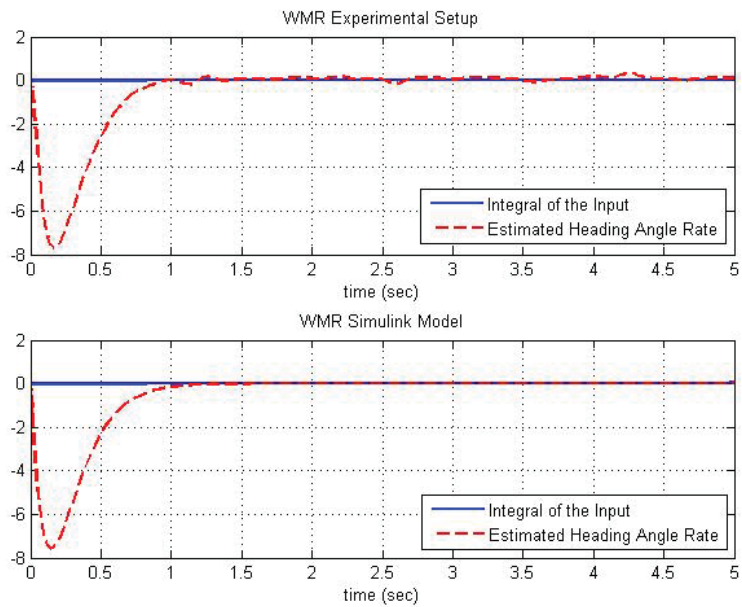
Figure 4.40: Heading Angle Rate "R" estimation of the WMR, using high-gain observer.
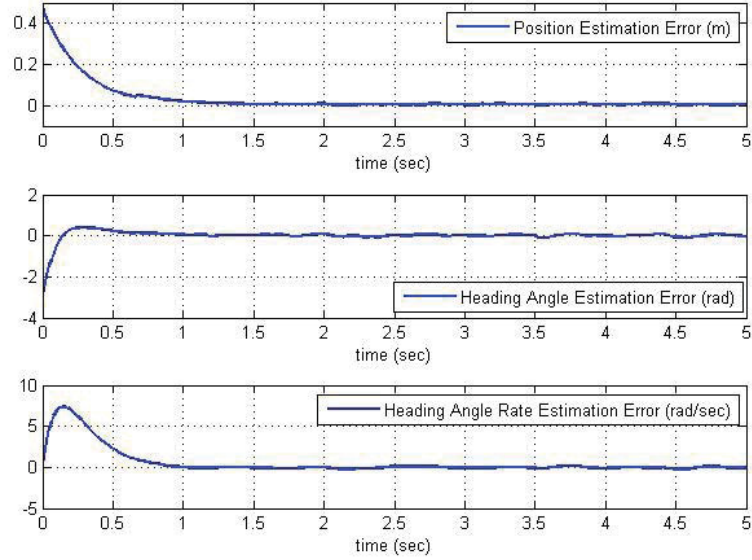
Figure 4.41: State estimation errors of real setup of the WMR sampled-data system ($T = 0.2s$), using high-gain observer.

observers. The PWA observer is implemented on the WMR. The results of the estimation and estimation error of the position, the heading angle and the heading angle rate are shown in Figures 4.42, 4.43 and 4.44, respectively. In this part the output of the system is sampled with sampling time $T = 0.2s$. The state estimation errors are shown in Figure 4.45.

Tables 4.3 and 4.4 summarize the results of the state estimation for the WMR system for different observers. Note that for the position y the maximum error in the transient (e_{max}) occurs at the initial condition and therefore it is not provided in the table.

Observers	Transient Performance (e_{max})		Steady State Performance (e_{rms})		
	ψ	R	y	ψ	R
PWA	0.7505	11.0954	0.0017	0.0422	0.158
Sliding Mode	1.8805	10.7923	0.0035	0.0556	0.2899
Backstepping	0.4352	5.5699	0.0066	0.0337	0.0829
High-Gain	0.4128	7.6748	0.0087	0.0358	0.1011
Output Injection	1.1807	16.2459	0.0065	0.0367	0.1194
Interconnected	0.4338	6.1442	0.0067	0.0313	0.0746

Table 4.3: Different observers implemented on the nonlinear WMR experimental setup.

To conclude, all the implemented observers are able to estimate the states of the
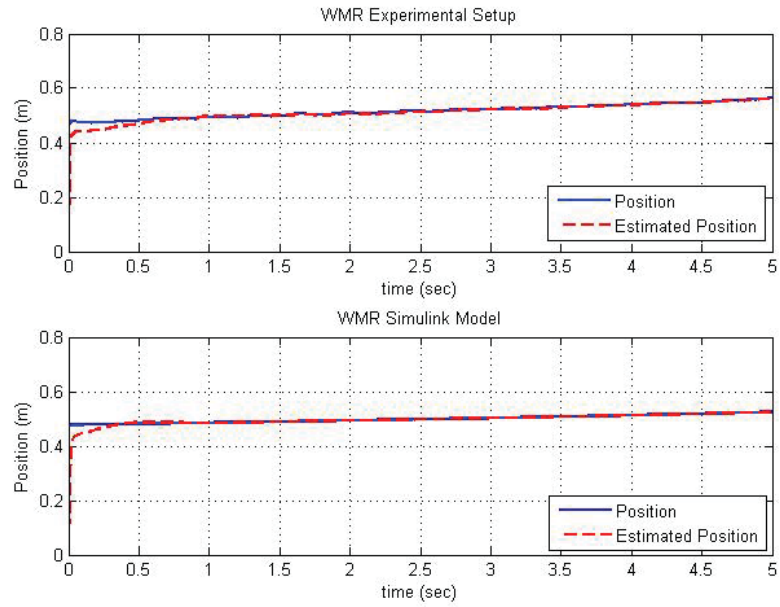
Figure 4.42: Position "*y*" estimation of the WMR, using PWA observer.
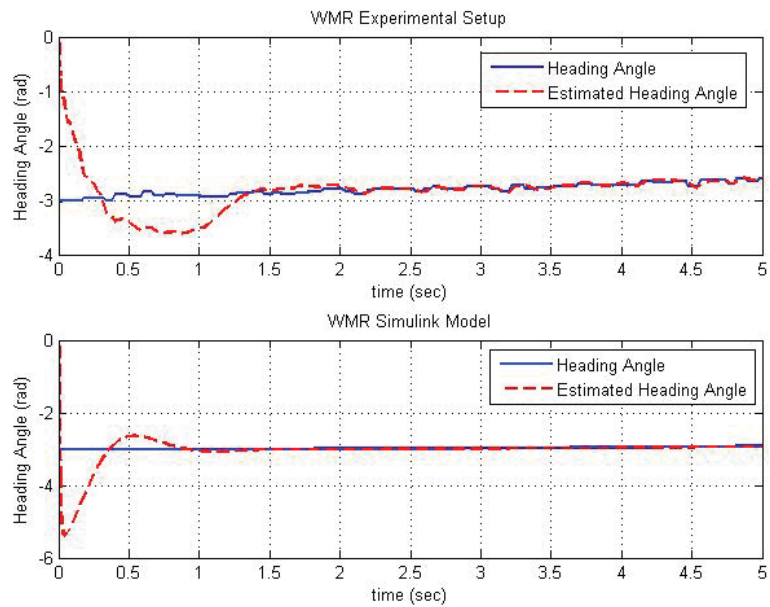
Figure 4.43: Heading angle "ψ" estimation of the WMR, using PWA observer.
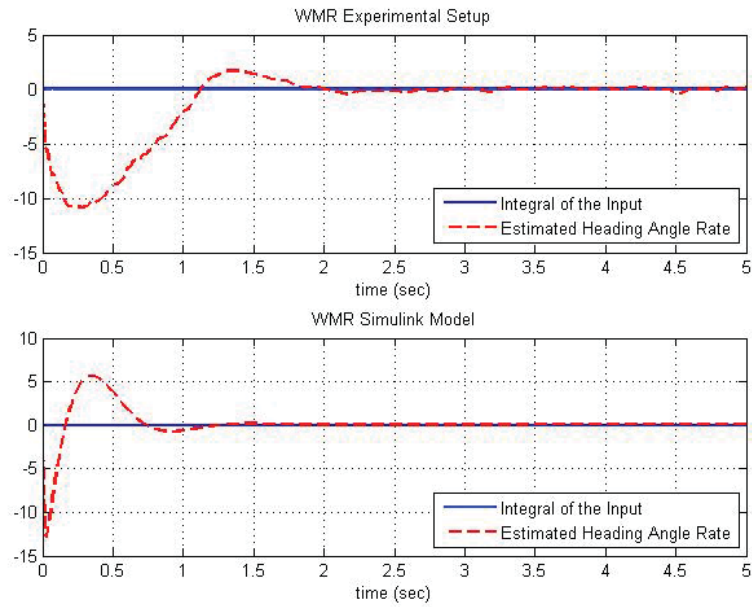
Figure 4.44: Heading angle rate "*R*" estimation of the WMR, using PWA observer.
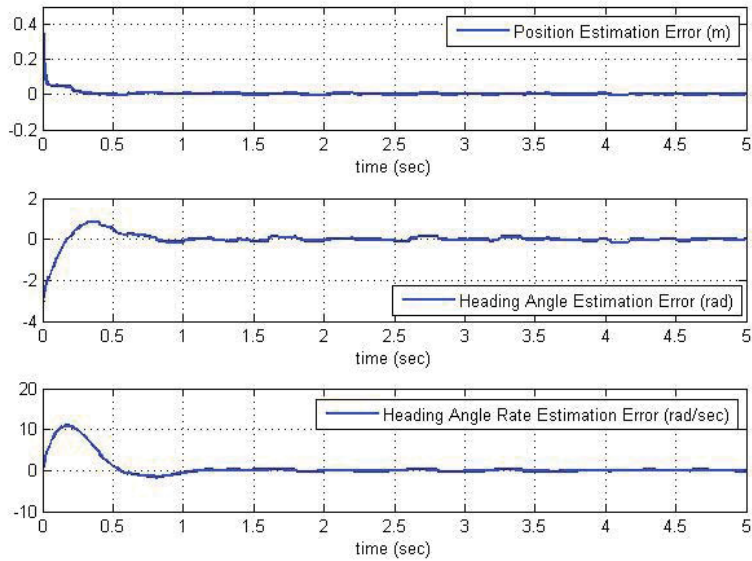
Figure 4.45: State estimation errors of real setup of the WMR sampled-data ($T = 0.2s$) experimental setup, using PWA observer.

Observers	Transient Performance(e_{max})		Steady State Performance (e_{rms})		
	ψ	R	y	ψ	R
PWA	0.847	10.9512	0.0048	0.0668	0.2018
Sliding Mode	1.9594	10.7969	0.0089	0.0718	0.3562
Backstepping	0.4109	5.485	0.0109	0.0581	0.0888
High-Gain	0.396	7.369	0.0125	0.0534	0.1027
Output Injection	1.1829	16.3329	0.0098	0.0613	0.1975
Interconnected	0.463	6.232	0.0114	0.0556	0.055

Table 4.4: Different observers implemented on the nonlinear sampled-data ($T = 0.2s$) WMR experimental setup.

WMR yielding a convergent state estimation error. When implementing the sliding mode observer the chattering phenomenon occurred and it was impossible to continue the real-time program, which lead to changing the *sign* function to *saturation* function. All the implemented observers show good steady state performance, which is defined by e_{rms} with almost equal values, except the sliding mode observer that has a large value for the heading angle estimation error when compared to other observers. Also, the sliding mode observer yields a larger value for e_{rms} of the heading angle rate in comparison with other observers. Moreover, the estimation errors of the sliding mode observer converge slower than other observers which can be due to more computation needed in the sliding mode observer structure. The high gain observer has the largest value for e_{rms} of the position. Comparing the transient behavior, the nonlinear observer with output injection has the largest value for the overshoot of the heading angle rate estimation error.

Table 4.5 compares different observers implemented on the WMR with the PWA observer, where $T - P$ stands for transient performance and $SS - P$ stands for steady state performance.

From Table 4.5 it can be concluded that the PWA observer and the sliding mode observer are the most robust observers in comparison with other observers. However, the sliding mode observer shoes poor steady state performance. Moreover, the PWA observer has a large value in transient time for the heading angle rate estimation error. On the other hand, the sliding mode observer has limitations such as occurrence of chattering in practical

implementation which makes the PWA observer more suitable to implement in practice.

4.5 Summary

In this chapter a continuous-time PWA observer is designed for a continuous-time PWA approximation of the WMR, which is an example of a nonlinear sampled-data system. The observer is implemented on the experimental setup of the WMR available at the HYCONS Laboratory of Concordia University. The position of the WMR is measured by capturing images with the camera and the heading angle is obtained based on the information regarding the position. Therefore, the estimations obtained from the observer are compared to these values. The estimated values have converged to real values after a short time. The heading angle rate is not measured, based on the WMR dynamic equations, the integral of the input is compared to the estimated heading angle rate and it is concluded that the heading angle rate is estimated correctly. The data given to the observer is only available at sampling instants and contains noise. As proven in the theorems proposed in Chapter 3, the observer is robust to the sampling error and the measurement noise which its type is not known but it is bounded. As a result, the state estimation errors are ultimately bounded and have converged to small regions around zero. In theory it was proven that a continuous-time piecewise affine observer can be used for state estimation of a class of nonlinear sampled-data systems yielding a convergent state estimation error and in this chapter real experiments resulted in the same conclusion. Moreover, some other nonlinear observers are implemented on the WMR and the results of the state estimation are compared to the ones regarding the PWA observer. The PWA observer and the sliding mode observer are the most robust observers to perturbations. However, the sliding mode observer has some practical limitations.

Observers	T-P (e_{max})			SS-P (e_{rms})			Robustness	Note
	y	ψ	R	y	ψ	R		
PWA	√	√	×	√	√	√	√	applicable to all smooth nonlinear systems (linear in the input, nonlinear in one of the states), scalable, can be efficiently solved by available software packages
Sliding Mode	√	√	√	×	×	×	√	occurrence of chattering, limitations in practical implementation, requires that the systems be in certain (triangular) form, unstable state estimation error for lower speeds of convergence
Backstepping	√	√	√	√	√	√	×	requires that the systems be in certain (triangular) form, many calculations needed to obtain gains
High-Gain	√	√	√	×	√	√	×	requires that the systems be in certain (triangular) form
Output Injection	√	√	×	√	√	√	×	only applicable to systems with measurable nonlinearities (otherwise, a transformation needed which requires necessary conditions which are difficult to be satisfied)
Interconnected	√	√	√	√	√	√	×	requires that the systems be in certain form, could be an interconnection between any above named observers

Table 4.5: Comparison of different observers.

Chapter 5

Conclusions and Future Research

In this chapter the contributions of the thesis are summarized and the conclusions from this research are made. Also, potential future work is discussed in this chapter.

In Chapter 2 some preliminaries on PWA systems and PWA observer design are reviewed. In addition, definitions of boundedness and ultimate boundedness and some nonlinear observer design methodologies are also studied in Chapter 2.

Building on the knowledge from Chapter 2, the problem of PWA observer design for a class of nonlinear systems is discussed in Chapter 3. The contributions of Chapter 3 include designing a continuous-time PWA observer for a class of nonlinear systems yielding ultimately bounded state estimation error. Moreover, it is proven that the state estimation error is still convergent and ultimately bounded when the output of the system is only available at sampling instants. Also, it is proven that when the continuous-time PWA observer is applied to the nonlinear sampled-data system in the presence of norm bounded measurement noise, the state estimation error is ultimately bounded. The proposed method of observer design can be cast as a set of LMIs and is based on a convex optimization approach which can be solved efficiently using available software packages. Performance, robustness and scalability of the proposed PWA observer makes this method an alternative approach for designing observers for nonlinear systems.

In Chapter 4 a practical experiment is performed on a WMR available at the HY-CONS Laboratory of Concordia University. After studying the WMR modeling, the wireless communication, electronics and sensors of the WMR are explained. The WMR is an example of the class of nonlinear systems studied in Chapter 3. The output of this system is available for the observer only at sampling instants. Therefore, the WMR system is an example of nonlinear sampled-data systems that can be approximated by a PWA system to be used for validating the proposed theorems in this thesis. Also, measurements from the outputs of the WMR contain noise. An observer is designed for this system and the results of the state estimation error, which are all convergent, validate the proposed theorems in Chapter 3.

Comparing different observers, the PWA observer and the sliding mode observer are the most robust observers. However, the sliding mode observer shows poor steady state performance and the PWA observer has a large value in transient time estimating the heading angle rate. In practical implementation the sliding mode observer has some limitations such as occurrence of chattering. The overall performance, robustness, practical implementation and scalability of PWA observer makes this method an alternative approach to design observers for nonlinear systems.

In what follows a few suggestions for future studies are made.

• Although there are many real applications that can be modeled by the class of nonlinear functions considered in this thesis, considering a more general class of nonlinear systems for solving the problem of observer design can be addressed in the future.

• It would be a good idea to solve the problem of obtaining the maximum allowable sampling time in order to have an exponentially stable state estimation error when the PWA observer is applied to a nonlinear sampled-data system.

• In many applications, the estimated states obtained from observers are used to control the systems. An extension of the work in this thesis could be to design a controller for the system using the states estimated by the PWA observer. Moreover, that would be

very interesting to try to control the experimental setup of the WMR using the estimated states from the PWA observer.

Bibliography

[1] G. Besançon, "An overview on observer tools for nonlinear systems," in *Nonlinear Observers and Applications*. Springer, 2007, pp. 1–33.

[2] B. Gholitabar Omrani, "Optimization-based control methodologies with applications to autonomous vehicle," Master's thesis, Concordia University, 2010.

[3] L. Rodrigues and J. P. How, "Observer-based control of piecewise-affine systems," *International Journal of Control*, vol. 76, no. 5, pp. 459–477, 2003.

[4] E. A. Misawa, "Observer-based discrete-time sliding mode control with computational time delay: The linear case," in *Proceedings of the American Control Conference*, vol. 2. IEEE, 1995, pp. 1323–1327.

[5] C. H. Lien, "Robust observer-based control of systems with state perturbations via LMI approach," *IEEE Transactions on Automatic Control*, vol. 49, no. 8, pp. 1365–1370, 2004.

[6] D. G. Luenberger, "Observing the state of a linear system," *IEEE Transactions on Military Electronics*, vol. 8, no. 2, pp. 74–80, 1964.

[7] D. Luenberger, "Observers for multivariable systems," *IEEE Transactions on Automatic Control*, vol. 11, no. 2, pp. 190–197, 1966.

[8] ——, "An introduction to observers," *IEEE Transactions on Automatic Control*, vol. 16, no. 6, pp. 596–602, 1971.

[9] N. H. Jo and J. H. Seo, "Input output linearization approach to state observer design for nonlinear system," *IEEE Transactions on Automatic Control*, vol. 45, no. 12, pp. 2388–2393, 2000.

[10] W. Baumann and W. Rugh, "Feedback control of nonlinear systems by extended linearization," *IEEE Transactions on Automatic Control*, vol. 31, no. 1, pp. 40–46, 1986.

[11] J. Primbs, "Survey of nonlinear observer design techniques," CDS122, Tech. Rep., 1996.

[12] J. Voros, "Parameter identification of Hammerstein systems with asymmetric dead-zones," *Journal Of Electrical Engineering*, vol. 55, no. 1-2, pp. 46–49, 2004.

[13] D. Dai, T. Hu, A. R. Teel, and L. Zaccarian, "Piecewise-quadratic Lyapunov functions for systems with deadzones or saturations," *Systems & Control Letters*, vol. 58, no. 5, pp. 365–371, 2009.

[14] A. Rantzer and M. Johansson, "Piecewise linear quadratic optimal control," *IEEE Transactions on Automatic Control*, vol. 45, no. 4, pp. 629–637, 2000.

[15] J. Sieber, "Dynamics of delayed relay control systems with large delays," in *Proceedings of 5th IFAC Workshop on Time-delay Systems*, 2005.

[16] J. I. Imura, "Well-posedness analysis of switch-driven piecewise affine systems," *IEEE Transactions on Automatic Control*, vol. 48, no. 11, pp. 1926–1935, 2003.

[17] M. Johansson and A. Rantzer, "Computation of piecewise quadratic Lyapunov functions for hybrid systems," *IEEE Transactions on Automatic Control*, vol. 43, no. 4, pp. 555–559, 1998.

[18] S. Lim and K. Chan, "Piecewise switching-dependent Lyapunov functional for analyzing systems with hysteresis," in *Proceedings of the American Control Conference*, vol. 1.   IEEE, 2001, pp. 206–211.

[19] B. Samadi and L. Rodrigues, "Stability of sampled-data piecewise-affine systems: A time-delay approach," *Automatica*, vol. 45, no. 9, pp. 1995–2001, 2009.

[20] L. Rodrigues, "Dynamic output feedback controller synthesis for piecewise-affine systems," Ph.D. dissertation, Stanford University, 2002.

[21] S. Casselman and L. Rodrigues, "A new methodology for piecewise affine models using Voronoi partitions," in *Proceedings of the 48th IEEE Conference on Decision and Control held jointly with the 28th Chinese Control Conference. CDC/CCC 2009.* IEEE, 2009, pp. 3920–3925.

[22] M. J. Chien and E. Kuh, "Solving nonlinear resistive networks using piecewise-linear analysis and simplicial subdivision," *IEEE Transactions on Circuits and Systems*, vol. 24, no. 6, pp. 305–317, 1977.

[23] P. Julian, A. Desages, and O. Agamennoni, "High-level canonical piecewise linear representation using a simplicial partition," *IEEE Transactions on Circuits and Systems I: Fundamental Theory and Applications*, vol. 46, no. 4, pp. 463–480, 1999.

[24] L. Rodrigues and J. P. How, "Automated control design for a piecewise-affine approximation of a class of nonlinear systems," in *Proceedings of the American Control Conference*, vol. 4.   IEEE, 2001, pp. 3189–3194.

[25] A. Hassibi and S. Boyd, "Quadratic stabilization and control of piecewise-linear systems," in *Proceedings of the American Control Conference*, vol. 6.   IEEE, 1998, pp. 3659–3664.

[26] L. Rodrigues and S. Boyd, "Piecewise-affine state feedback for piecewise-affine slab systems using convex optimization," *Systems & Control Letters*, vol. 54, no. 9, pp. 835–853, 2005.

[27] B. Samadi and L. Rodrigues, "Extension of a local linear controller to a stabilizing semi-global piecewise affine controller," in *7th Portuguese Conf. on Automatic Control*, 2006.

[28] S. Paoletti, A. L. Juloski, G. Ferrari-Trecate, and R. Vidal, "Identification of hybrid systems a tutorial," *European Journal of Control*, vol. 13, no. 2, pp. 242–260, 2007.

[29] J. Roll, "Local and piecewise affine approaches to system identification," Ph.D. dissertation, Linkoping University, 2003.

[30] G. Ferrari-Trecate, M. Muselli, D. Liberati, and M. Morari, "A clustering technique for the identification of piecewise affine systems," *Automatica*, vol. 39, no. 2, pp. 205–217, 2003.

[31] S. Paoletti, A. Garulli, E. Pepona *et al.*, "Exploiting structure in piecewise affine identification of LFT systems," in *15th IFAC Symposium on System Identification SYSID, Saint-Malo, July 2009. In press*, 2009.

[32] S. Paoletti, "Identification of piecewise affine models," Ph.D. dissertation, Department of Information Engineering, University of Siena, Siena, Italy, 2004.

[33] G. Ferrari-Trecate and M. Schinkel, "Conditions of optimal classification for piecewise affine regression," in *Hybrid systems: computation and control*. Springer, 2003, pp. 188–202.

[34] E. Asarin, T. Dang, and A. Girard, "Reachability analysis of nonlinear systems using conservative approximation," in *Hybrid Systems: Computation and Control*. Springer, 2003, pp. 20–35.

[35] L. Rodrigues, A. Hassibi, and J. P. How, "Output feedback controller synthesis for piecewise-affine systems with multiple equilibria," in *Proceedings of the American Control Conference*, vol. 3. IEEE, 2000, pp. 1784–1789.

[36] N. Nayebpanah, L. Rodrigues, and Y. Zhang, "Fault detection and identification for bimodal piecewise affine systems," in *Proceedings of the American Control Conference*. IEEE, 2009, pp. 2362–2366.

[37] A. L. Juloski, W. Heemels, Y. Boers, and F. Verschure, "Two approaches to state estimation for a class of piecewise affine systems," in *Proceedings. 42nd IEEE Conference on Decision and Control (CDC)*, vol. 1. IEEE, 2003, pp. 143–148.

[38] A. L. Juloski, W. Heemels, and S. Weiland, "Observer design for a class of piecewise affine systems," in *Proceedings of the 41st IEEE Conference on Decision and Control (CDC)*, vol. 3. IEEE, 2002, pp. 2606–2611.

[39] S. P. Boyd and L. Vandenberghe, *Convex optimization*. Cambridge university press, 2004.

[40] S. Kaynama, "Convex formulation of controller synthesis for piecewise-affine systems," Master's thesis, Concordia University, 2012.

[41] "Academic dictionaries and encyclopedias," http://en.academic.ru/dic.nsf/enwiki/1255374.

[42] F. Thau, "Observing the state of non-linear dynamic systems," *International Journal of Control*, vol. 17, no. 3, pp. 471–479, 1973.

[43] C. Leondes and L. Novak, "Reduced-order observers for linear discrete-time systems," *IEEE Transactions on Automatic Control*, vol. 19, no. 1, pp. 42–46, 1974.

[44] S. Bhattacharyya, "Observer design for linear systems with unknown inputs," *IEEE Transactions on Automatic Control*, vol. 23, no. 3, pp. 483–484, 1978.

[45] E. De Santis, M. D. Di Benedetto, and G. Pola, "On observability and detectability of continuous-time linear switching systems," in *Proceedings. 42nd IEEE Conference on Decision and Control*, vol. 6.   IEEE, 2003, pp. 5777–5782.

[46] C.-F. Lin and W.-C. Su, "Linear observer design using the inverse method for systems with matched disturbances," in *Proc. American Control Conference*.   IEEE, 2010, pp. 617–622.

[47] T. Raff, P. Menold, C. Ebenbauer, and F. Allgower, "A finite time functional observer for linear systems," in *Proc. 44th IEEE Conference on Decision and Control and 2005 European Control Conference. CDC-ECC'05*.   IEEE, 2005, pp. 7198–7203.

[48] B. A. Charandabi and H. J. Marquez, "Observer design for discrete-time linear systems with unknown disturbances," in *Proc. 51st Annual Conference on Decision and Control (CDC)*.   IEEE, 2012, pp. 2563–2568.

[49] Y. Xiong and M. Saif, "Sliding-mode observer for uncertain systems. I linear systems case," in *Proceedings of the 39th IEEE Conference on Decision and Control*, vol. 1. IEEE, 2000, pp. 316–321.

[50] A. Seuret, T. Floquet, J.-P. Richard, and S. K. Spurgeon, "A sliding mode observer for linear systems with unknown time varying delay," in *Proc. American Control Conference*.   IEEE, 2007, pp. 4558–4563.

[51] A. J. Koshkouei and A. Zinober, "Sliding mode state observers for linear multivariable systems," in *Proceedings of the 34th IEEE Conference on Decision and Control*, vol. 3.   IEEE, 1995, pp. 2115–2120.

[52] S. Drakunov and V. Utkin, "Sliding mode observers. tutorial," in *Proceedings of the 34th IEEE Conference on Decision and Control*, vol. 4.   IEEE, 1995, pp. 3376–3378.

[53] C. P. Tan and C. Edwards, "Robust fault reconstruction in uncertain linear systems using multiple sliding mode observers in cascade," *IEEE Transactions on Automatic Control*, vol. 55, no. 4, pp. 855–867, 2010.

[54] ——, "An LMI approach for designing sliding mode observers," *International Journal of Control*, vol. 74, no. 16, pp. 1559–1568, 2001.

[55] F. Celle, J. Gauthier, D. Kazakos, and G. Sallet, "Synthesis of nonlinear observers: A harmonic-analysis approach," *Mathematical systems theory*, vol. 22, no. 1, pp. 291–322, 1989.

[56] S. R. Kou, D. L. Elliott, and T. J. Tarn, "Exponential observers for nonlinear dynamic systems," *Information and Control*, vol. 29, no. 3, pp. 204–216, 1975.

[57] S. P. Banks, "A note on non-linear observers," *International Journal of Control*, vol. 34, no. 1, pp. 185–190, 1981.

[58] S. Raghavan and J. K. Hedrick, "Observer design for a class of nonlinear systems," *International Journal of Control*, vol. 59, no. 2, pp. 515–528, 1994.

[59] N. Kazantzis and C. Kravaris, "Nonlinear observer design using Lyapunovs auxiliary theorem," *Systems & Control Letters*, vol. 34, no. 5, pp. 241–247, 1998.

[60] J. Deutscher, "Numerical design of nonlinear observers with approximately linear error dynamics," in *Proc. International Conference on Computer Aided Control System Design*. IEEE, 2006, pp. 2985–2990.

[61] A. Howell and J. K. Hedrick, "Nonlinear observer design via convex optimization," in *Proceedings of the American Control Conference*, vol. 3. IEEE, 2002, pp. 2088–2093.

[62] G. I. Bara, A. Zemouche, and M. Boutayeb, "Observer synthesis for Lipschitz discrete-time systems," in *International Symposium on Circuits and Systems, ISCAS*. IEEE, 2005, pp. 3195–3198.

[63] F. Yan and J. Wang, "In-cylinder oxygen mass fraction cycle-by-cycle estimation via a Lyapunov-based observer design," in *Proc. American Control Conference*. IEEE, 2010, pp. 652–657.

[64] X. Sen and W. Yu, "Designs and applications of observer for nonlinear control system," in *Proceedings of the Twenty-Eighth Southeastern Symposium on System Theory*. IEEE, 1996, pp. 190–194.

[65] A. Banaszuk and W. M. Sluis, "On nonlinear observers with approximately linear error dynamics," in *Proceedings of the American Control Conference*, vol. 5. IEEE, 1997, pp. 3460–3464.

[66] A. F. Lynch and S. A. Bortoff, "Nonlinear observers with approximately linear error dynamics: The multivariable case," *IEEE Transactions on Automatic Control*, vol. 46, no. 6, pp. 927–932, 2001.

[67] J. Birk and M. Zeitz, "Extended Luenberger observer for non-linear multivariable systems," *International Journal of Control*, vol. 47, no. 6, pp. 1823–1836, 1988.

[68] Z. Ding, "Observer design in convergent series for a class of nonlinear systems," *IEEE Transactions on Automatic Control*, vol. 57, no. 7, pp. 1849–1854, 2012.

[69] T. Meurer, "On the extended Luenberger-type observer for semilinear distributed-parameter systems," *IEEE Transactions on Automatic Control*, vol. 58, no. 7, pp. 1732–1743, 2013.

[70] T. Pana and O. Stoicuta, "Design of an extended Luenberger observer for sensorless vector control of induction machines under regenerating mode," in *12th International Conference on Optimization of Electrical and Electronic Equipment (OPTIM)*. IEEE, 2010, pp. 469–478.

[71] A. J. Krener and A. Isidori, "Linearization by output injection and nonlinear observers," *Systems & Control Letters*, vol. 3, no. 1, pp. 47–52, 1983.

[72] D. Bestle and M. Zeitz, "Canonical form observer design for non-linear time-variable systems," *International Journal of Control*, vol. 38, no. 2, pp. 419–431, 1983.

[73] A. J. Krener and W. Respondek, "Nonlinear observers with linearizable error dynamics," *SIAM Journal on Control and Optimization*, vol. 23, no. 2, pp. 197–216, 1985.

[74] R. Marino, "Adaptive observers for single output nonlinear systems," *IEEE Transactions on Automatic Control*, vol. 35, no. 9, pp. 1054–1058, 1990.

[75] R. Marino and P. Tomei, "Adaptive observers for a class of multi-output non-linear systems," *International journal of adaptive control and signal processing*, vol. 6, no. 4, pp. 353–365, 1992.

[76] H. Cho, J. Yang, and J. H. Seo, "Geometric characterization of reduced-order dynamic observer error linearization for uncontrolled multi-output systems," in *Proc. 51st Annual Conference on Decision and Control (CDC)*. IEEE, 2012, pp. 338–343.

[77] M. Koldychev and C. Nielsen, "Local full-state observers on linear Lie groups with linear error dynamics," in *Proc. 51st Annual Conference on Decision and Control (CDC)*. IEEE, 2012, pp. 5918–5923.

[78] H. K. Khalil, "High-gain observers in nonlinear feedback control," in *New directions in nonlinear observer design*. Springer, 1999, pp. 249–268.

[79] F. Esfandiari and H. K. Khalil, "Output feedback stabilization of fully linearizable systems," *International Journal of Control*, vol. 56, no. 5, pp. 1007–1037, 1992.

[80] H. K. Khalil, "Adaptive output feedback control of nonlinear systems represented by input-output models," *IEEE Transactions on Automatic Control*, vol. 41, no. 2, pp. 177–188, 1996.

[81] S. Oh and H. K. Khalil, "Output feedback stabilization using variable structure control," *International Journal of Control*, vol. 62, no. 4, pp. 831–848, 1995.

[82] ——, "Nonlinear output-feedback tracking using high-gain observer and variable structure control," *Automatica*, vol. 33, no. 10, pp. 1845–1856, 1997.

[83] L. B. Freidovich and H. K. Khalil, "Lyapunov-based switching control of nonlinear systems using high-gain observers," *Automatica*, vol. 43, no. 1, pp. 150–157, 2007.

[84] A. A. Prasov and H. K. Khalil, "A nonlinear high-gain observer for systems with measurement noise in a feedback control framework," *IEEE Transactions on Automatic Control*, vol. 58, no. 3, pp. 569–580, 2013.

[85] C. P. Tan and C. Edwards, "Sliding mode observers for robust detection and reconstruction of actuator and sensor faults," *International Journal of Robust and Nonlinear Control*, vol. 13, no. 5, pp. 443–463, 2003.

[86] ——, "Sliding mode observers for detection and reconstruction of sensor faults," *Automatica*, vol. 38, no. 10, pp. 1815–1821, 2002.

[87] C. Edwards, S. K. Spurgeon, and R. J. Patton, "Sliding mode observers for fault detection and isolation," *Automatica*, vol. 36, no. 4, pp. 541–553, 2000.

[88] S. V. Drakunov, "Sliding-mode observers based on equivalent control method," in *Proceedings of the 31st IEEE Conference on Decision and Control*. IEEE, 1992, pp. 2368–2369.

[89] Y. Xiong and M. Saif, "Sliding mode observer for nonlinear uncertain systems," *IEEE Transactions on Automatic Control*, vol. 46, no. 12, pp. 2012–2017, 2001.

[90] J. A. Moreno and M. Osorio, "A Lyapunov approach to second-order sliding mode controllers and observers," in *Proc. 47th IEEE Conference on Decision and Control (CDC)*.   IEEE, 2008, pp. 2856–2861.

[91] K. Kalsi, J. Lian, S. Hui, and S. H. Zak, "Sliding-mode observers for uncertain systems," in *Proc. American Control Conference*.   IEEE, 2009, pp. 1189–1194.

[92] X. Han, E. Fridman, and S. K. Spurgeon, "A sliding mode observer for fault reconstruction under output sampling: A time-delay approach," in *Proc. 50th IEEE Conference on Decision and Control and European Control Conference (CDC-ECC)*. IEEE, 2011, pp. 77–82.

[93] J. Diego Sanchez-Torres, A. G. Loukianov, J. A. Moreno, and S. V. Drakunov, "An equivalent control based sliding mode observer using high order uniform robust sliding operators," in *Proc. American Control Conference*.   IEEE, 2012, pp. 6160–6165.

[94] B. Walcott and S. Zak, "Observation of dynamical systems in the presence of bounded nonlinearities/uncertainties," in *Proc. 25th IEEE Conference on Decision and Control (CDC)*, vol. 25.   IEEE, 1986, pp. 961–966.

[95] ——, "State observation of nonlinear uncertain dynamical systems," *IEEE Transactions on Automatic Control*, vol. 32, no. 2, pp. 166–170, 1987.

[96] M.-W. Thein and E. A. Misawa, "Comparison of the sliding observer to several state estimators using a rotational inverted pendulum," in *Proceedings of the 34th IEEE Conference on Decision and Control (CDC)*, vol. 4.   IEEE, 1995, pp. 3385–3390.

[97] W. Wang and Z. Gao, "A comparison study of advanced state observer design techniques," in *Proceedings of the American Control Conference*, vol. 6.   IEEE, 2003, pp. 4754–4759.

[98] J. Tsinias, "Observer design for nonlinear systems," *Systems & Control Letters*, vol. 13, no. 2, pp. 135–142, 1989.

[99] X.-h. Xia and W.-b. Gao, "On exponential observers for nonlinear systems," *Systems & Control Letters*, vol. 11, no. 4, pp. 319–325, 1988.

[100] J. P. Gauthier, H. Hammouri, and S. Othman, "A simple observer for nonlinear systems applications to bioreactors," *IEEE Transactions on Automatic Control*, vol. 37, no. 6, pp. 875–880, 1992.

[101] R. Rajamani, "Observers for Lipschitz nonlinear systems," *IEEE Transactions on Automatic Control*, vol. 43, no. 3, pp. 397–401, 1998.

[102] B. Walcott, M. Corless, and S. Żak, "Comparative study of non-linear state-observation techniques," *International Journal of Control*, vol. 45, no. 6, pp. 2109–2132, 1987.

[103] A. Smyshlyaev and M. Krstic, "Backstepping observers for a class of parabolic PDEs," *Systems & Control Letters*, vol. 54, no. 7, pp. 613–625, 2005.

[104] A. J. Krener and W. Kang, "Locally convergent nonlinear observers," *SIAM Journal on Control and Optimization*, vol. 42, no. 1, pp. 155–177, 2003.

[105] M. Jankovic, "Adaptive nonlinear output feedback tracking with a partial high-gain observer and backstepping," *IEEE Transactions on Automatic Control*, vol. 42, no. 1, pp. 106–113, 1997.

[106] C. Di Persis, "A necessary condition and a backstepping observer for nonlinear fault detection," in *Proceedings of the 38th IEEE Conference on Decision and Control (CDC)*, vol. 3.   IEEE, 1999, pp. 2896–2901.

[107] A. Robertsson and R. Johansson, "Observer backstepping for a class of nonminimum-phase systems," in *Proceedings of the 38th IEEE Conference on Decision and Control (CDC)*, vol. 5.   IEEE, 1999, pp. 4866–4871.

[108] J. d. Leon, I. Souleiman, A. Glumineau, and G. Schreier, "On nonlinear equivalence and backstepping observer," *Kybernetika*, vol. 37, no. 5, pp. 521–546, 2001.

[109] R. Galeazzi, M. P. Gryning, and M. Blanke, "Observer backstepping control for variable speed wind turbine," in *Proc. American Control Conference*.   IEEE, 2013, pp. 1036–1043.

[110] H. K. Khalil, *Nonlinear systems*.   Prentice hall Upper Saddle River, 2002, vol. 3.

[111] V. I. Utkin and H.-C. Chang, "Sliding mode control on electro-mechanical systems," *Mathematical Problems in Engineering*, vol. 8, no. 4-5, pp. 451–473, 2002.

[112] S. Aubouet, L. Dugard, and O. Sename, "H_∞-LPV observer for an industrial semi-active suspension," in *Control Applications,(CCA) & Intelligent Control, (ISIC)*.   IEEE, 2009, pp. 756–763.

[113] X. Wei and M. Verhaegen, "Mixed H_-/H_∞ fault detection observer design for LPV systems," in *47th IEEE Conference on Decision and Control*.   IEEE, 2008, pp. 1073–1078.

[114] G. I. Bara, J. Daafouz, F. Kratz, and J. Ragot, "Parameter-dependent state observer design for affine LPV systems," *International Journal of Control*, vol. 74, no. 16, pp. 1601–1611, 2001.

[115] J. Daafouz, G. I. Bara, F. Kratz, and J. Ragot, "State observers for discrete-time LPV systems: An interpolation based approach," in *39th IEEE Conference on Decision and Control*, vol. 5.   IEEE, 2000, pp. 4571–4572.

[116] X. Yang and Y. Huang, "Capabilities of extended state observer for estimating uncertainties," in *Proceedings of the American Control Conference*. IEEE, 2009, pp. 3700–3705.

[117] Y. Zhang, Z. Zhao, T. Lu, L. Yuan, W. Xu, and J. Zhu, "A comparative study of Luenberger observer, sliding mode observer and extended Kalman filter for sensorless vector control of induction motor drives," in *Energy Conversion Congress and Exposition, ECCE*. IEEE, 2009, pp. 2466–2473.

[118] A. H. Al-Bayati, Z. Skaf, and H. Wang, "A comparative study of nonlinear observers applied to a DC servo motor," in *8th World Congress on Intelligent Control and Automation (WCICA)*. IEEE, 2010, pp. 855–860.

[119] M. A. Fallah, "Optimal control and estimation strategies for nonlinear and switched systems," Master's thesis, Concordia University, 2011.

[120] A. Balluchi, L. Benvenuti, M. D. Di Benedetto, and A. L. Sangiovanni-Vincentelli, "Design of observers for hybrid systems," in *Hybrid Systems: Computation and Control*. Springer, 2002, pp. 76–89.

[121] G. Ferrari-Trecate, D. Mignone, and M. Morari, "Moving horizon estimation for hybrid systems," *IEEE Transactions on Automatic Control*, vol. 47, no. 10, pp. 1663–1676, 2002.

[122] L. Pina and M. A. Botto, "Simultaneous state and input estimation of hybrid systems with unknown inputs," *Automatica*, vol. 42, no. 5, pp. 755–762, 2006.

[123] G. Böker and J. Lunze, "Stability and performance of switching Kalman filters," *International Journal of Control*, vol. 75, no. 16-17, pp. 1269–1281, 2002.

[124] L. Rodrigues and J. P. How, "Observer-based control of piecewise-affine systems," in *Proceedings. 40th IEEE Conference on Decision and Control (CDC)*, vol. 2. IEEE, 2001, pp. 1366–1371.

[125] N. Nayebpanah, "Fault tolerant control for bimodal piecewise affine systems," Master's thesis, Concordia University, 2010.

[126] A. Alessandri and P. Coletta, "Switching observers for continuous-time and discrete-time linear systems," in *Proceedings of the American Control Conference*, vol. 3. IEEE, 2001, pp. 2516–2521.

[127] ——, "Design of observers for switched discrete-time linear systems," in *Proceedings of the American Control Conference*, vol. 4. IEEE, 2003, pp. 2785–2790.

[128] A. Alessandri, M. Baglietto, and G. Battistelli, "Luenberger observers for switching discrete-time linear systems," *International Journal of Control*, vol. 80, no. 12, pp. 1931–1943, 2007.

[129] A. Tanwani, H. Shim, and D. Liberzon, "Observability for switched linear systems: characterization and observer design," *IEEE Transactions on Automatic Control*, vol. 58, no. 4, pp. 891–904, 2013.

[130] W. Heemels, S. Weiland *et al.*, "Observer design for a class of piecewise linear systems," *International Journal of Robust and Nonlinear Control*, vol. 17, no. 15, pp. 1387–1404, 2007.

[131] A. Doris, A. Juloski, M. Heemels, N. van de Wouw, and H. Nijmeijer, "Switching observer design for an experimental piece-wise linear beam system," in *16th IFAC Conf., Prague, Czech Republic*, 2005.

[132] J. Xu, K. Y. Lum, and A. P. Loh, "Observer-based fault detection for piecewise linear systems: discrete-time cases," in *International Conference on Control Applications, CCA*. IEEE, 2007, pp. 373–378.

[133] S.-T. Chung and J. Grizzle, "Observer error linearization for sampled-data systems," in *Proceedings of the 28th IEEE Conference on Decision and Control (CDC)*. IEEE, 1989, pp. 90–95.

[134] M. Arcak and D. Nešić, "A framework for nonlinear sampled-data observer design via approximate discrete-time models and emulation," *Automatica*, vol. 40, no. 11, pp. 1931–1938, 2004.

[135] M. Abbaszadeh and H. J. Marquez, "Robust H_∞ observer design for sampled-data Lipschitz nonlinear systems with exact and Euler approximate models," *Automatica*, vol. 44, no. 3, pp. 799–806, 2008.

[136] Z. Mao, B. Jiang, and P. Shi, "Fault-tolerant control for a class of nonlinear sampled-data systems via a Euler approximate observer," *Automatica*, vol. 46, no. 11, pp. 1852–1859, 2010.

[137] M. Arcak and D. Nesic, "Observer design for sampled-data nonlinear systems via approximate discrete-time models," in *Proceedings. 42nd IEEE Conference on Decision and Control (CDC)*, vol. 1. IEEE, 2003, pp. 49–54.

[138] M. Nadri, H. Hammouri, and R. Grajales, "Observer design for uniformly observable systems with sampled measurements," *IEEE Transactions on Automatic Control*, vol. 58, no. 3, pp. 757–762, 2013.

[139] L. Rodrigues, "Stability of sampled-data piecewise-affine systems under state feedback," *Automatica*, vol. 43, no. 7, pp. 1249–1256, 2007.

[140] ——, "Sampled-data state feedback control of piecewise-affine systems," in *Proc. 44th IEEE Conference on Decision and Control and 2005 European Control Conference. CDC-ECC'05*. IEEE, 2005, pp. 4487–4492.

[141] A. Hably, M. Alamir, J. Dumon *et al.*, "Observer-based control of a tethered wing wind power system: indoor real-time experiment," in *Proc. American Control Conference*, 2013.

[142] J. R. LeSage and R. G. Longoria, "Hybrid observer design for online battery state-of-charge estimation," in *Proc. American Control Conference*, 2013.

142

[143] W. Zhang, S. A. Gadsden, and S. R. Habibi, "Nonlinear estimation of stator winding resistance in a brushless DC motor," in *Proc. American Control Conference*, 2013.

[144] J. Lee, R. Mukherjee, and H. K. Khalil, "Application of dynamic inversion with extended high-gain observers to inverted pendulum on a cart," in *Proc. American Control Conference*, 2013.

[145] A.-R. Meghnous, M. T. Pham, X. Lin-Shi *et al.*, "Nonlinear observer and Lyapunov-based control for sepic converter: Design and experimental results," in *Proc. of the American Control Conference*, 2013.

[146] G. Schreier, J. DeLeon, A. Glumineau, and R. Boisliveau, "Cascade nonlinear observers: Application to an experimental induction motor benchmark," *IEE Proceedings-Control Theory and Applications*, vol. 148, no. 6, pp. 509–515, 2001.

[147] J. Gudino-Lau, M. A. Arteaga, L. A. Muñoz, and V. Parra-Vega, "On the control of cooperative robots without velocity measurements," *IEEE Transactions on Control Systems Technology*, vol. 12, no. 4, pp. 600–608, 2004.

[148] A. Ticlea and G. Besancon, "Observer design for state and parameter estimation in induction motors with simulation and experimental validation," in *32nd Annual Conference on Industrial Electronics, IECON*. IEEE, 2006, pp. 5075–5080.

[149] D. Traore, J. De Leon, A. Glumineau, and L. Loron, "Interconnected observers for sensorless induction motor in dq frame: Experimental tests," in *32nd Annual Conference on Industrial Electronics, IECON*. IEEE, 2006, pp. 5093–5100.

[150] D. Traoré, J. De Leon, and A. Glumineau, "Speed sensorless field-oriented control of induction motor with interconnected observers: experimental tests on low frequencies benchmark," *Control Theory & Applications, IET*, vol. 1, no. 6, pp. 1681–1692, 2007.

[151] S. E. Talole, J. P. Kolhe, and S. B. Phadke, "Extended-state-observer-based control of flexible-joint system with experimental validation," *IEEE Transactions on Industrial Electronics*, vol. 57, no. 4, pp. 1411–1419, 2010.

[152] A. Doris, A. L. Juloski, N. Mihajlovic, W. Heemels, N. van de Wouw, and H. Nijmeijer, "Observer designs for experimental non-smooth and discontinuous systems," *IEEE Transactions on Control Systems Technology*, vol. 16, no. 6, pp. 1323–1332, 2008.

[153] G. Phanomchoeng, R. Rajamani, and D. Piyabongkarn, "Nonlinear observer for bounded Jacobian systems, with applications to automotive slip angle estimation," *IEEE Transactions on Automatic Control*, vol. 56, no. 5, pp. 1163–1170, 2011.

[154] S.-C. Yang and R. D. Lorenz, "Surface permanent-magnet machine self-sensing at zero and low speeds using improved observer for position, velocity, and disturbance torque estimation," *IEEE Transactions on Industry Applications*, vol. 48, no. 1, pp. 151–160, 2012.

[155] R. Trabelsi, A. Khedher, M. F. Mimouni, and F. MSahli, "An adaptive backstepping observer for on-line rotor resistance adaptation," *International Journal IJ-STA*, vol. 4, no. 1, pp. 1246–1267, 2010.

[156] P. Sahoo and T. Riedel, *Mean value theorems and Functional Equations*. World Scientific, 1998.

[157] K. Eriksson, D. Estep, and C. Johnson, "Applied mathematics body and soul: Vol I-III," in *Springer-Verlag Publishing*. Citeseer, 2003.

[158] S. Casselman, "A new methodology for obtaining piecewise affine models using a set of linearisation points and Voronoi partitions," Master's thesis, Concordia University, 2009.

[159] S. M. A. Seyedahmady Zavieh, "Pseudo Euler-Lagrange and piecewise affine control applied to surge and stall in axial compressors," Master's thesis, Concordia University, 2013.

[160] R. E. Groff, "Piecewise linear homeomorphisms for approximation of invertible maps," Ph.D. dissertation, The University of Michigan, 2003.

[161] S. I. Azuma, J. I. Imura, and T. Sugie, "Lebesgue piecewise affine approximation of nonlinear systems and its application to hybrid system modeling of biosystems," in *Proc. 45th IEEE Conference on Decision and Control (CDC)*. IEEE, 2006, pp. 2128–2133.

[162] B. Llanas and F. J. Sáinz, "Uniform tree approximation by global optimization techniques," *Computing and visualization in science*, vol. 13, no. 2, pp. 83–97, 2010.

[163] M. Storace and O. De Feo, "Piecewise-linear approximation of nonlinear dynamical systems," *IEEE Transactions on Circuits and Systems I: Regular Papers*, vol. 51, no. 4, pp. 830–842, 2004.

[164] M. Johansson, *Piecewise linear control systems: a computational approach*. Springer Berlin, 2003.

[165] S. Pettersson, "Analysis and design of hybrid systems," School of Electrical and Computer Engineering, Chalmers University of Technology, Gteborg, Sweden, Tech. Rep., 1999.

[166] L. Rodrigues, "Stability analysis of piecewise-affine systems using controlled invariant sets," *Systems & control letters*, vol. 53, no. 2, pp. 157–169, 2004.

[167] A. Bemporad, G. Ferrari-Trecate, and M. Morari, "Observability and controllability of piecewise affine and hybrid systems," *IEEE Transactions on Automatic Control*, vol. 45, no. 10, pp. 1864–1876, 2000.

[168] A. Pavlov, N. van de Wouw, and H. Nijmeijer, "Convergent piecewise affine systems: analysis and design part I: continuous case," in *Proc. 44th IEEE Conference on Decision and Control and 2005 European Control Conference. CDC-ECC'05*. IEEE, 2005, pp. 5391–5396.

[169] B. Samadi and L. Rodrigues, "Backstepping controller synthesis for piecewise affine systems: A sum of squares approach," in *International Conference on Systems, Man and Cybernetics, ISIC*. IEEE, 2007, pp. 58–63.

[170] ——, "Controller synthesis for piecewise affine slab differential inclusions: A duality-based convex optimization approach," in *Proc. 46th IEEE Conference on Decision and Control (CDC)*. IEEE, 2007, pp. 4999–5004.

[171] J. F. Sturm, "Using sedumi 1.02, a matlab toolbox for optimization over symmetric cones," *Optimization methods and software*, vol. 11, no. 1-4, pp. 625–653, 1999.

[172] J. Lofberg, "Yalmip: A toolbox for modeling and optimization in matlab," in *Computer Aided Control Systems Design, 2004 IEEE International Symposium on*. IEEE, 2004, pp. 284–289.

[173] S. P. Boyd, *Linear matrix inequalities in system and control theory*. SIAM, 1994, vol. 15.

[174] V. A. Yakubovich, "S-procedure in nonlinear control theory," *Vestnik Leningrad University*, vol. 1, pp. 62–77, 1971.

[175] S. Weiland, A. L. Juloski, and B. Vet, "On the equivalence of switched affine models and switched ARX models," in *45th IEEE Conference on Decision and Control*. IEEE, 2006, pp. 2614–2618.

[176] S. Paoletti, A. Garulli, J. Roll, and A. Vicino, "A necessary and sufficient condition for input-output realization of switched affine state space models," in *47th IEEE Conference on Decision and Control*. IEEE, 2008, pp. 935–940.

[177] P. Collins and J. H. Van Schuppen, "Observability of piecewise-affine hybrid systems," in *Hybrid Systems: Computation and Control*. Springer, 2004, pp. 265–279.

[178] P. Axelsson, "Evaluation of six different sensor fusion methods for an industrial robot using experimental data," in *10th IFAC Symposium on Robot Control*, 2004.

[179] R. Henriksson, M. Norrlof, S. Moberg, E. Wernholt, and T. Schon, "Experimental comparison of observers for tool position estimation of industrial robots," in *48th IEEE Conference on Decision and Control held jointly with the 28th Chinese Control Conference. CDC/CCC 2009*. IEEE, 2009, pp. 8065–8070.

[180] J. Wallén, S. Gunnarsson, R. Henriksson, S. Moberg, and M. Norrlof, "ILC applied to a flexible two-link robot model using sensor-fusion-based estimates," in *48th IEEE Conference on Decision and Control held jointly with the 28th Chinese Control Conference. CDC/CCC 2009*. IEEE, 2009, pp. 458–463.

[181] W. Chen and M. Tomizuka, "Direct joint space state estimation in robots with multiple elastic joints," in *IEEE/ASME Transactions on Mechatronics*. IEEE, 2013, pp. 1–10.

[182] C. Ossa, "Design, construction and control of a quadrotor helicopter using a new multirate technique," Master's thesis, Concordia University, 2012.

[183] D. I. Inc, "Digi XBee Wireless RF Modules," http://www.digi.com/xbee/.

[184] S. K. Chilakala, *Development and Flight Testing of a Wireless Avionics Network Based on the IEEE 802.11 Protocols*. ProQuest, 2008.

[185] R. C. Gonzalez and R. E. Woods, *Digital Image Processing: Introduction*, 2002.

[186] S. B. by Sergey Shapovalov, "RTsync Blockset - File Exchange - MATLAB Central," http://www.mathworks.com/matlabcentral/fileexchange/24975-rtsync-blockset.

[187] OpenCVWebsite, "Open Source Computer Vision," http://opencv.willowgarage. com.

Appendix

The following parameters are used for designing the backstepping observer as explained in Section 2.5.

$$g_{2,1} = C_1 + \frac{\partial b_1}{\partial \hat{x}_1}$$

$$g_{3,1} = 1 + c_2(g_{2,1} - \phi_1) + (g_{2,1} - \phi_1)(\frac{\partial b_1}{\partial \hat{x}_1} - \phi_1) + \frac{d}{dt}(g_{2,1} - \phi_1) + K_1\frac{\partial b_2}{\partial \hat{x}_2}$$

$$g_{3,2} = K_1 C_2 + a_1 g_{2,1} + \frac{dK_1}{dt} + K_1\frac{\partial b_2}{\partial \hat{x}_2}$$

$$g_{4,1} = g_{2,1} - \phi_1 + c_3(g_{3,1} - K_1\phi_2) + (g_{3,1} - K_1\phi_2)(\frac{\partial b_1}{\partial \hat{x}_1} - \phi_1) + \frac{d}{dt}(g_{3,1} - K_1\phi_2) +$$

$$(g_{3,2} - K_1\phi_1)(\frac{\partial b_2}{\partial \hat{x}_1} - \phi_2) + K_2\frac{\partial b_3}{\partial \hat{x}_1}$$

$$g_{4,2} = a_1 + c_3(g_{3,2} - K_1\phi_1) + K_1 g_{3,1} + (g_{3,2} - K_1\phi_1)\frac{\partial b_2}{\partial \hat{x}_2} + \frac{d}{dt}(g_{3,2} - K_1\phi_1) + K_2\frac{\partial b_3}{\partial \hat{x}_2}$$

$$g_{4,3} = c_3 K_2 + a_2 g_{3,2} + \frac{d}{dt}(K_2) + K_2\frac{\partial b_3}{\partial \hat{x}_3}$$